

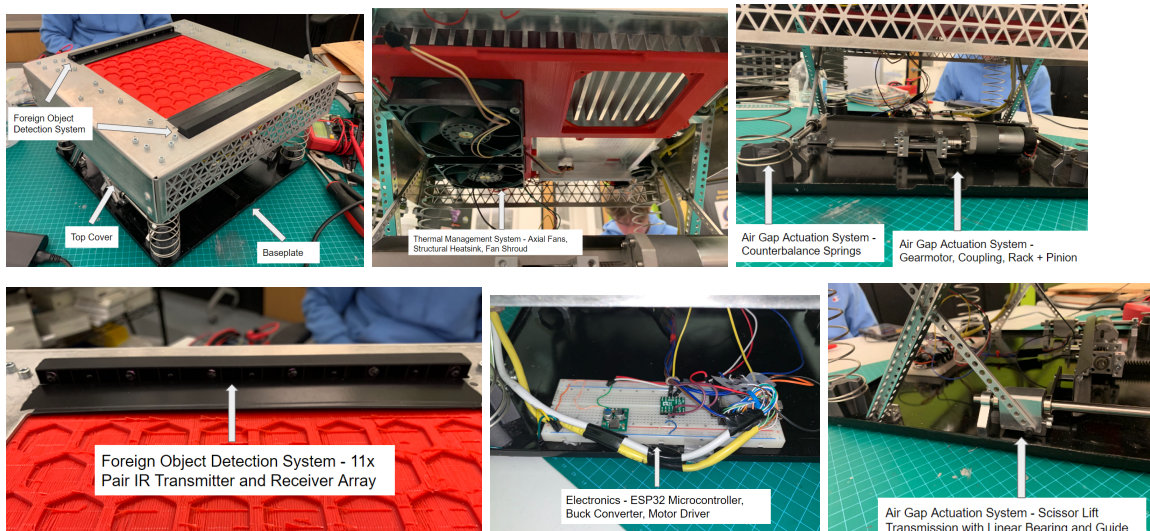
Wireless Charger Air Gap Actuation System

Opportunity: “Improve the charging experience of electric vehicles.”

High-level Strategy and Design v/s Achieved Specs

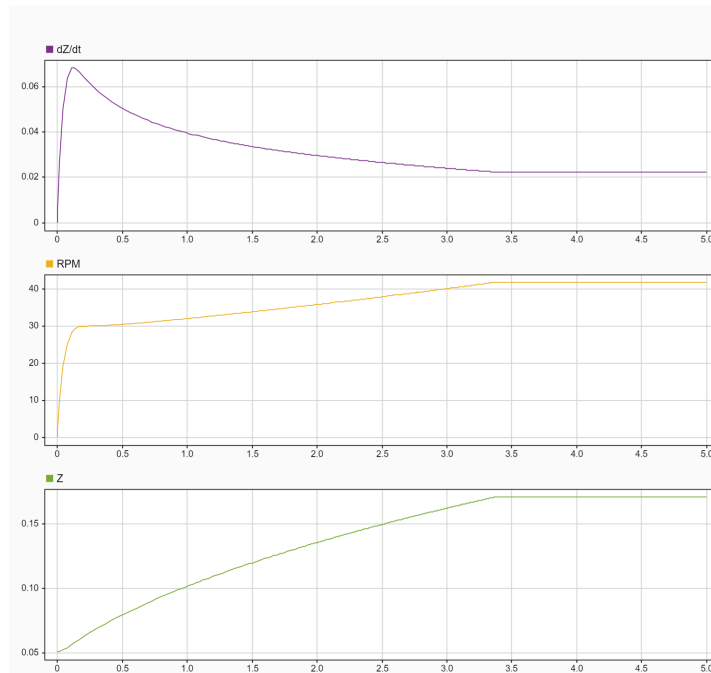
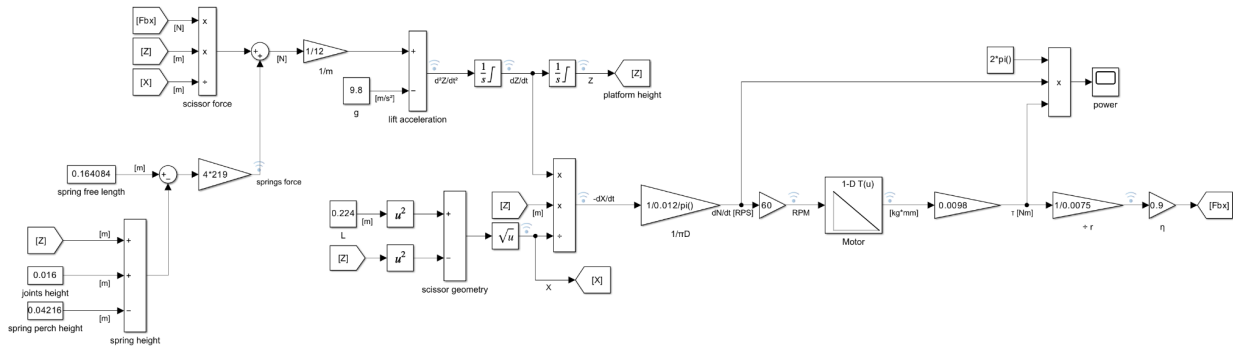
Our strategy to “improve the charging experience of EVs” is to create a resonant inductive wireless charger for various autonomous electric vehicles and micro-mobility forms of transport (wheelchairs, e-scooters, e-bikes, golf carts, e-skateboards, etc) equipped with ‘air gap actuation’ and ‘foreign object detection systems,’ with the latter 2 subsystems being the primary scope of this project. The foreign object detection system ensures the charging system is inactive when foreign objects (pets, metal objects, implants, people, etc.) are present in between the overlapped and perimeter regions of the vehicle (transmitter) and ground (receiver) charging pads. This system is necessary, especially for high frequency power transfer, as exposure to the magnetic field generated by the electromagnetic induction in the coils can have several negative impacts including joule heating of various systems and organs in the body as well as inducing a biased, oscillating current flow in the neural systems leading to overwritten body functions and signals. This system is implemented using an array of digital break beam sensor suite of infrared transmitters and receivers which, upon being broken, deactivate charging. The air gap actuation system linearly translates the vehicle pad in the Z-axis to a specified air gap for the inductive power coupling that has been modeled for the system’s electromagnetic design and power rating requirements, allowing for uncommon spacings between the vehicle and the ground surfaces. This allows all vehicle types to use one hardware configuration which is much more scalable than having multiple variants for each expected air gaps with smaller quantities. This system is implemented via a scissors mechanism driven by a rack and pinion and a DC motor. The primary design spec for the actuation system was to lift a platform (wireless charging transmitter coil module and peripherals) weighing 17 kg up 0.15 meters in 5 seconds. Our real-life assembly achieved 17 kg up 0.15 meters in 9 seconds, as evidenced by Appendix E.

Photos



Function-critical Decision Discussion

- Motor selection for scissor lift mechanism
 - Motor: <https://www.pololu.com/product/4697>; Motor Driver: [Pololu DRV8874](#)
 - Upon simulating various motors, the Pololu 4697 150:1 24V gearmotor is best predicted to raise the scissor lift to max height within 3.5 seconds, with the help of the springs. The 131:1 and 100:1 are also able, but the 150:1 will be in a more efficient RPM range during the overall run.
 - Estimation (based on linear approximation) of average power needed to lift 17kg by 0.15m within 5 secs: $\eta \bar{P} = \frac{W}{t}$; $\bar{P} = \frac{mg\Delta Z}{\eta \Delta t} = \frac{(17kg)(9.8m/s^2)(0.15m)}{(0.25)(5s)} \approx 20W$
 - This Simulink model uses the force balance equations derived earlier and the motor torque curve from datasheet to simulate the scissor lift's trajectory.

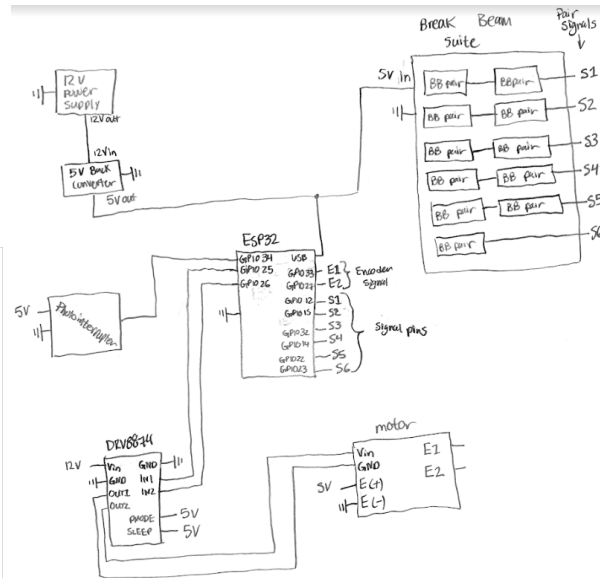
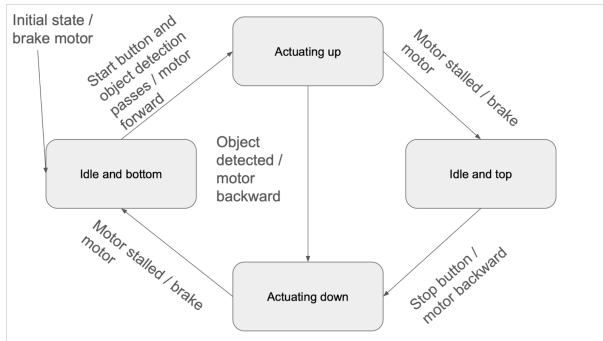


	Lead screw	Rack & pinion	Belt
Backdrivability	less	more	more

Maintenance	Requires lubrication	minimal	Requires belt tensioning
Dust resistance	bad	good	good
Cost	\$\$ (\$17)	\$\$ (~\$15)	\$

- Goal: find the radial reaction forces on the 2 bearings in the transmission during max torque conditions.
 - Knowns: $T_{max} = 560 \text{ kg} * \text{mm}$; $D_{pitch} = 15 \text{ mm}$; $\phi_{pressure} = 20 \text{ deg}$
 - Assume: treat tooth reaction forces as acting at the contact point between the 2 meshing gear pitch circles, independent of real tooth location.
 - Calculation: $T = F * r$; $F_{max} = T_{max} / r_{pitch}$;
 - $F_{max} = (560 \text{ kg} * \text{mm}) / (15/2 \text{ mm}) = 74.67 \text{ kgf}$
 - $F_{max} / \cos(\phi_{pressure}) = (74.67 \text{ kgf}) / \cos(20 \text{ deg}) = 79.46 \text{ kgf}$
 - $(79.46 \text{ kgf}) / (2 \text{ bearings}) = 39.73 \text{ kgf}$ reaction load on each bearing at max motor torque

Circuit Diagram and State Transition Diagram



Reflection

Our group was pleased to form a team early in the semester with complementary skills - we advise future groups to do the same (e.g. strong mechanical designer, electrical designer, coder, hands-on skills). We wish we had left more time for integration testing of the final assembly to gain confidence in the hardware's reliability - we advise to allocate time accordingly for future groups.

Appendix A: Bill of Materials

ME102B Group 5: Brad Ling, Shane Lee, David Kurniawan, Isak Knox, David Kurniawan

Level 0	Level 1	Level 2	Qty	Supplier	Mfr Part Number	Unit Cost	Ext. Cost	Product Link
	Scissor Lift Linkages SYSTEM		2			\$84.55	\$169.09	
	Slider Pillow Block ASSEMBLY		2			\$15.23	\$30.46	
		Slider Pillow Block	1	self. manual milling aluminum	6061-T6	\$1.71	\$1.71	https://www.mcmaster.com/9008K13/
		LM8SUU linear ball bearing	1	ServoCity	1612-0815-0045	\$4.00	\$4.00	https://www.servocity.com/8mm-id-x-45mm-length-linear-ball-bearings/
		15mm snap ring	2	ServoCity	632150	\$0.59	\$1.18	https://www.servocity.com/15mm-snap-ring/
		4x25mm shoulder bolt	1	McMaster	92981A745	\$3.20	\$3.20	https://www.mcmaster.com/92981a745/
		4x7-0.5mm shim	3	ServoCity	2807-0407-0500	\$0.17	\$0.50	https://www.servocity.com/2807-series-stainless-steel-shim-4mm-id-x-7mm-od-0-50mm-thickness-12-pack/
		M3 nylon nut	1	McMaster	90576A102	\$4.65	\$4.65	https://www.mcmaster.com/catalog/90576A102
	Stationary Joint ASSEMBLY		2			\$9.90	\$19.81	
		24mm U-Beam	1	ServoCity	1101-0003-0024	\$0.89	\$0.89	https://www.servocity.com/1101-series-u-beam-3-hole-24mm-length/
		M4x10mm socket head bolt	2	ServoCity	2800-0004-0010	\$0.14	\$0.27	https://www.servocity.com/2800-series-zinc-plated-steel-socket-head-screw-m4-x-0-7mm-10mm-length-25-pack/
		M4 square nut	2	ServoCity	2803-0007-0007	\$0.21	\$0.42	https://www.servocity.com/2803-series-stainless-steel-threaded-plate-7-7-24-pack/
		4x18mm shoulder bolt	1	McMaster	92981A744	\$3.18	\$3.18	https://www.mcmaster.com/92981A744/
		M3 nylon nut	1	McMaster	90576A102	\$4.65	\$4.65	https://www.mcmaster.com/catalog/90576A102
		4x7-0.5mm shim	3	ServoCity	2807-0407-0500	\$0.17	\$0.50	https://www.servocity.com/2807-series-stainless-steel-shim-4mm-id-x-7mm-od-0-50mm-thickness-12-pack/
	Linear Shaft ASSEMBLY		2			\$17.14	\$34.28	
		8mm x 150mm shaft	1	ServoCity	2100-0008-0150	\$2.89	\$2.89	https://www.servocity.com/8mm-x-150mm-stainless-steel-precision-shafting/
		clamp shaft support	2	ServoCity	1400-0032-0008	\$6.99	\$13.98	https://www.servocity.com/1400-series-1-side-2-post-clamping-mount-8mm-bore/
		M4x10mm socket head bolt	2	ServoCity	2800-0004-0010	\$0.14	\$0.27	https://www.servocity.com/2800-series-zinc-plated-steel-socket-head-screw-m4-x-0-7mm-10mm-length-25-pack/
	Crossbeam SYSTEM		1			\$128.76	\$128.76	
		Crossbeam	1	self. laser cutting & bending aluminum	5052	\$5.60	\$5.60	https://moosemetal.com/home
		L-bracket	2	self. manual milling mild steel		\$1.20	\$2.40	https://www.acehardware.com/metal-angles/5014360
		M4x16mm hex standoff	4	ServoCity	1516-4008-0160	\$0.67	\$2.69	https://www.servocity.com/1516-series-8mm-rex-standoff-m4-x-0-7mm-threads-16mm-length-4-pack/
		M4x10mm socket head bolt	4	ServoCity	2800-0004-0010	\$0.14	\$0.54	https://www.servocity.com/2800-series-zinc-plated-steel-socket-head-screw-m4-x-0-7mm-10mm-length-25-pack/
		M4x7mm socket head bolt	6	ServoCity	2800-0004-0007	\$0.12	\$0.74	https://www.servocity.com/2800-series-zinc-plated-steel-socket-head-screw-m4-x-0-7mm-7mm-length-25-pack/
		gear rack (100mm, 1.0 module)	1	McMaster	2485N217	\$16.12	\$16.12	https://www.mcmaster.com/2485N217/
	Drivetrain ASSEMBLY		1			\$100.66	\$100.66	
		150:1, 37mm gearmotor with encoder	1	Pololu	4697	\$51.95	\$51.95	https://www.pololu.com/product/4697
		6mm flexible shaft coupler	1	ServoCity	4002-0006-0006	\$5.99	\$5.99	https://www.servocity.com/6mm-to-6mm-flexible-clamping-shaft-coupler/
		pinion gear (15T, 1.0 module)	1	McMaster	2664N11	\$13.68	\$13.68	https://www.mcmaster.com/2664N11/
		6x14.5mm flanged bearing	2	ServoCity	1611-0514-0006	\$2.00	\$3.99	https://www.servocity.com/1611-series-flanged-ball-bearing-6mm-id-x-14mm-od-5mm-thickness-2-pack/
		BelleVue washer	1	McMaster	96445K276	\$3.85	\$3.85	https://www.mcmaster.com/96445K276/
		6x9-1mm shim	2	ServoCity	2807-0609-1000	\$0.19	\$0.38	https://www.servocity.com/2807-series-stainless-steel-shim-6mm-id-x-9mm-od-1mm-thickness-12-pack/
		6x9-0.25mm shim	1	ServoCity	2807-0609-0250	\$0.19	\$0.19	https://www.servocity.com/2807-series-stainless-steel-shim-6mm-id-x-9mm-od-0-25mm-thickness-12-pack/
		Quad Block Pattern Mount	2	ServoCity	1201-0024-0001	\$6.99	\$13.98	https://www.servocity.com/1201-series-quad-block-pattern-mount-24-1/
		M4x43mm hex standoff	2	ServoCity	1516-4008-0430	\$1.01	\$2.02	https://www.servocity.com/1516-series-8mm-rex-standoff-m4-x-0-7mm-threads-43mm-length-4-pack/
		Motor Mount	1	self. waterjet aluminum	6061-T6	\$3.22	\$3.22	https://www.mcmaster.com/8975K89/
		M4x10mm socket head bolt	6	ServoCity	2800-0004-0010	\$0.14	\$0.81	https://www.servocity.com/2800-series-zinc-plated-steel-socket-head-screw-m4-x-0-7mm-10mm-length-25-pack/
		M3x10mm socket head bolt	6	found spare	-	\$0.10	\$0.60	-
	Roof SYSTEM		1			\$153.36	\$153.36	
		Roof	1	self. laser cutting & bending aluminum	5052	\$48.00	\$48.00	https://moosemetal.com/home
		1/4" blind rivet	4	found spare	-	\$0.10	\$0.40	-
		Photointerrupter Sensor	1	found spare (EE16B kit)	HCMDU240	\$2.54	\$2.54	https://hobbycomponents.com/sensors/1147-compact-ir-infrared-rotary-speed-sensing-module
	Break Beam Sensor Cartridge ASSEMBLY		2			\$51.21	\$102.42	
		M4x24mm round standoff	2	ServoCity	1501-0006-0240	\$0.87	\$1.75	https://www.servocity.com/1501-series-m4-x-0-7mm-standoff-6mm-od-24mm-length-4-pack/
		M4x6mm flange head bolt	2	McMaster	96660A204	\$0.57	\$1.13	https://www.mcmaster.com/96660A204/
		Break Beam Sensor Cartridge	1	self. 3D print	-	\$0.92	\$0.92	https://www.amazon.com/HATCHBOX-3D-Filament-Dimensional-Accuracy/dp/B014VM951K/
		IR Break Beam Sensor (pair)	6	Adafruit	2168	\$5.95	\$35.70	https://www.adafruit.com/ProductDetail/Adafruit/2168?qs=GIURawfaeGuDdM1bPD%2FDieQ%3D%3D
		M3x14mm flat-head self-tapping screws	11	McMaster	90434A146	\$0.12	\$1.37	https://www.mcmaster.com/90434A146/
		conical spring (0.75", 1.215 lbs/in)	4	Access Spring	PCC022-328-421-7500-SST-0750-C-N-IN	\$2.15	\$8.60	https://www.thespringstore.com/catalog/product/view/id/124868/s/pcc022-328-421-7500-sst-0750-c-n-in/category/2/
		M3x6mm hex standoff	2	McMaster	95947A030	\$0.67	\$1.34	https://www.mcmaster.com/95947A030/
		M3x8mm socket head bolt	4	found spare	-	\$0.10	\$0.40	-
	Spring SYSTEM		4			\$16.06	\$64.24	
		compression spring, 6.5", 1.25 lbs/in	1	Access Spring	PC080-1734-11000-SST-6460-C-N-IN	\$12.06	\$12.06	https://www.thespringstore.com/pc080-1734-11000-sst-6460-c-n-in.html
		Spring Perch	2	self. 3D print	-	\$2.00	\$4.00	https://prusament.com/materials/prusament-pc-blend-carbon-fiber/
	Electronics SYSTEM		1			\$27.20	\$27.20	
		CAT5e solid core cable	2	found spare	-	\$1.00	\$2.00	-
		Dupont crimp connector	32	found spare	-	\$0.02	\$0.64	-
		Dupont male-male jumper	30	class kit	-	\$0.00	\$0.00	-
		adhesive zip tie mount	3	YUANHONGJIAN	-	\$0.47	\$1.42	https://www.amazon.com/dp/B0BY59DRL8?psc=1&ref=ppx_yo2ov_dt_b_product_details
		zip tie	12	found spare	-	\$0.02	\$0.24	-
		breadboard	1	class kit	-	\$0.00	\$0.00	-
		5V 3.4A step-down regulator board	1	Pololu	2831 (D30V30F5)	\$12.95	\$12.95	https://www.pololu.com/product/4892
		motor driver board	1	Pololu	4035 (DRV8874)	\$9.95	\$9.95	https://www.pololu.com/product/4035
		Huzzah ESP32 Feather	1	class kit	3405	\$0.00	\$0.00	-
	Inductive Transmitter SYSTEM		1	self (outside ME102B scope)		\$1,260.00	\$1,260.00	
						TOTAL:	\$1,802.64	

Appendix B: CAD Screenshots

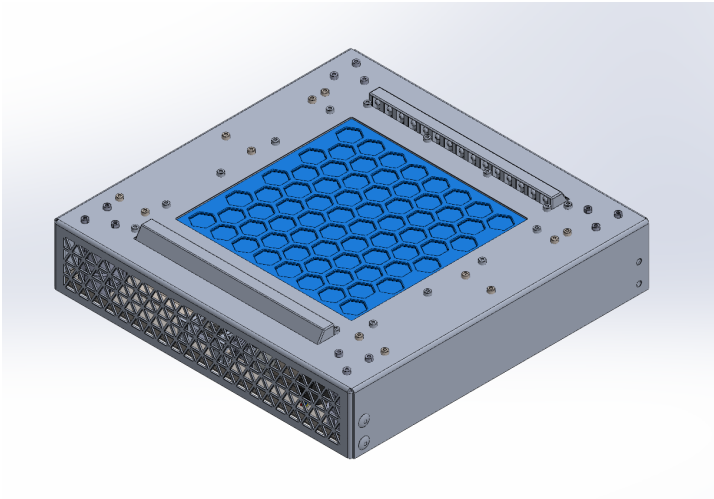


Fig. Top level assembly, retracted position.

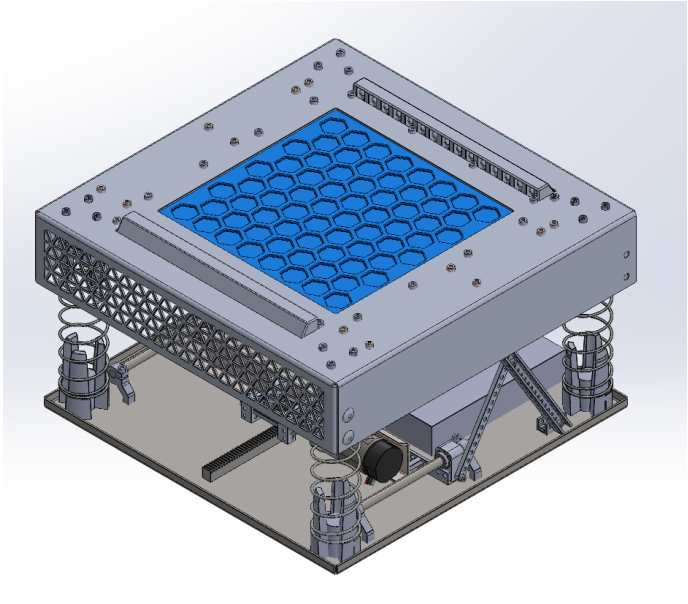


Fig. Top level assembly, extended position.

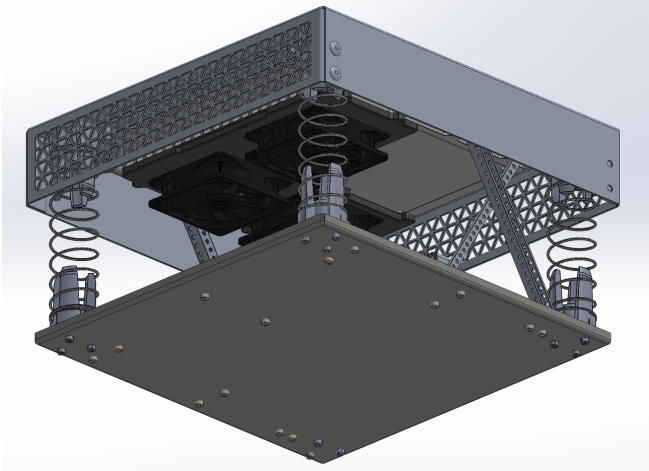


Fig. Top level assembly, bottom isometric extended position

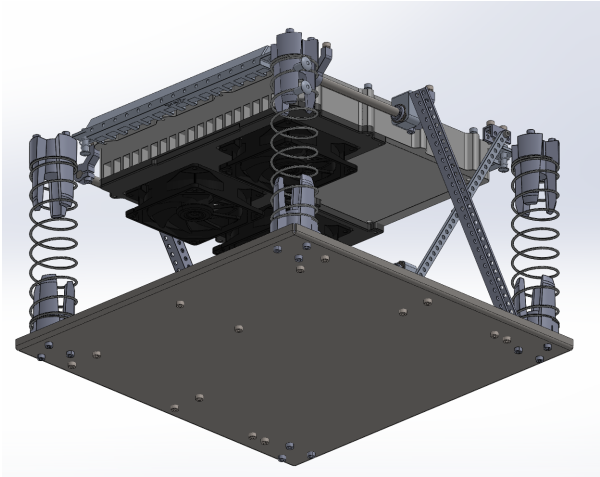


Fig. Top level assembly, bottom isometric, extended position, without roof enclosure

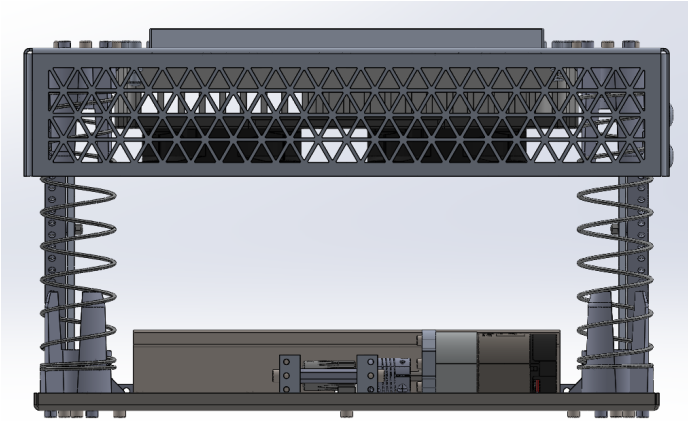


Fig. Top level assembly, side view, extended position.

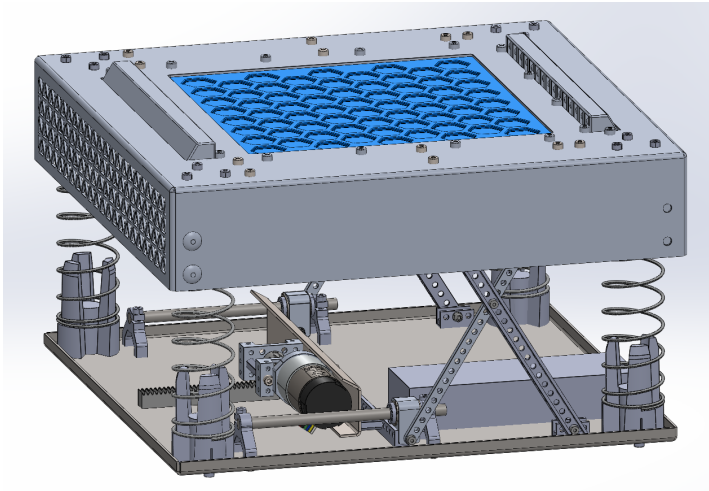


Fig. Top level assembly, trimetric view, extended position

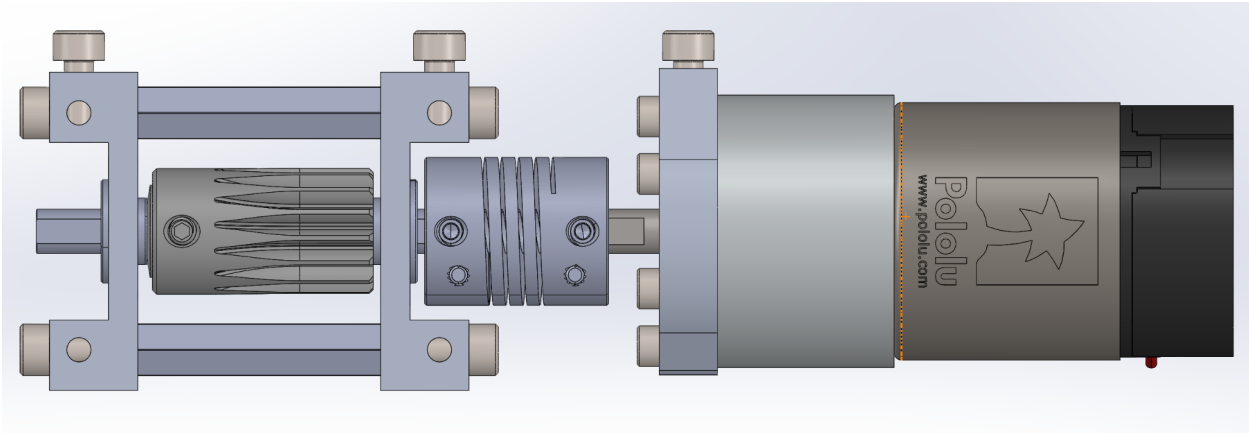
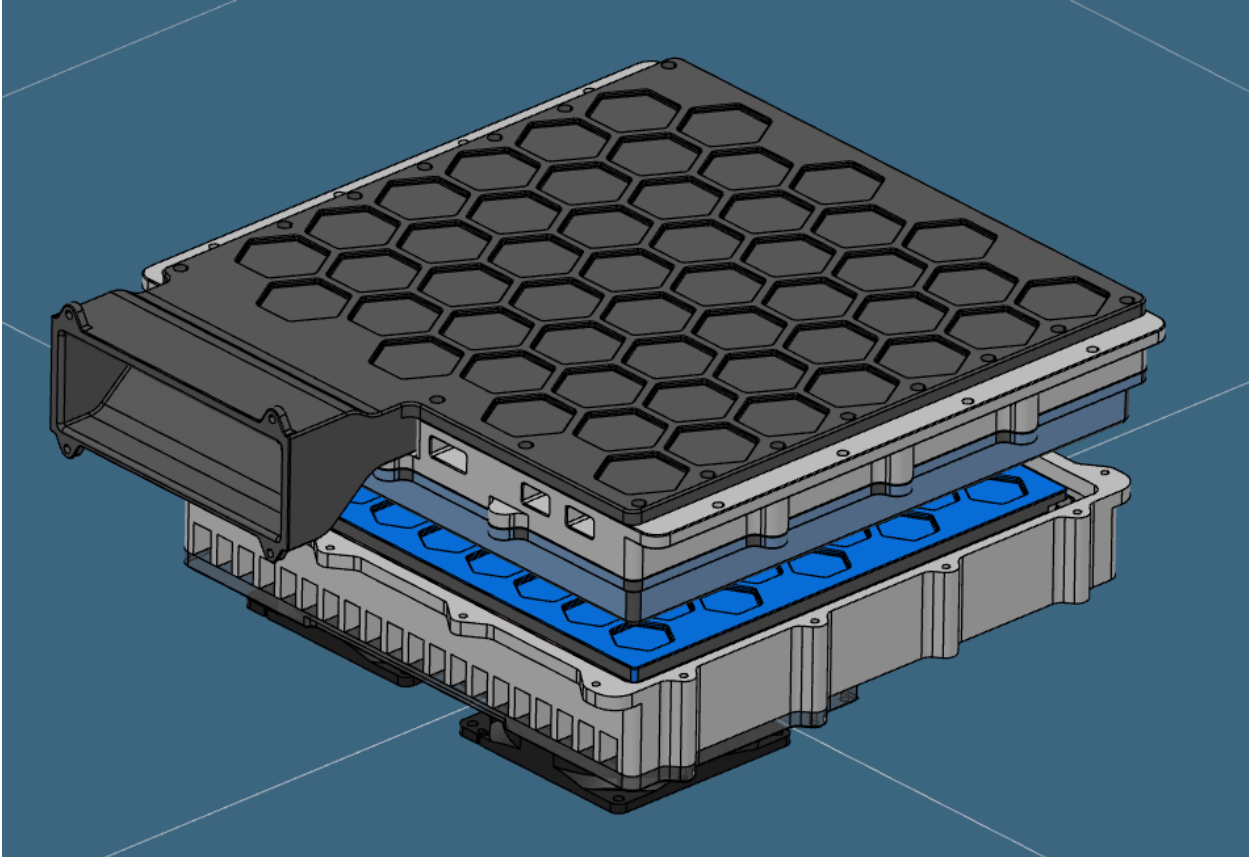
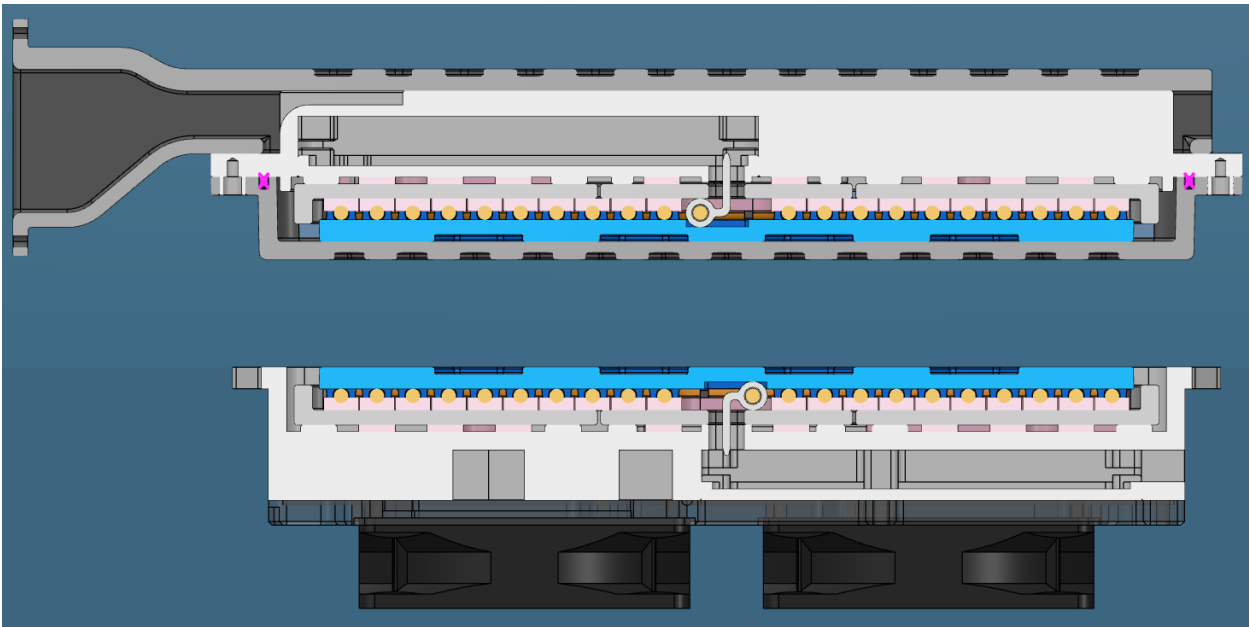


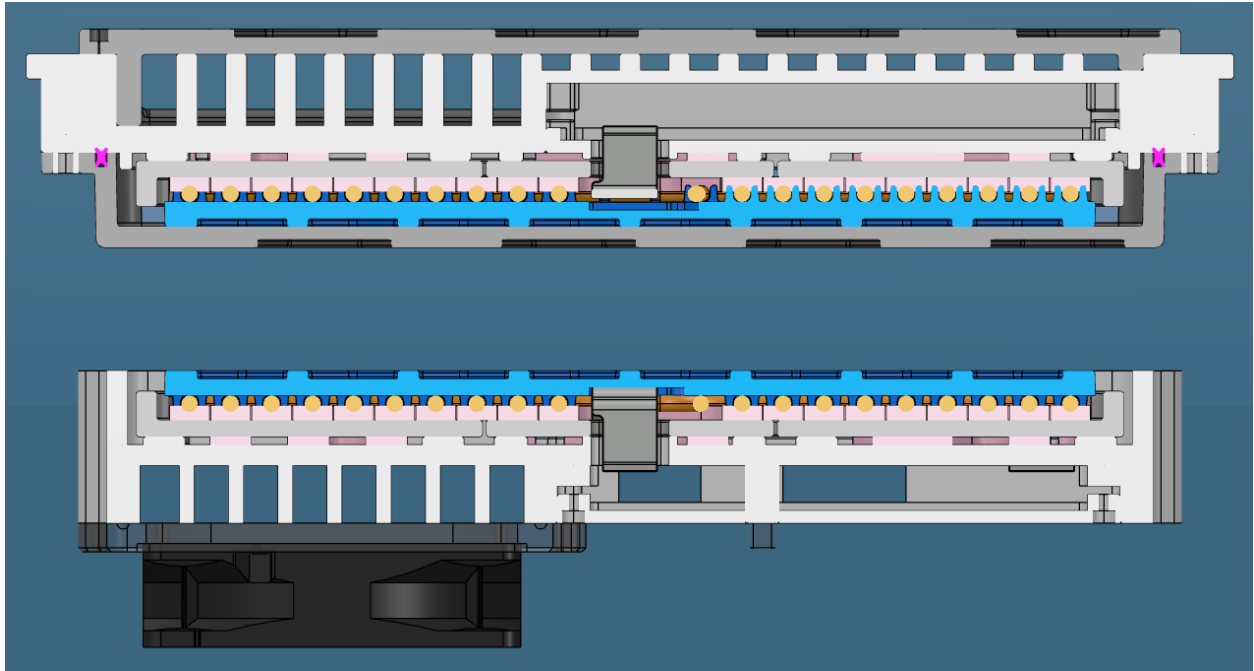
Fig. Transmission system



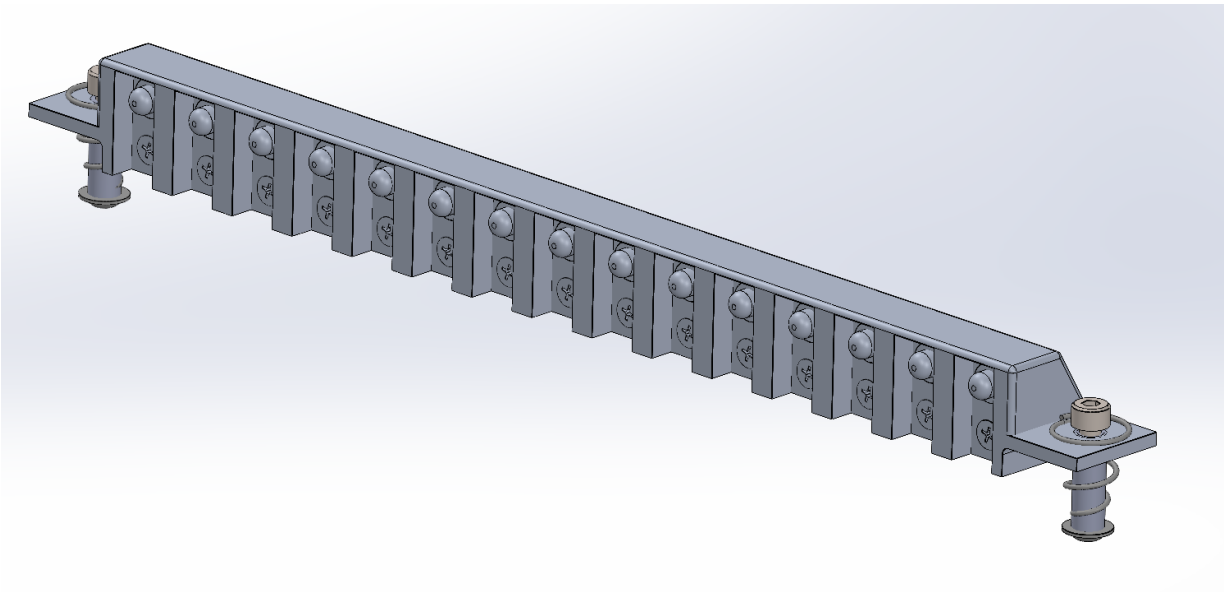
Vehicle Pad (Receiver Module) & Ground Pad (Transmitter Module) Isometric View

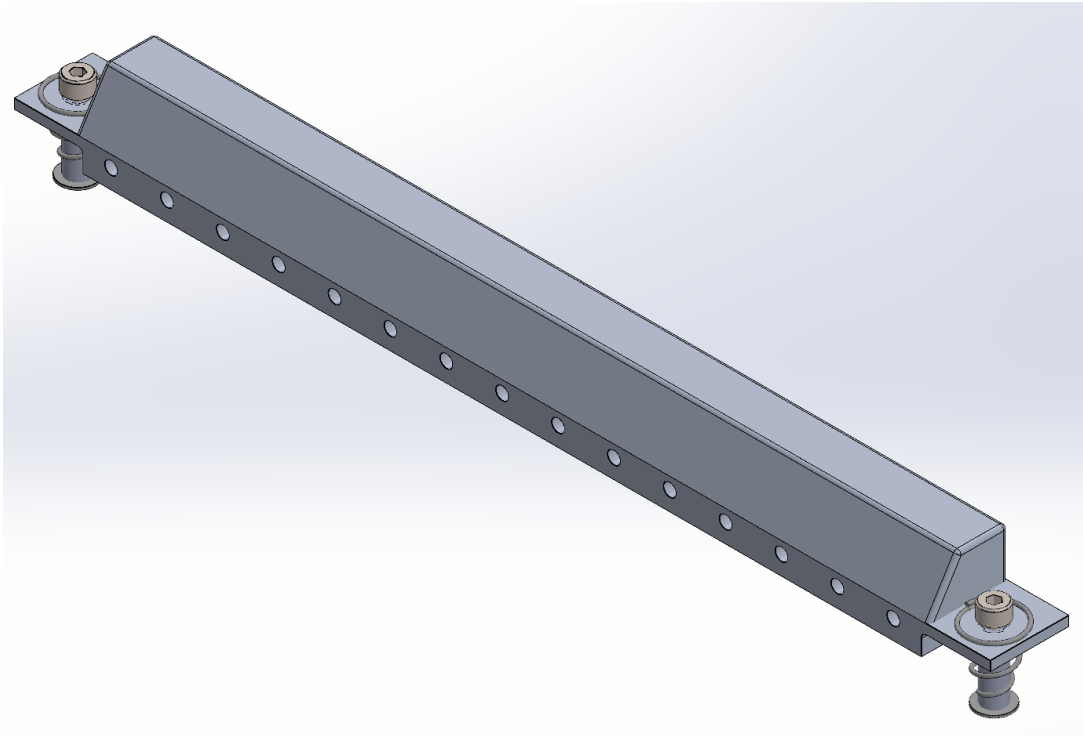
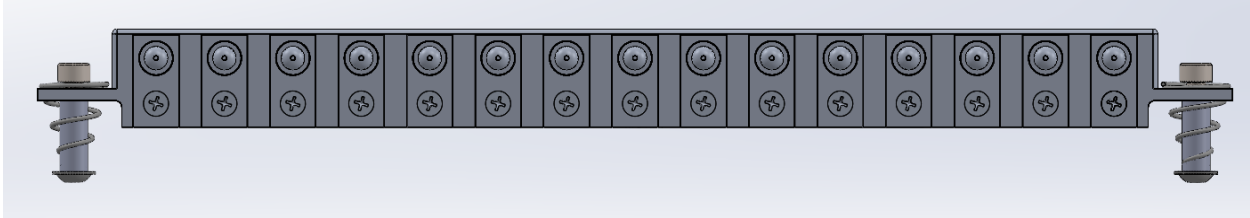


Vehicle Pad (Receiver Module) & Ground Pad (Transmitter Module) Cross Section



Vehicle Pad (Receiver Module) & Ground Pad (Transmitter Module) Cross Section





Figs. Foreign object detection infrared sensor cartridge, front and rear isometric view

Appendix C: Code Screenshots

```
1  #include <Arduino.h>
2  #include <ArduinoMqttClient.h>
3  #include <ESP32Encoder.h>
4  #include <WiFi.h>
5  WiFiClient wifiClient;
6  MqttClient mqttClient(wifiClient);
7  // const char* ssid = "iPhone (19)";
8  // const char* password = "shinhee3";
9  const char* ssid = "Berkeley-IoT";
10 const char* password = "n5ggZc(B";
11 const char* broker = "io.adafruit.com";
12 const char* user = "isaknox";
13 const char* key = "aio_acfe90JLF5q6Mz41FaP5nHjH5TYQ";
14 const int port = 1883;
15 const char* topic = "isaknox/feeds/luis";
16 #define disablePin 34 //declare pin for limit break
17 #define beam1 14
18 #define beam2 32
19 #define beam3 15
20 #define beam4 23
21 #define beam5 22
22 #define beam6 12
23 int beam;
24 int motorPin1 = 25;
25 int motorPin2 = 26;
26
27 //Setup variables -----
28 // Setting PWM properties
29 const int freq = 20000;
30 const int pwmChannel1 = 0;
31 const int pwmChannel2 = 1;
32 const int resolution = 8;
33 int dutyCycle = 220;
34 // Encoder
35 ESP32Encoder encoder;
36 volatile int count = 0; // encoder count
37
38 // declare timer
39 hw_timer_t * timer = NULL;
40
```

ME102B Group 5: Brad Ling, Shane Lee, David Kurniawan, Isak Knox, David Kurniawan

```
41 //Set bools to use for interrupts
42 volatile bool button = false;
43 volatile bool broken = false;
44 volatile bool disable = false;
45 int state = 1;
46 /* Possible States:
47 State 1: Idle and bottom
48 State 2: Actuating up
49 State 3: Idle and top
50 State 4: Actuating down
51 */
52
53 //Initialization -----
54 void IRAM_ATTR isr_disable() { // the function to be called when interrupt is triggered
55     disable = !disable;
56 }
57
58 void IRAM_ATTR isr_beam_suite() {
59     if (digitalRead(beam1) && digitalRead(beam2) && digitalRead(beam3)
60         && digitalRead(beam4) && digitalRead(beam5) && digitalRead(beam6)) {
61         broken = false;
62     } else {
63         broken = true;
64     }
65 }
66
67
68 void IRAM_ATTR onTime() {
69     timerStop(timer);
70 }
71
72
73 void TimerInterruptInit() {
74     timer = timerBegin(0, 80, true);
75     timerAttachInterrupt(timer, &onTime, true);
76     timerAlarmWrite(timer, 600000, true);
77     timerAlarmEnable(timer);
78 }
79
80
81 void startup() {
82     actuate_down();
83     while (true) {
84         count = encoder.getCount( );
85         if (count == 0) {
86             brake_motor();
87             return;
88         }
89         encoder.clearCount ( );
90     }
91 }
92
93 void setup() {
94     // configure pin modes
95     pinMode(motorPin1, OUTPUT);
96     pinMode(motorPin2, OUTPUT);
97     // set internal pullup resistor on esp for break beam sensors
98     pinMode(beam1, INPUT_PULLUP);
99     pinMode(beam2, INPUT_PULLUP);
100    pinMode(beam3, INPUT_PULLUP);
101    pinMode(beam4, INPUT_PULLUP);
102    pinMode(beam5, INPUT_PULLUP);
103    pinMode(beam6, INPUT_PULLUP);
104    pinMode(disablePin, INPUT);
105    // turn on internal pullup in break beams
106    digitalWrite(beam1, HIGH);
107    digitalWrite(beam2, HIGH);
108    digitalWrite(beam3, HIGH);
109    digitalWrite(beam4, HIGH);
110    digitalWrite(beam5, HIGH);
111    digitalWrite(beam6, HIGH);
112    // configure PWM on motor pins
113    ledcSetup(pwmChannel1, freq, resolution);
114    ledcAttachPin(motorPin1, pwmChannel1);
115    ledcAttachPin(motorPin2, pwmChannel2);
116    // setup interrupt triggers
117    attachInterrupt(disablePin, isr_disable, CHANGE);
```

ME102B Group 5: Brad Ling, Shane Lee, David Kurniawan, Isak Knox, David Kurniawan

```
118 attachInterrupt(beam1, isr_beam_suite, CHANGE);
119 attachInterrupt(beam2, isr_beam_suite, CHANGE);
120 attachInterrupt(beam3, isr_beam_suite, CHANGE);
121 attachInterrupt(beam4, isr_beam_suite, CHANGE);
122 attachInterrupt(beam5, isr_beam_suite, CHANGE);
123 attachInterrupt(beam6, isr_beam_suite, CHANGE);
124 // init timer
125 TimerInterruptInit();
126 timerStop(timer);
127 // Encoder
128 ESP32Encoder::useInternalWeakPullResistors = UP; // Enable the weak pull up resistors
129 encoder.attachHalfQuad(33, 27); // Attach pins for use as encoder pins
130 encoder.setCount(0); // set starting count value after attaching
131 // setup wifi connection
132 WiFi.begin(ssid, password);
133 Serial.println("Connecting");
134 while (WiFi.status() != WL_CONNECTED) {
135     delay(500);
136     Serial.println(".");
137 }
138 Serial.println("Connected to the WiFi network");
139 mqttClient.setUsernamePassword(user, key);
140 if (!mqttClient.connect(broker, port)) {
141     Serial.print("MQTT connection failed! Error code = ");
142     Serial.println(mqttClient.connectError());
143 }
144 Serial.println("You're connected to the MQTT broker!");
145 mqttClient.onMessage(toggle_button);
146 mqttClient.subscribe(topic);
147 startup();
148 Serial.begin(115200);
149 }
150

151 void loop() {
152     // put your main code here, to run repeatedly:
153     Serial.print("Broken: ");
154     Serial.println(broken);
155     Serial.print("Button: ");
156     Serial.println(button);
157     Serial.print("Disabled: ");
158     Serial.println(disable);
159     Serial.print("System state: ");
160     switch (state) {
161         case 1:
162             Serial.println("Idle bottom");
163             mqttClient.poll();
164             if (button && !CheckObstruction()) {
165                 button = false;
166                 actuate_up();
167                 state = 2;
168                 timerStart(timer);
169                 encoder.clearCount ( );
170             }
171             break;
172
173         case 2:
174             Serial.println("Actuating up");
175             if (CheckStall()) {
176                 stalled();
177                 state = 3;
178             } else if (CheckObstruction()) {
179                 actuate_down();
180                 state = 4;
181             }
182             break;
```

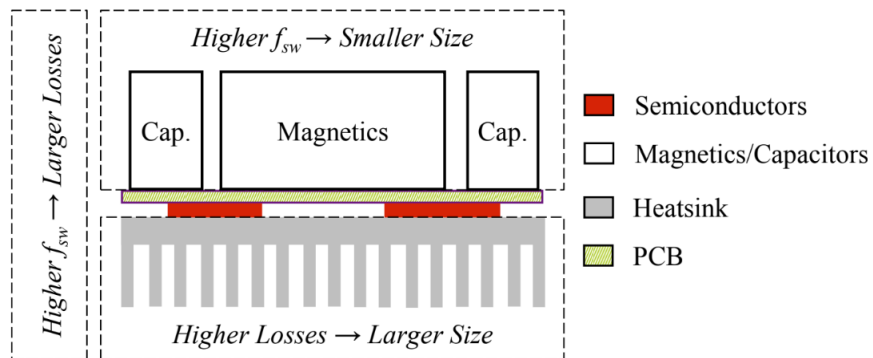
ME102B Group 5: Brad Ling, Shane Lee, David Kurniawan, Isak Knox, David Kurniawan

```
183     case 3:
184         Serial.println("Idle and top");
185         mqttClient.poll();
186         if (button) {
187             actuate_down();
188             button = false;
189             encoder.clearCount ( );
190             state = 4;
191         }
192         break;
193
194     case 4:
195         Serial.println("Actuating down");
196         if (CheckStall()) {
197             stalled();
198             state = 1;
199         }
200         break;
201     }
202 }
203
204
205 // Event Checker functions!!
206 bool CheckObstruction() {
207     if (broken && !disable) {
208         return true;
209     }
210     return false;
211 }
212
213 bool CheckStall() {
214     count = encoder.getCount( );
215     if (count == 0 && !timerStarted(timer)) {
216         encoder.clearCount ( );
217         return true;
218     }
219     encoder.clearCount ( );
220     return false;
221 }
222 ---
223
224 // Service Functions!!
225 void actuate_up() {
226     ledcWrite(pwmChannel1, dutyCycle);
227     ledcWrite(pwmChannel2, 0);
228     disable = false;
229 }
230
231 void actuate_down() {
232     ledcWrite(pwmChannel2, dutyCycle);
233     ledcWrite(pwmChannel1, 0);
234 }
235
236 void brake_motor() {
237     ledcWrite(pwmChannel2, dutyCycle);
238     ledcWrite(pwmChannel1, dutyCycle);
239 }
240
241 void stalled() {
242     brake_motor();
243     timerStart(timer);
244 }
245
246 void toggle_button(int message) {
247     button = true;
248     Serial.print("Received signal!");
249 }
250
```

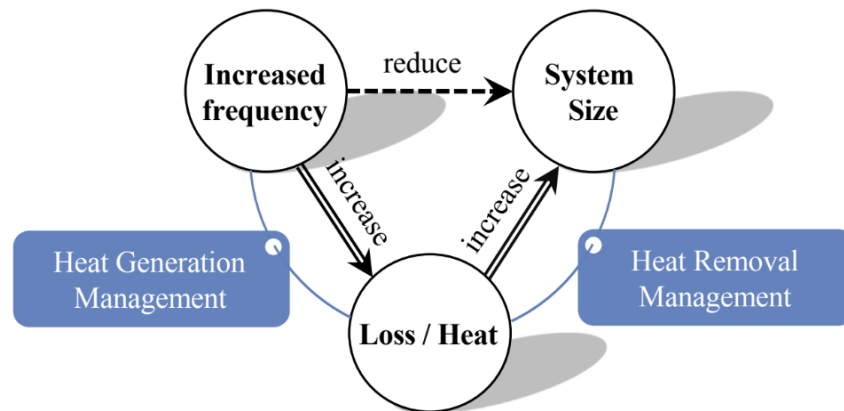
Appendix D: Wireless Charger and Thermal System Design Doc

● **Background: Why do we need thermal management?**

- Thermal management systems are implemented in order to ensure components are operating at or below their maximum operating temperature which helps both performance objectives as well as long-term reliability. In power electronics converters with high power density, the loss density increases for power flow components as the converter is more compact at both a component and system level. Advancements in the world of power electronics are driven by the following goals: higher energy efficiency, better reliability, increased production automation capability, and increased power density.
- Higher energy efficiency is achieved directly as a result of generating lower losses which not only improves efficiency, but also improves long-term reliability as well as increased power density. Lower losses will lead to reduced hot-spot temperatures which will improve reliability as the leading cause of failure in electronics is failures as a function of temperature delta.
- The main factors which deteriorate the power density of power electronics include the following: poor spatial consumption/large amounts of ineffective internal ambient air (use of standard components leads to non-uniform profiles and volumes that lead to many pockets of waste air that do not provide any additional cooling capability during normal operation); inefficient operation (losses generated are dissipated in the form of heat which in overabundance can lead to large internal temperature deltas for components that will shorten the lifetime of the component or lead to a runaway and short-term damage); and inefficient heat dissipation methods (typical loss density ranges for components in power electronics converters are 1-100 W/cm² for semiconductors, 0.1-1 W/cm² for magnetics, and < 0.1 W/cm² for capacitors; however, semiconductors have minimal volume relative to other components while possessing cooling systems far greater in volume while magnetics and other components possess larger volumes with less effective cooling systems which leads to overall inefficient cooling systems with greater than needed volumes).



- At fixed power levels, increased power density is achieved by the reduction in the converter system volume. In most converters, volume is dominated by passive components as well as thermal management systems and their ancillaries. Generally, increasing the switching frequency of the power semiconductor devices in the system can effectively reduce volume of passive components (except cases such as capacitors being used to line frequency energy storage). The downside to increased frequency is that the switching losses of semiconductors and the core losses of magnetic components is increased, which subsequently leads to increased cooling system volume to manage component temperatures below operating limits.



- The solutions to increased losses from increasing frequency to reduce system volume is: 1) effective heat generation management to control component losses from higher switching frequencies and 2) heat dissipation management to control temperature rises of components.
- The loss characteristics of a power electronics converter are primarily derived from the topology of the circuit as different topologies can vary in terms of component stresses, component count, semiconductor modulation methods, power delivering pattern/sequence, etc. A selected topology that can intrinsically generate less loss in a specified application will also facilitate heat generation management. For example, if a topology requires capacitors to carry power current, then larger capacitors are required to thermally manage the significant losses which is inherently not a suitable candidate for higher power density designs.
- Beyond the converter topology and expected component types, there are a number of component and system design parameters to optimize system performance. These parameters include switching frequency, inductance values, modulation methods, materials, number of units in parallel, number of winding turns, winding configurations, and more. The optimal values for these parameters can and will likely change with temperature and the converter operating range. In order to optimize the power converter's efficiency, loss models that can accurately and rapidly estimate system and component losses based on the previously mentioned parameters will facilitate the optimal design.

- For instance, the winding loss of a high-current transformer is extensive, so to reduce this the lower voltage winding must have the minimum turn count possible to decrease winding resistance. However, less winding turns will increase the flux density of the magnetic cores which will tend to increase core losses and thus the temperature of the cores. A larger core can be employed to restrain increases in flux density, but this results in increased transformer volume. In this case, a balance must be struck between loss generation and transformer volume.
- Furthermore, due to the advent of wide bandgap power semiconductor devices such as silicon carbide (SiC) and gallium nitride (GaN), there has been a trend of increased miniaturization of power electronics converters to increase power density. The downstream effect of this is reduced area for dissipating heat which is a challenge for thermal management of newer power converter designs.
- The efforts of this project document will primarily focus on the design of effective thermal management systems and their ancillaries to reduce temperature rise in critical power electronics components. Effective thermal generation management design will be covered in greater depth in the power electronic project documentation found below. Without a carefully analyzed and well-thought-out cooling design, even minimal loss generation can lead to enough heat accumulated for a temperature delta that can burn or melt components along with overall decreased loss density. Generally, power semiconductors can easily be coupled to flat cooling surfaces thanks to newer design architectures incorporating larger embedded heat spreaders that are on the surface opposite of the die attach and PCB connections. However, bulky passive components, which are volume-heating components, are often decoupled from the cooling methods engaged for the semiconductors. Older and existing designs rely on heat generated by these passive components to be released to ambient via their exposed surface areas which results in poor cooling efficiency. If we design a thermal management system that integrates both active and passive components into the same cooling structure, we can achieve greater cooling efficiency. The objective of this project is to limit component temperature rise in a volumetrically efficient manner by collecting heat from primary loss-generating components through different thermal interfaces to a common heat exchange surface where heat is dissipated in a centralized manner.

Power Electronics Documentation: [☰ Wireless Charger | Power Electronics Topology Notes](#)

- **Air-Cooled vs Liquid-Cooled**

- Liquid cooled systems add complexity and mass to the system due to all the additional components needed to drive the liquid flow system (pumps, reservoirs, tubing, etc.)
-


- **(Ground Pad) Natural Convective Air-Cooling**

- **+** Wireless Charger | Heatsink Design Analysis
 - Can we get away with natural convective cooling as well as all the additional thermal mass of the ground pad to increase the transient thermal profile
-

- **Forced-Convective Air Cooling**

- **First Principles Hand Calc**

- **+** Wireless Charger | Heatsink Design Analysis
- Estimated total losses ($[1-\text{efficiency}] \times [\text{continuous power}]$) applied as a heat flux to top surface of finned heat sink
 - Refine with eventual component locations to apply heat flux to accurate source locations on the heatsink and each component's continuous power loss
 - Efficiency Target: 70%
 - Continuous Power Rating: 1 kW
 - Estimated Total Losses: 300 W
 - Constant Heat Flux Input
 - Area
 - 0.057 m^2
 - Rth Stack from TIM to Heatsink
 - Assumptions:
 - Full TIM Coverage between magnetics and heatsink (in reality this is a mix of TIM, aluminum, and air)
 - System total losses applied over surface of the heatsink baseplate
 - Rth Stack
 - Rth, TIM, Cond
 - Thermal conductivity
 - $K = 3.7 \text{ W/m-k}$
 - Thickness
 - 2 mm (0.002 m)
 - Area
 - 0.019 m^2 (19000 mm^2)
 - Rth, Heatsink Base, Cond
 - Thermal conductivity
 - $K = 237 \text{ W/m-K}$
 - Thickness
 - 6.5 mm (0.0065 m)
 - Area
 - 0.033 m^2 (33000 mm^2)

- Rth, Heatsink Fins, Conv
 - Convection Coefficient, h
 - Surface Area
 - 0.349 m²
 - T_{internal_ambient} = 40 C (obtain max allowable T_{rise} when h is known or get h is max allowable T_{rise} is known)
 - T_{ferrite} = 120C
 - **Calculated h = 12.070 W/m²-K**
 - **Conservative 1.5 FOS => 18 W/m²-K design target**
- **Predicted air flow characteristics, surface area/fin geometry, h (convective coefficient)**
 -  Wireless Charger | Heatsink Design Analysis
 - Properties of air (1 atm, 25C)
 - Density
 - 1.18 kg/m³
 - Thermal conductivity
 - 0.02624 W/m*K
 - Specific heat capacity
 - 1006 J/kg*K
 - Kinematic viscosity
 - 1.55*10⁻⁵ m²/s
 - Dynamic viscosity
 - 1.84*10⁻⁵ kg/m*s
 - Thermal diffusivity
 - 2.21*10⁻⁵ m²/s
 - Properties of air (1 atm, 40C)
 - Density
 - 1.13 kg/m³
 - Thermal conductivity
 - 0.02735 W/m*K
 - Specific heat capacity
 - 1007 J/kg*K
 - Kinematic viscosity
 - 1.66 * 10⁻⁵ m²/s
 - Dynamic viscosity
 - 1.87 * 10⁻⁵ kg/m*s
 - Thermal diffusivity
 - 2.40*10⁻⁵ m²/s
 - Relation between h and Nusselt Number

$$Nu = \frac{h D}{k}$$

-
- D_h = characteristic length

$$D_H = \frac{4A}{P}$$

-
- Wetted Perimeter
- Flow Cross-Sectional Area
- Use Gnielinski Empirical Correlation to estimate Nusselt Number

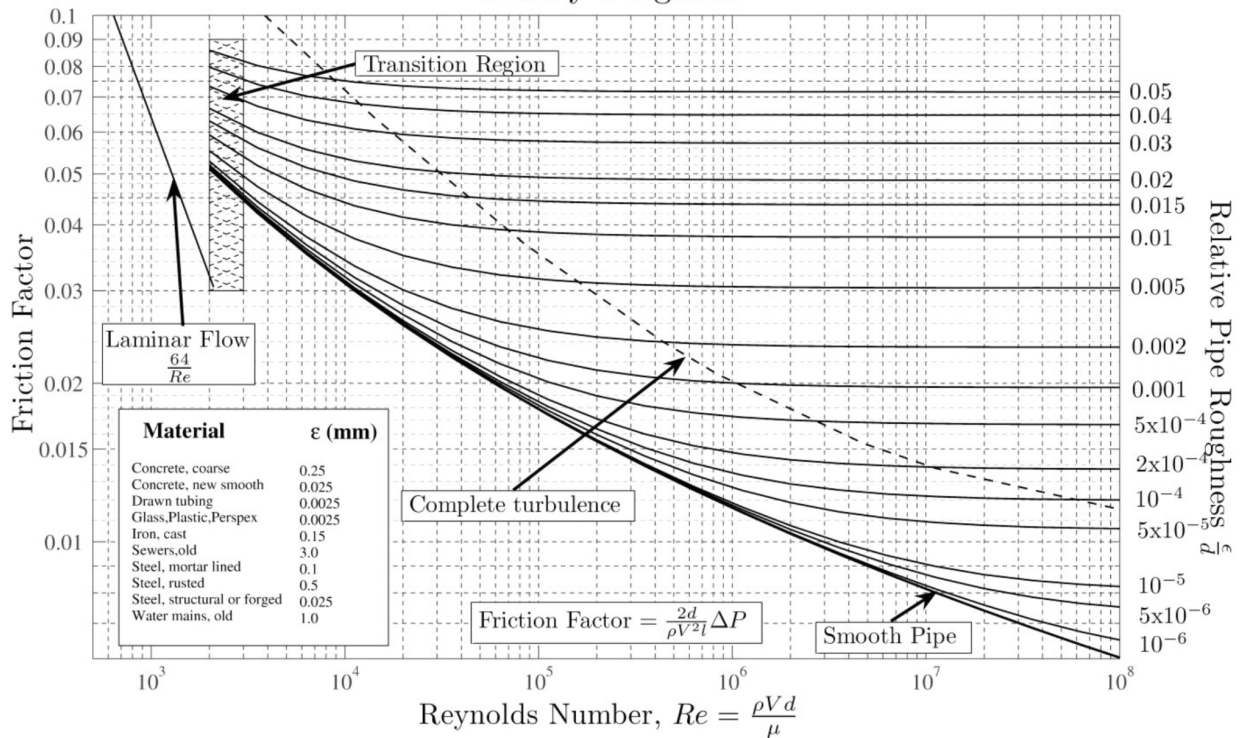
$$Nu_D = \frac{(f/8) (Re_D - 1000) Pr}{1 + 12.7(f/8)^{1/2} (Pr^{2/3} - 1)}$$

-
- Calculate Prandtl Number

$$Pr = \frac{\nu}{\alpha}$$

- Darcy Friction Factor
 - Moody Diagram

Moody Diagram



- Reynolds Number

$$Re_D = \frac{\rho u_m D}{\mu} = \frac{u_m D}{\nu} = \frac{4\dot{m}}{\pi D \mu}$$

- Use CFD results to obtain flow velocity (u_m) and pressure drop
- Select fan once target h is met along with any other metrics
- **General Convective Heat Transfer Process (Estimate h)**

- + Wireless Charger | Heatsink Design Analysis
- Check whether fluid flow is laminar or turbulent (Reynolds number)
 - For internal flow:
 - $Re_{D_cr} \sim 2300$ (Critical Reynolds Number)
 - If $Re_D < Re_{D_cr} \Rightarrow$ Laminar Regime
 - If $Re_{D_cr} < Re_D < 4000 \Rightarrow$ Transition Regime
 - If $Re_D > 4000 \Rightarrow$ Turbulent Regime
 - If $Re_D > 10000 \Rightarrow$ Fully Turbulent Regime

$$Re_D = \frac{\rho u_m D}{\mu} = \frac{u_m D}{\nu} = \frac{4\dot{m}}{\pi D \mu}$$

- Where μ is the dynamic viscosity (Ns/m²)
- Where ν is the kinematic viscosity (m²/s)
- Where u_m is the fluid velocity (m/s)
- Where ρ is the fluid density (kg/m³)
- Where D is the hydraulic diameter (m)
- Where \dot{m} is the mass flow rate (kg/s)
- Use correlations to find Nusselt Number based on Prandtl, Pr and Reynolds, Re Numbers
 - Reynolds Number is based on the hydraulic diameter as shown above
 - Prandtl number can be calculated as:

$$Pr = \frac{\nu}{\alpha}$$

- $Pr = \nu/\alpha$
- Where ν is the kinematic viscosity (m²/s)
 - Where $\nu = \mu/\rho$ where μ is the dynamic viscosity
- Where α is the thermal diffusivity (m²/s)
 - Where $\alpha = k/(\rho \cdot c_p)$

$$\alpha = \frac{k}{\rho C_p}$$

- Use Nusselt number, Nu and flow parameters (geometry - characteristic length, fluid velocity, and thermal conductivity) to calculate convective coefficient, h
 - Characteristic Length is the dimension in the direction of growth (or thickness) of the boundary layer
 - For complex shapes, the characteristic length may be defined as the volume of the fluid body divided by the surface area
 - Average vs Local Nusselt Number
- Check if estimated h is enough to for convective cooling requirements (q_conv)
 - From CFD, we can use estimated temperature across the heatsink and the delta with the ambient temperature (fan inlet temperature) to determine h as we will have q and surface area of the fin array
- Empirical Correlations for Nusselt Number
 - For forced convection the Nusselt number is generally a function of the Reynolds Number and the Prandtl Number (for natural convection, the Nusselt number is a function of the Rayleigh number and the Prandtl number)
 - Enclosed fin heatsink => internal flow correlations
 - Circular Tubes
 - Chilton-Colburn Analogy (Colburn Equation)
 - Second Petukhov
 - Gnielinski

$$Nu_D = \frac{(f/8) (Re_D - 1000) Pr}{1 + 12.7(f/8)^{1/2} (Pr^{2/3} - 1)}$$

-
- Which is valid for:
 - $0.5 \leq Pr \leq 2000$
 - $3000 \leq Re_D \leq 5 \times 10^6$
- Where f is the Darcy Friction Factor
 - This can be obtained from a Moody diagram or in the case of smooth tubes, from the Petukhov relation:
 - $f = (0.79 \ln(Re_D) - 1.64)^{-2}$
 - The friction factor can also be approximated using the Colebrook Equation for turbulent flows (relation holds for Re > 4000):

$$\frac{1}{\sqrt{f}} = -2 \log \left(\frac{\epsilon}{3.7D_h} + \frac{2.51}{\text{Re}\sqrt{f}} \right)$$

■ Dittus-Boelter

$$\bullet \quad \text{Nu}_D = 0.023 \text{Re}_D^{4/5} \text{Pr}^n$$

- Which is valid for

$$0.6 \leq \text{Pr} \leq 160$$

$$\text{Re}_D \gtrsim 10\,000$$

$$\frac{L}{D} \gtrsim 10$$

- Where $n = 0.4$ for fluid heating, $n = 0.3$ for fluid cooling
- Caution: Dittus-boelter is tailored for smooth tubes which for general machined heatsinks can lead to non-negligible inaccuracies

■ Sieder-Tate

$$\text{Nu}_D = 0.027 \text{Re}_D^{4/5} \text{Pr}^{1/3} \left(\frac{\mu}{\mu_s} \right)^{0.14}$$

- Where μ is the fluid viscosity at the bulk fluid temperature and μ_s is the fluid viscosity at the heat-transfer boundary surface temperature
- Which is valid for

$$0.7 \leq \text{Pr} \leq 16\,700$$

$$\text{Re}_D \geq 10\,000$$

$$\frac{L}{D} \gtrsim 10$$

○ Non-Circular Tubes

- Use the hydraulic diameter for both the Reynolds and Nusselt numbers using same correlations (for Turbulent flow)

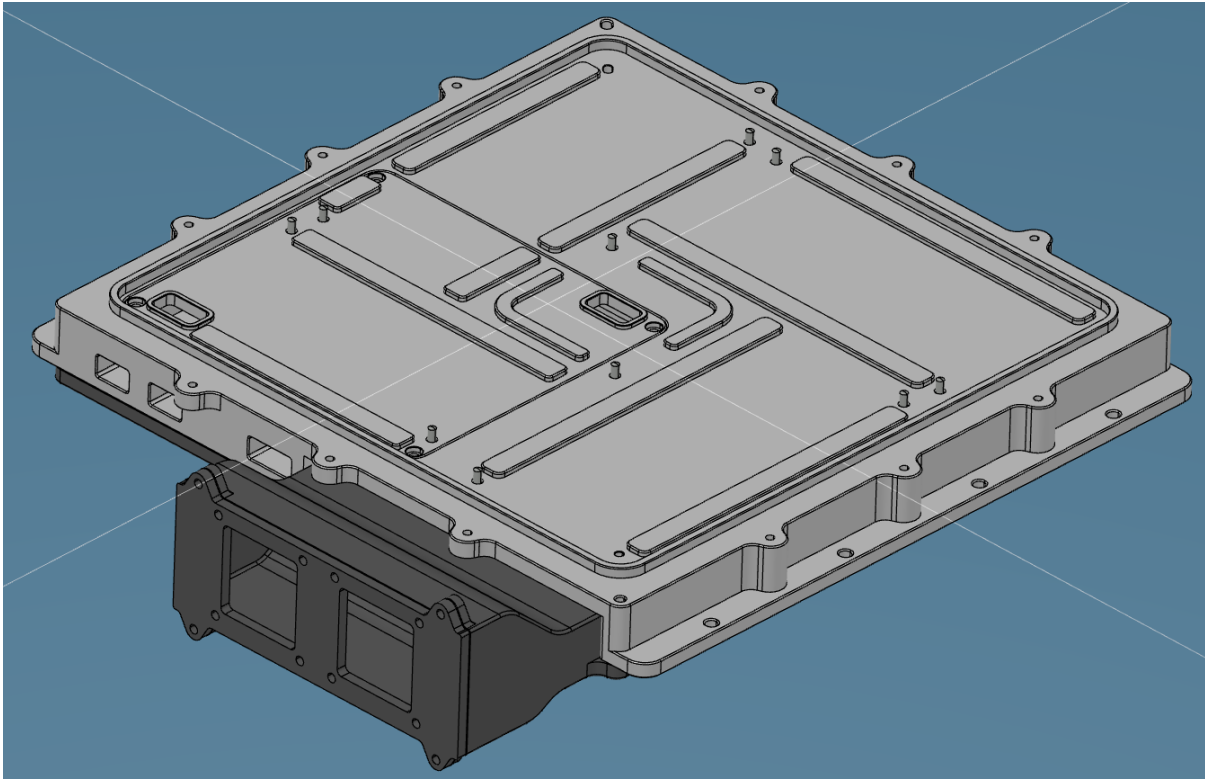
- Hydraulic diameter $D_h = (4 \cdot A_c) / p$

$$D_H = \frac{4A}{P}$$

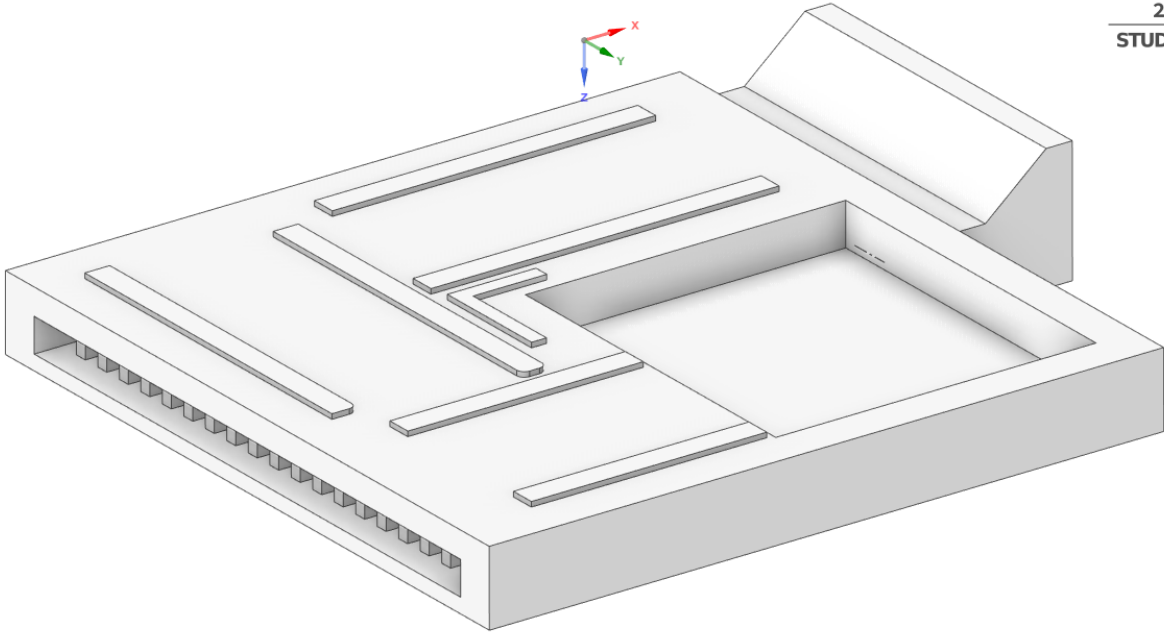
- Where P is wetted perimeter
- Where A_c is the flow cross-sectional area

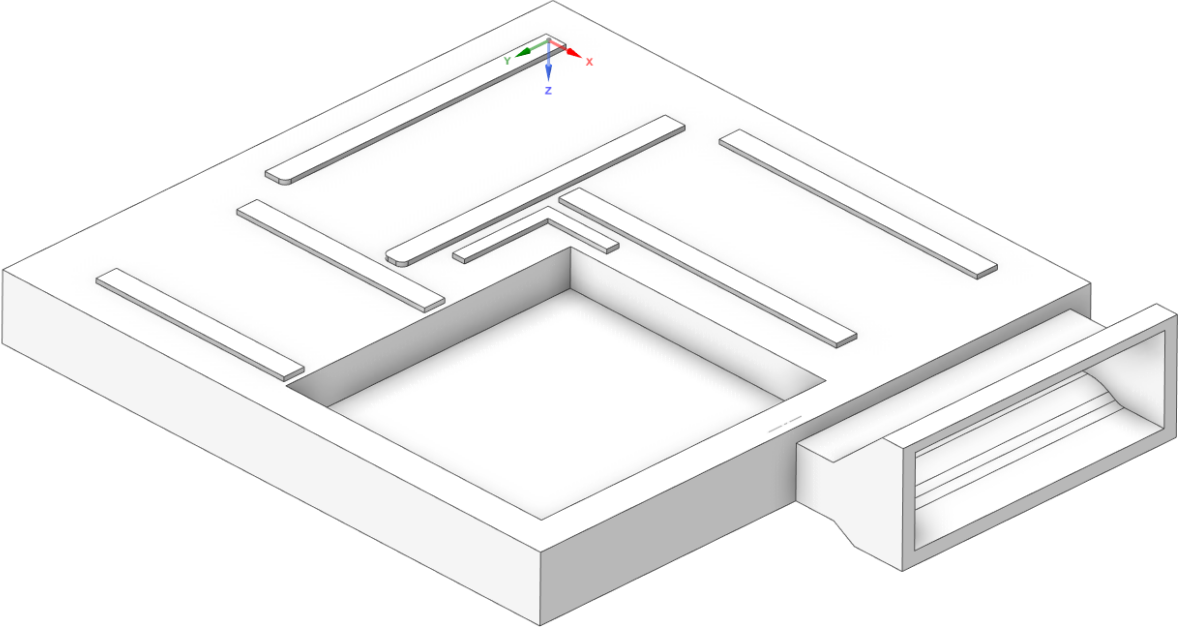
- In the case of laminar flow regimes, the Nusselt number depends heavily on aspect ratio as well as the entry region and surface thermal conditions
- Parallel Plate Correlations
- Common Dimensionless Numbers in Heat Transfer
 - Reynolds Number
 - A dimensionless number that is the ratio of forces (inertia forces to viscous forces) that influence the behavior of fluid flow in a boundary layer
 - Nusselt Number
 - A dimensionless number that represents the ratio of convection (both advection - fluid motion, and diffusion - conduction) to conduction for a layer of fluid
 - Prandtl Number
 - A dimensionless number which relates the viscous diffusion rate (viscosity) with the thermal diffusion rate (thermal diffusivity => measures a material's ability to conduct thermal/heat energy relative to its ability to store thermal/heat energy, i.e. a high diffusivity means that heat transfers rapidly through the material)
 - Another way to think of the Prandtl number is that its a ratio of the velocity boundary layer to the thermal boundary layer => or in other words, it assesses the relation between momentum transport and thermal transport capacity of a fluid
 - With increasing viscosity, momentum transport dominates over heat transport
 - The mode of heat transfer in the velocity boundary layer is predominantly convection
 - The mode of heat transfer in the thermal boundary layer is predominantly conduction
 - A high Prandtl number means that heat transfer is more favorable to occur by fluid momentum than by thermal diffusion => heat transfer is favored to occur by fluid momentum/convection than by fluid conduction
 - When examining various correlations for Nusselt number, heat transfer coefficient increases with an increase in Prandtl number and the thermal boundary layer thickness is reduced
 - Sherwood Number (Nusselt number for mass transport)
 - Grashof Number (pertains to natural convection)
 - Rayleigh Number (pertains to natural convection)

- Vehicle Pad CFD Flow/Pressure Drop Analysis
 - Normal Heatsink Model

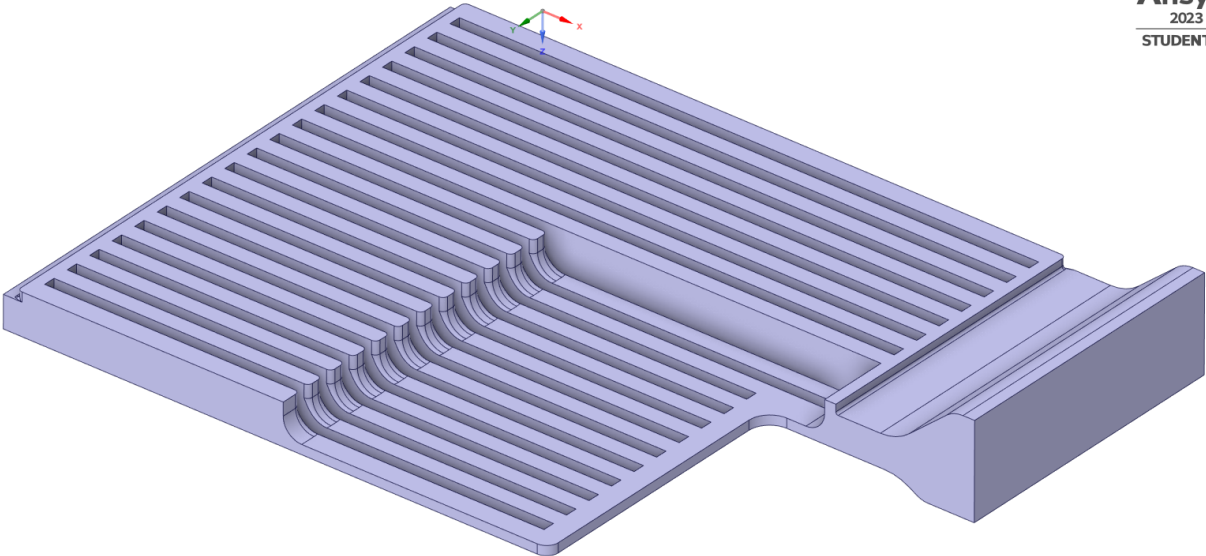


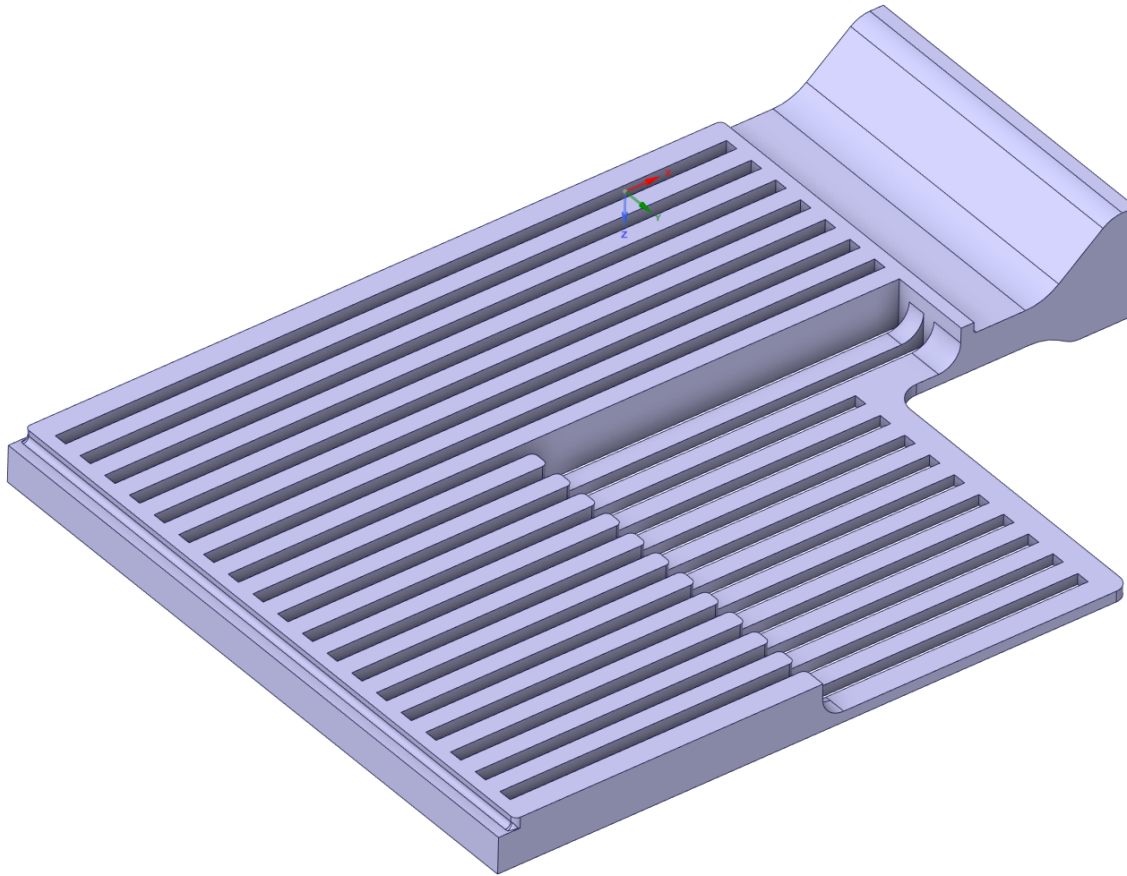
- De-featured heatsink Model



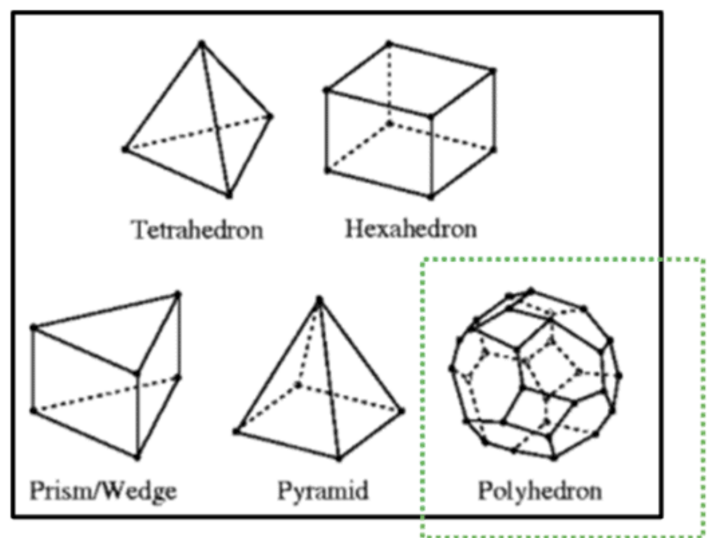


- Fluid Volume Extract





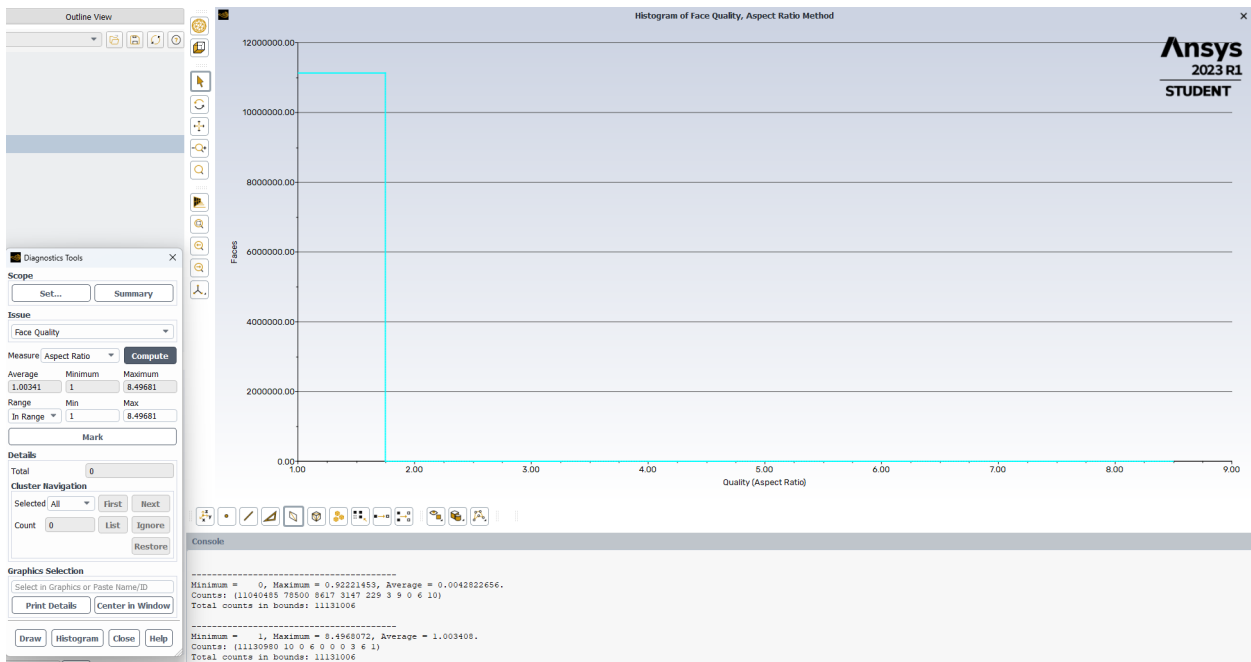
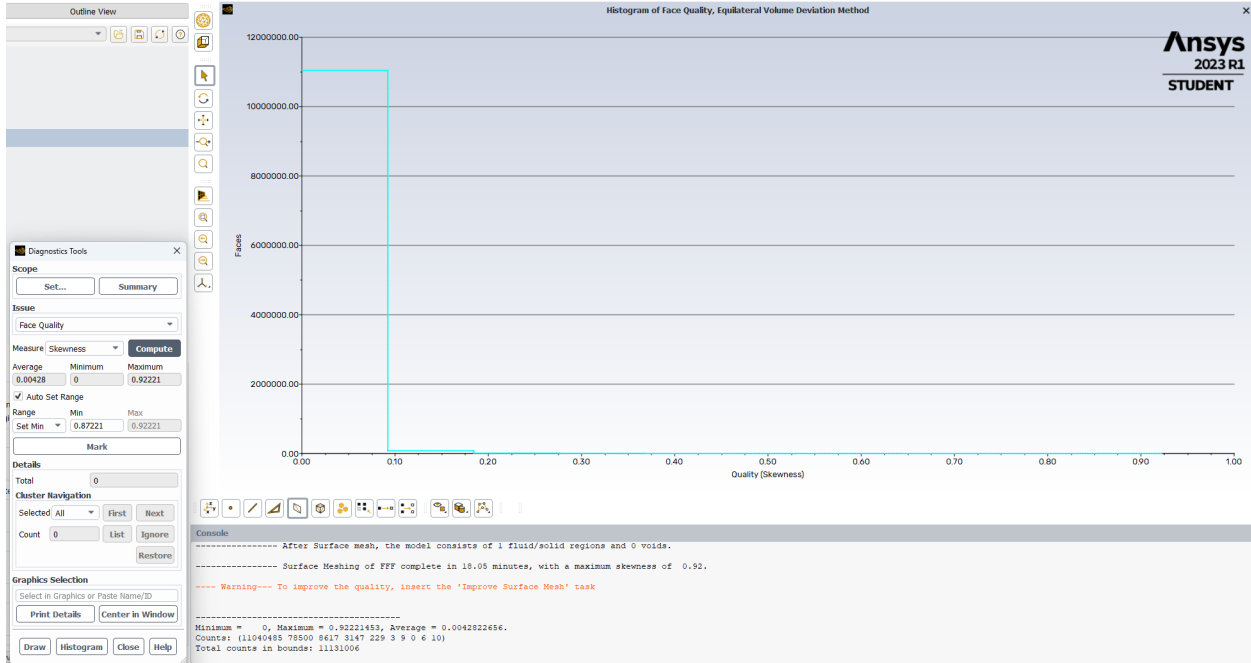
- Mesh Workflow
 - Import defeatured CAD => surface mesh => generate fluid medium regions => volume mesh => solution mode
 - Note: Fluent Meshing vs Ansys Meshing



○ Figure 3: 3D Element Types, Polyhedrons are Only Available in Fluent Meshing

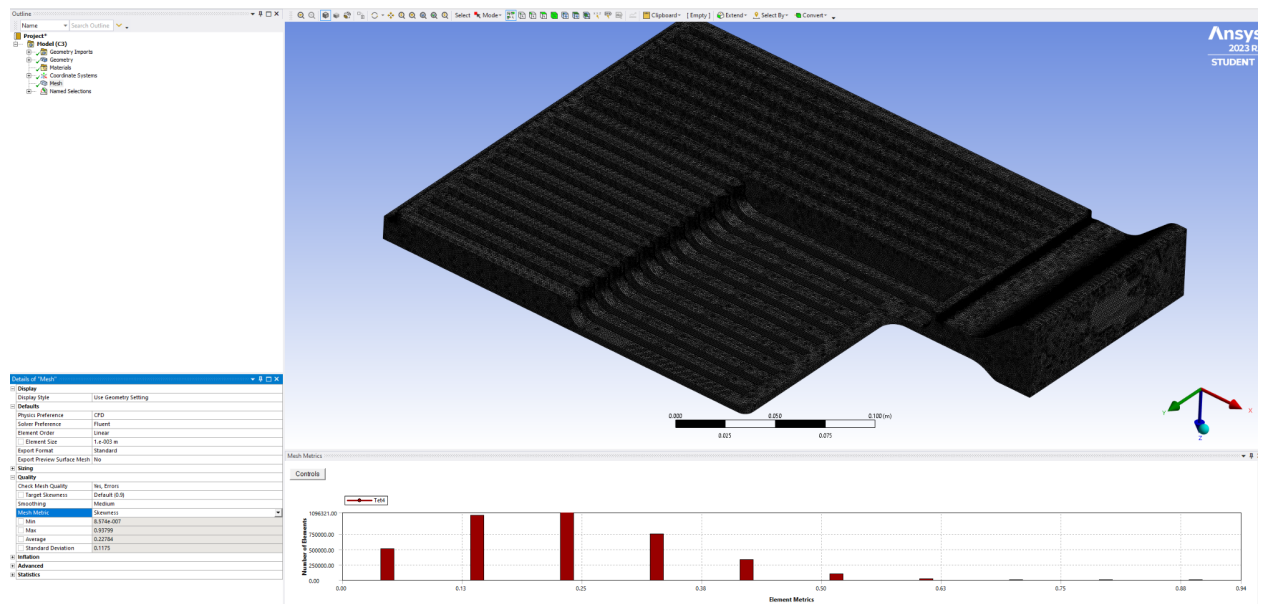
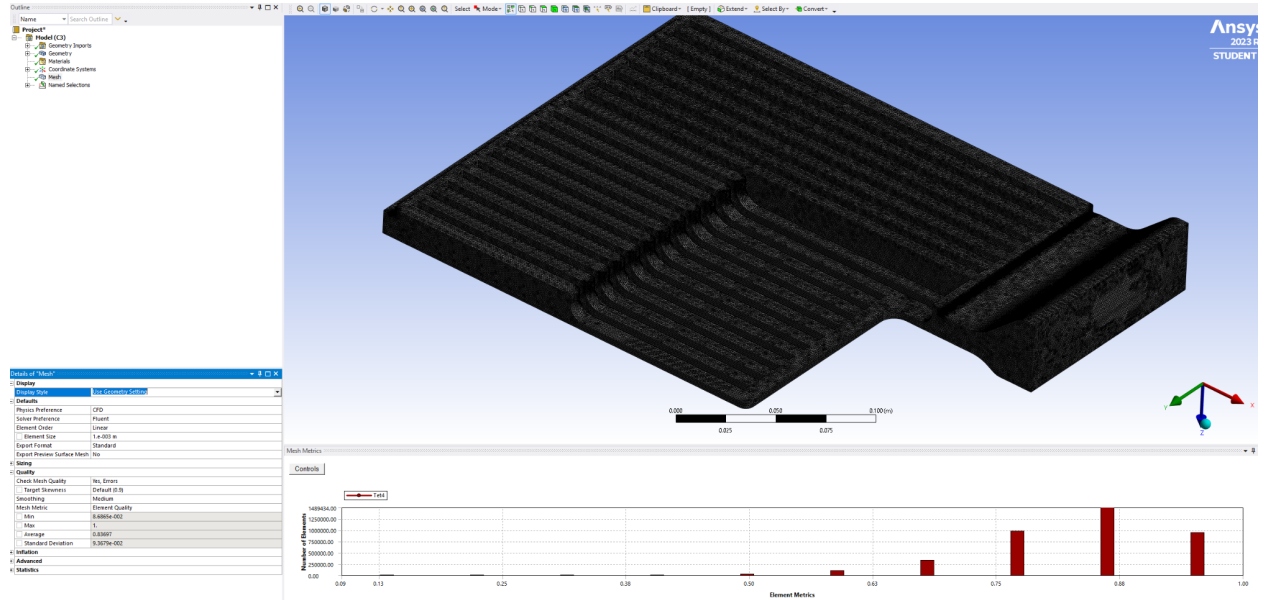
- Cell types/ Methods:

- Fluent Meshing's Mosaic-Enabled Parallel Poly-Hex Core Meshing combines high geometry fidelity, cell quality and fast solve time.
- Ansys Meshing Sweep and Multi zone meshing enable users to create structured (primarily) hex meshes with intuitive control and flexibility.
- Workflows
 - Fluent Meshing's task-based workflows are easy to use and tailored to the most common CFD applications.
 - Ansys Meshing provides a flexible environment allowing users to leverage smart physics-based global controls while also providing detailed local mesh control.
- Usability Features
 - Fluent meshing offers the ability to create custom workflows that can include journal files, local sizing and automatic mesh improvement tasks.
 - Ansys meshing worksheets enable mesh operation recording and name selection definition based on size, location, or topology for mesh control
- Mesh Parameters & Setup
 - Local Sizing
 - Face Sizing
 - 0.0003 m
 - Surface Mesh
 - Min Size
 - 0.0003 m
 - Max Size
 - 0.005 m
 - Growth Rate
 - 1.2
 - Size Functions
 - Curvature & Proximity
 - Curvature Normal Angle
 - 18
 - Mesh Quality
 - Skewness

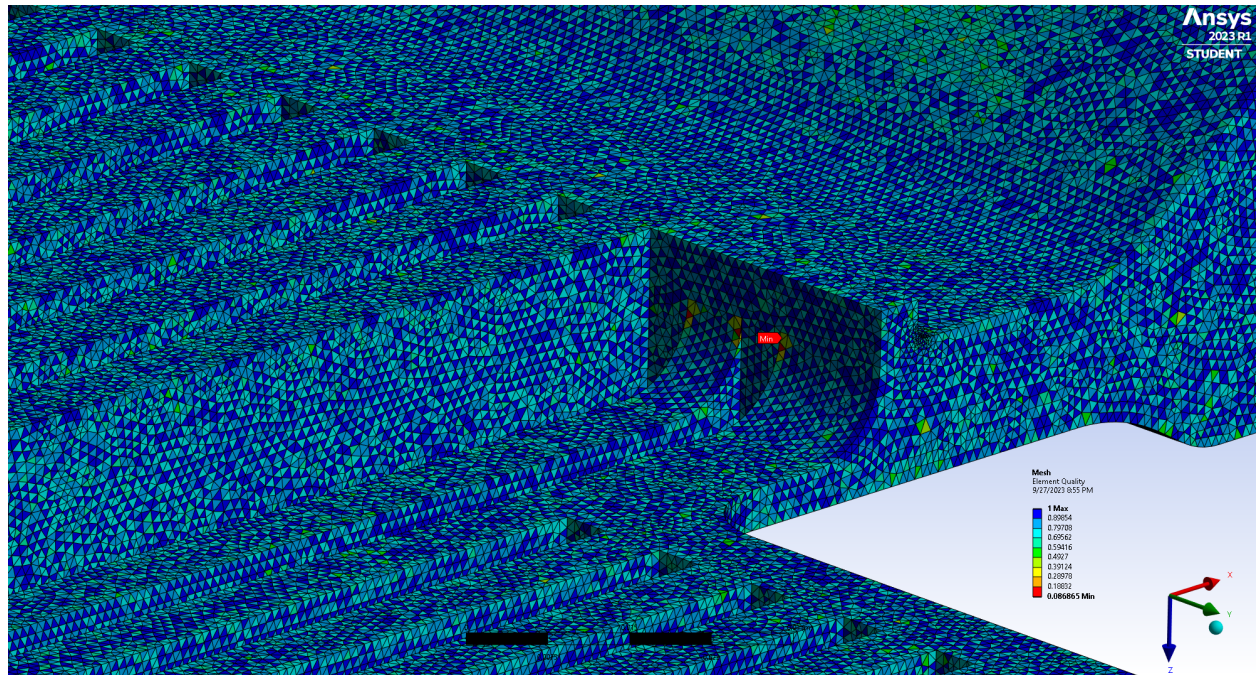
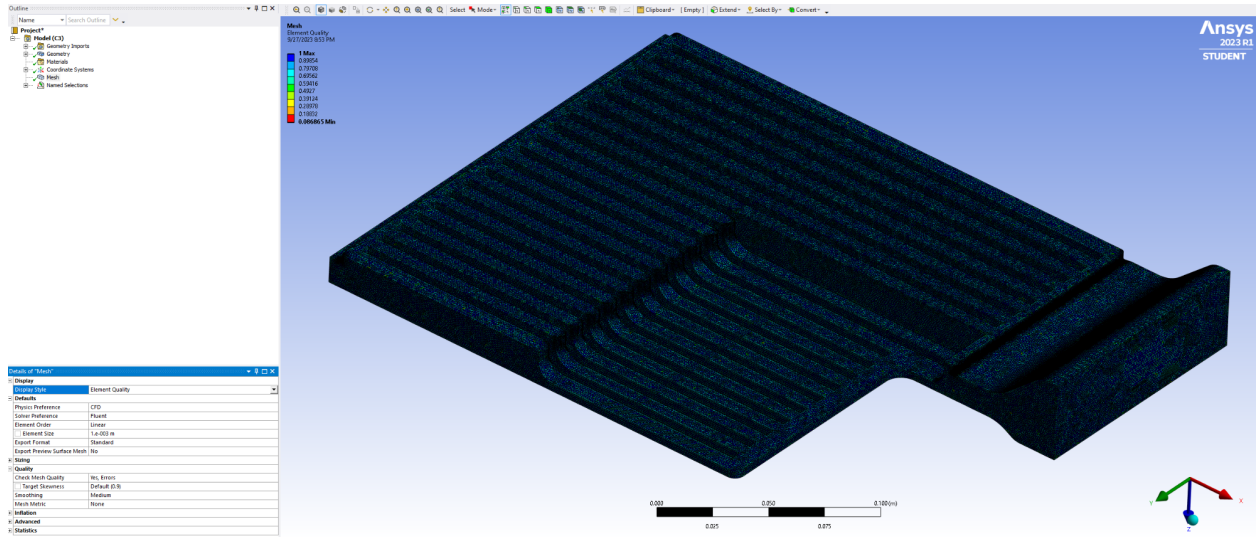


- Ansys Meshing
 - Mesh Settings
 - Mesh Quality
 - 0.001 m Element Size

ME102B Group 5: Brad Ling, Shane Lee, David Kurniawan, Isak Knox, David Kurniawan

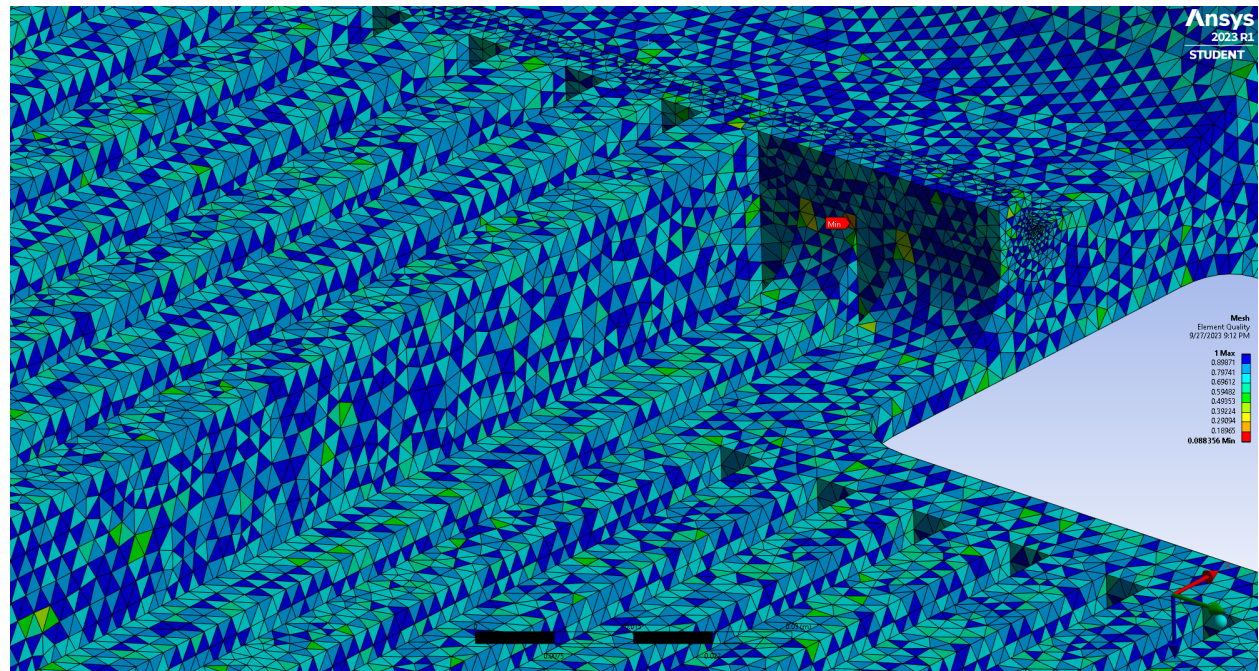
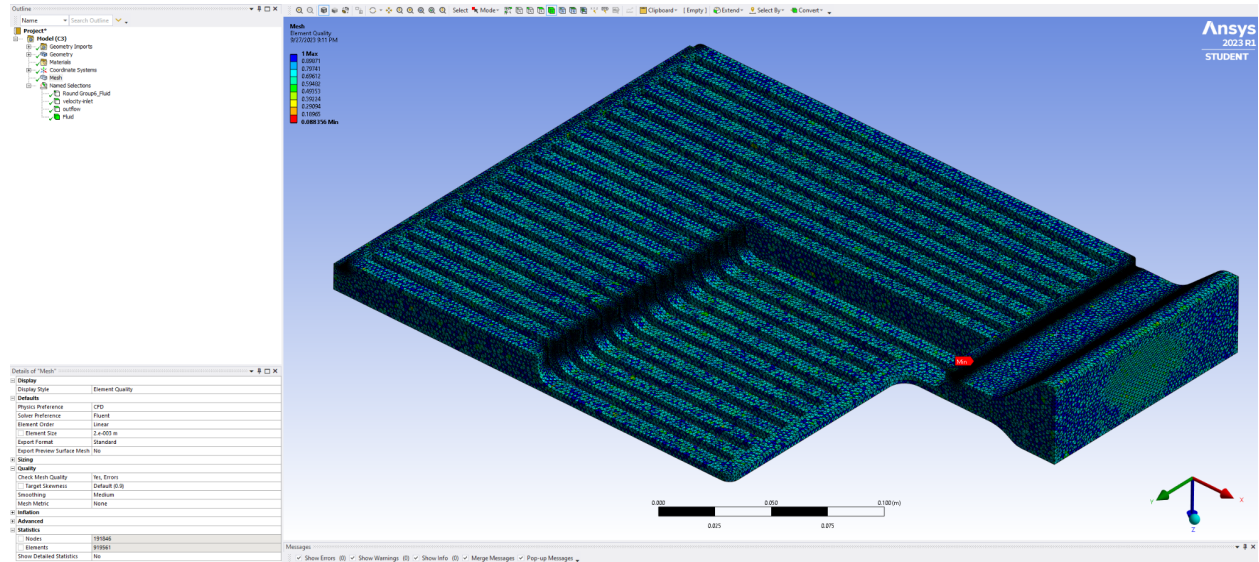


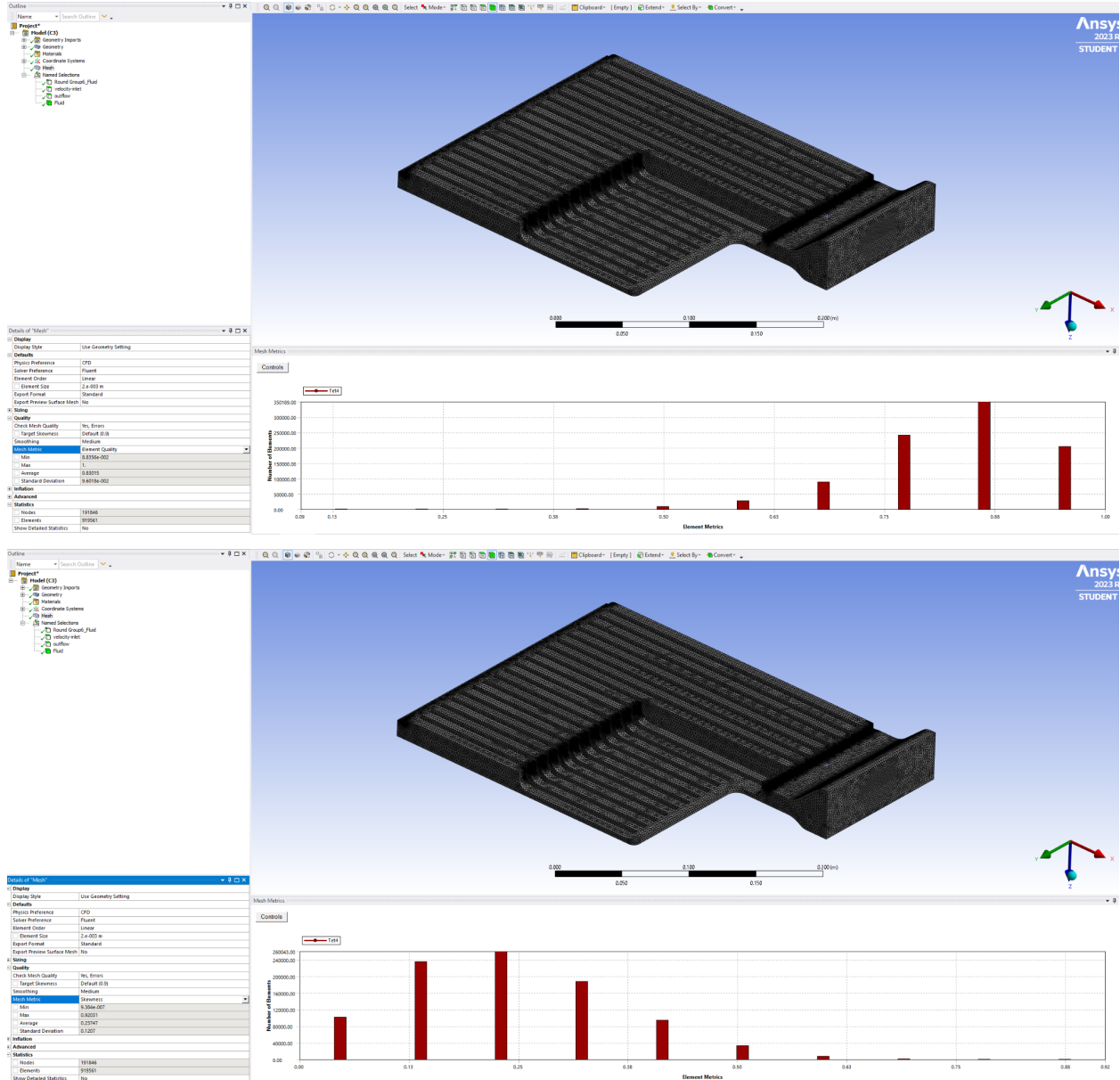
ME102B Group 5: Brad Ling, Shane Lee, David Kurniawan, Isak Knox, David Kurniawan



■ 0.002 Element Size

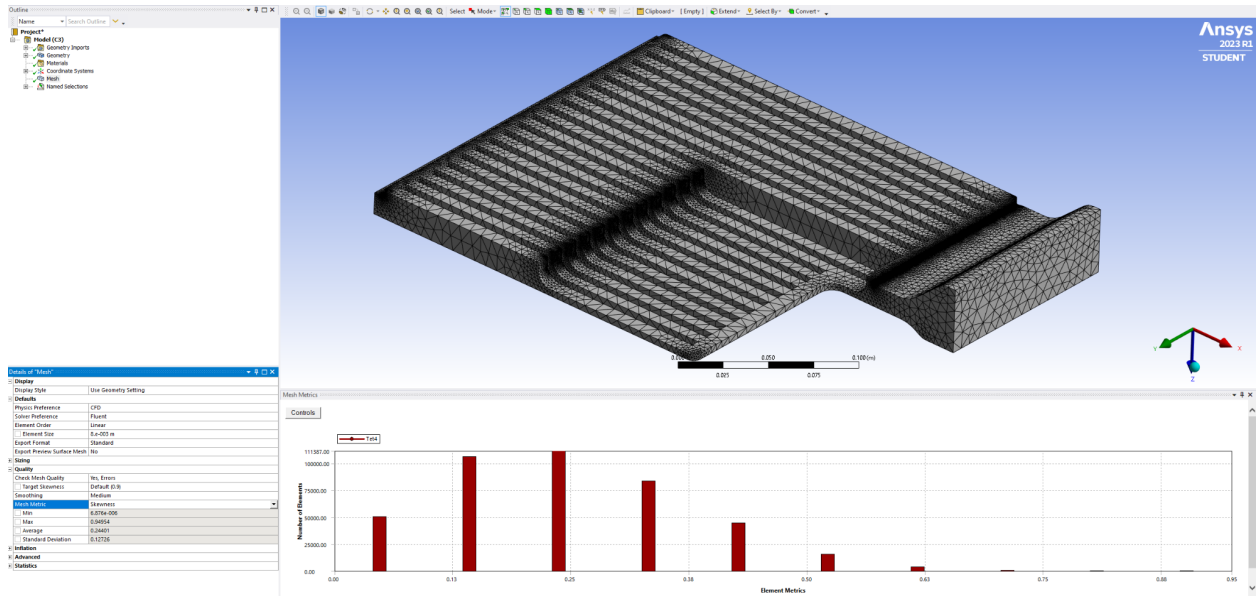
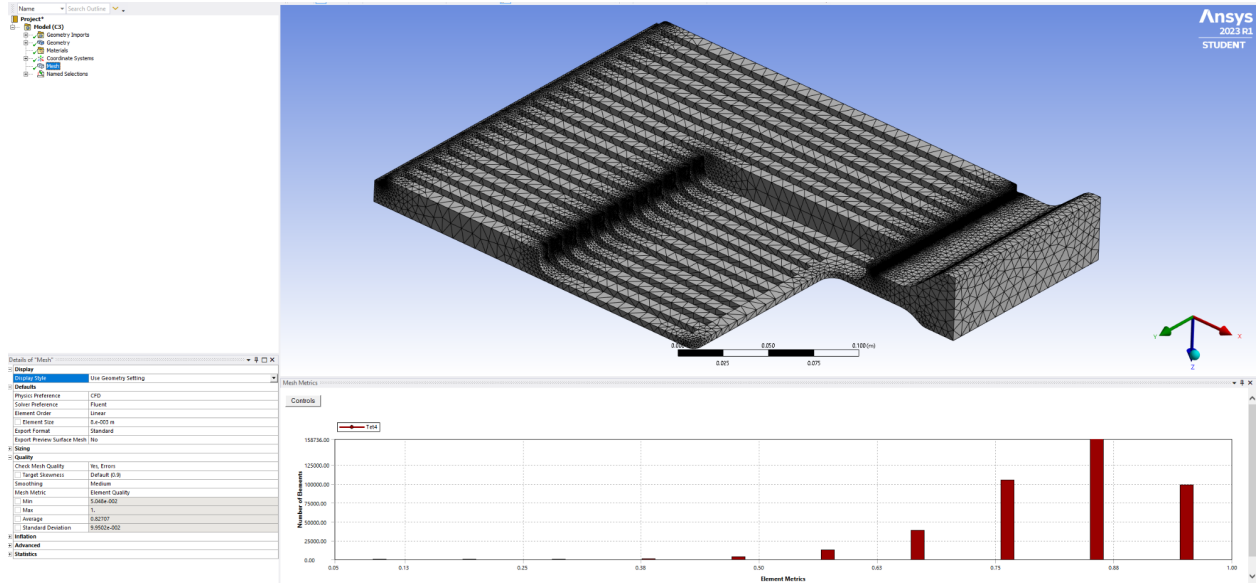
ME102B Group 5: Brad Ling, Shane Lee, David Kurniawan, Isak Knox, David Kurniawan

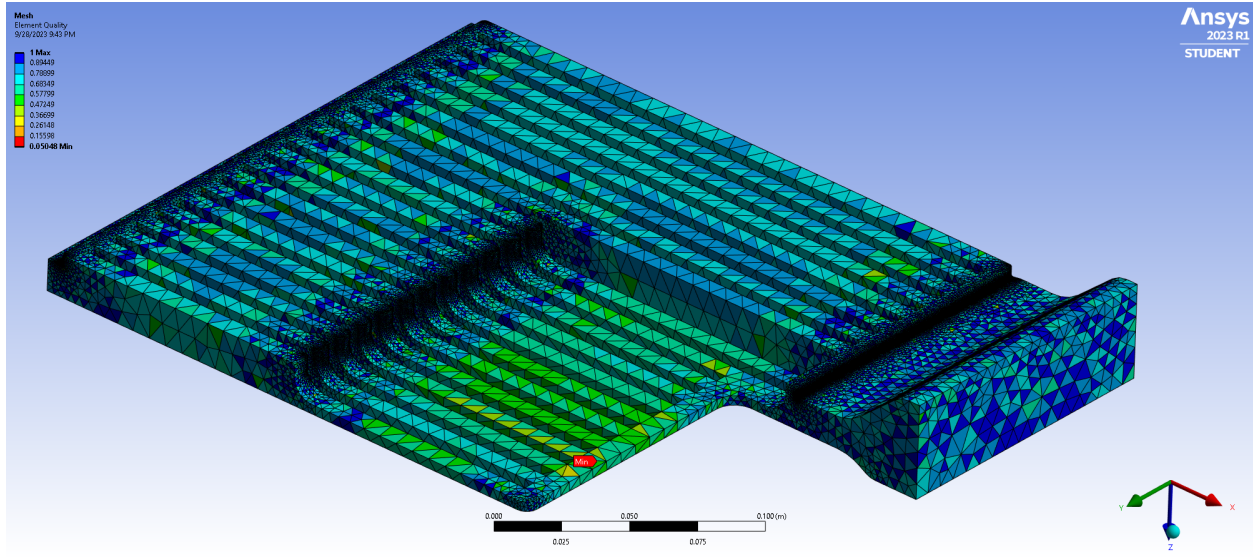




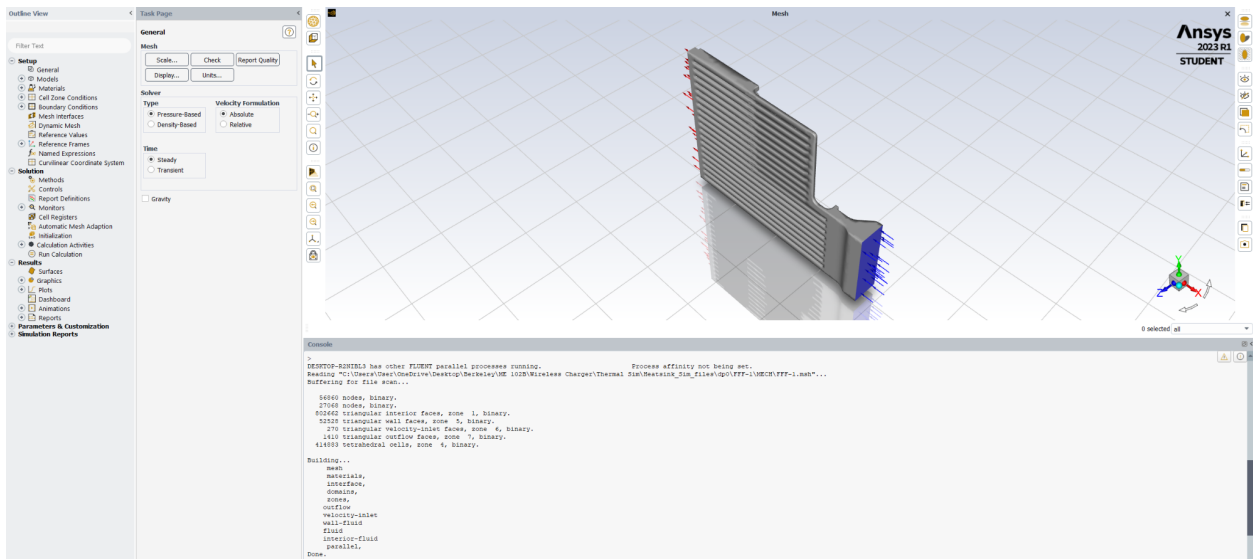
- Note: Difficult to lower number of cells for Ansys mesh (Fluent mesh uses cells while Ansys uses elements/nodes => doubled mesh size and still didn't go below student license limit)
 - 0.008 Element Size

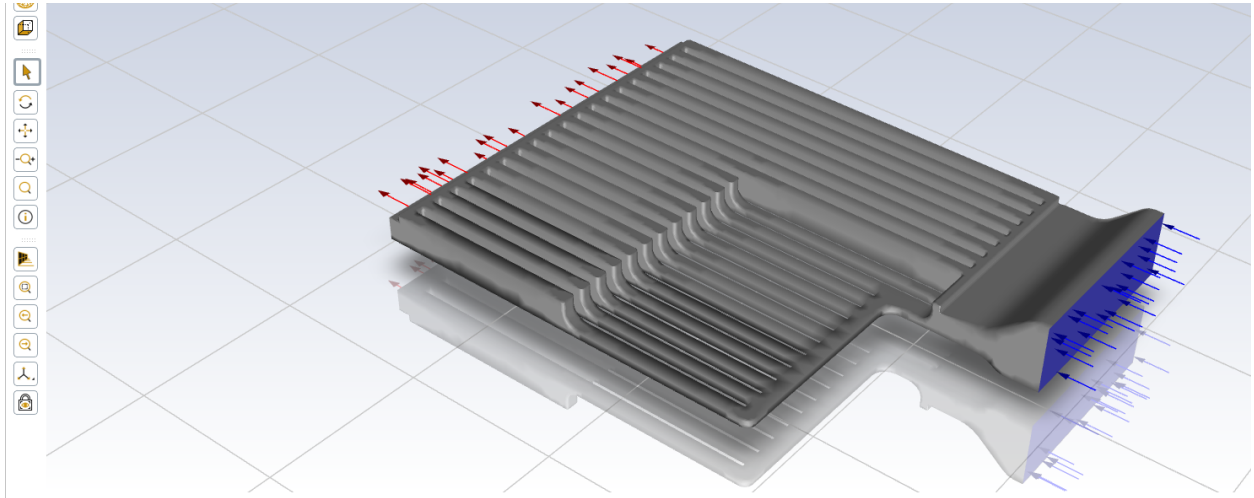
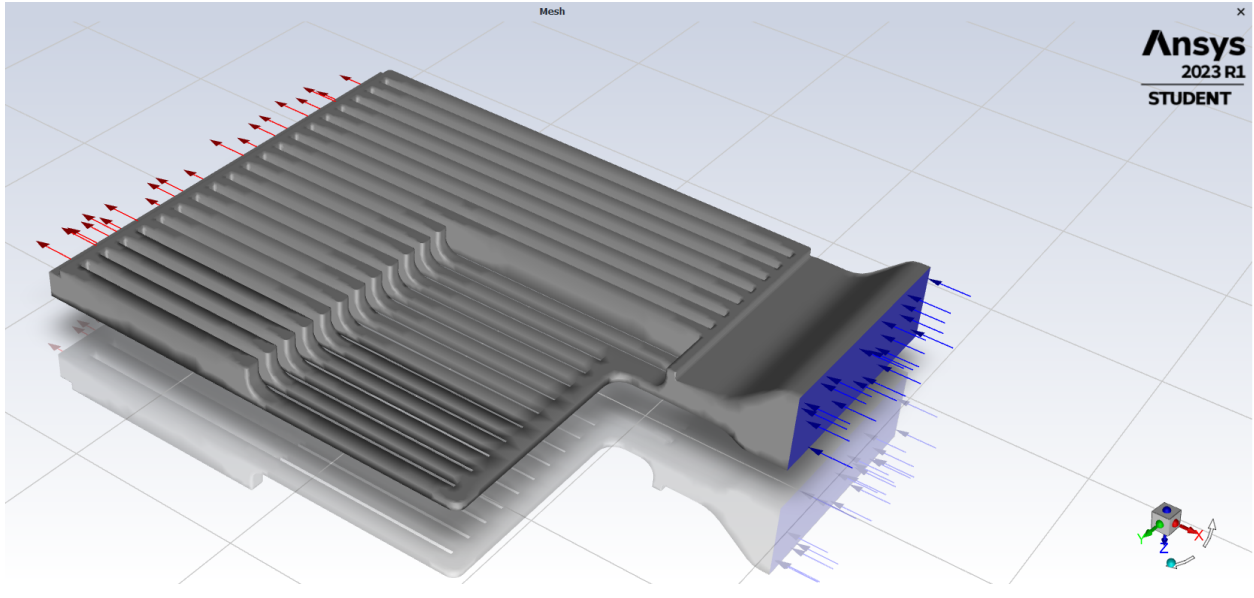
ME102B Group 5: Brad Ling, Shane Lee, David Kurniawan, Isak Knox, David Kurniawan





- 0.008 element size was successful in reducing cell count under 512000 limit for student license
 - 414883 tetrahedral cells
- Named Selections
 - Velocity Inlet
 - Pressure Outlet vs Outflow
- Setting up Mesh Domain in Fluent (Mesh Check & Mesh Quality Evaluation)





```
Console
interior-fluid
parallel,
Done.

Preparing mesh for display...
Done.

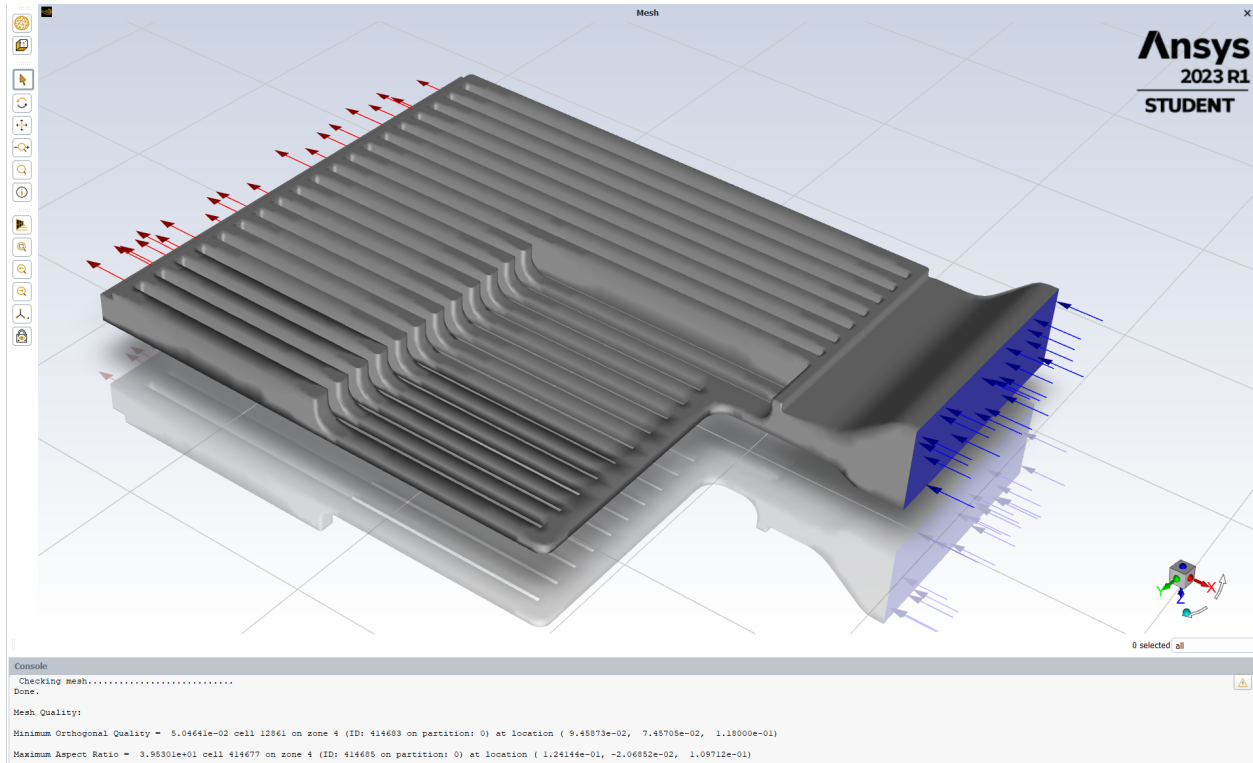
Writing Settings file "C:\Users\User\OneDrive\Desktop\Berkeley\ME 102B\Wireless Charger\Thermal Sim\Heatsink_Sim_files\dp0\FFF-1\Fluent\FFF-1.set"...
writing ip variables ... Done.
writing domain variables ... Done.
writing fluid (type fluid) (mixture) ... Done.
writing interior-fluid (type interior) (mixture) ... Done.
writing wall-fluid (type wall) (mixture) ... Done.
writing velocity-inlet (type velocity-inlet) (mixture) ... Done.
writing outflow (type outflow) (mixture) ... Done.
writing zones map name-id ... Done.

Domain Extents:
x-coordinate: min (m) = -1.350873e-01, max (m) = 1.885873e-01
y-coordinate: min (m) = -1.190873e-01, max (m) = 1.190873e-01
z-coordinate: min (m) = 8.600000e-02, max (m) = 1.260000e-01

Volume statistics:
minimum volume (m3): 4.696468e-14
maximum volume (m3): 1.234989e-07
total volume (m3): 6.810050e-04

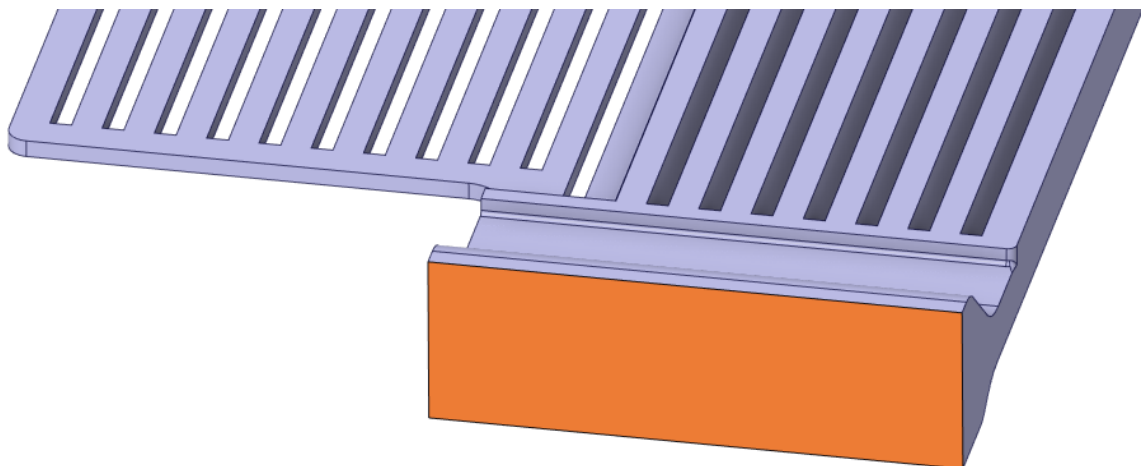
Face area statistics:
minimum face area (m2): 2.061719e-09
maximum face area (m2): 5.501891e-05

Checking mesh.....
Done.
```



- Models
- Material Properties
- Boundary Conditions
 - Velocity Inlet

■ Cross-Sectional Area

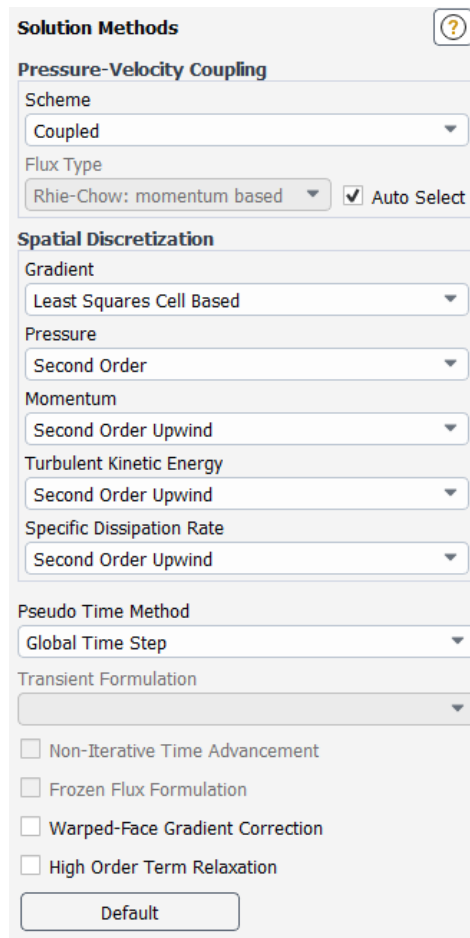


Area	4903.491mm ²
Perimeter	325.1746mm

■ Momentum Boundary Conditions

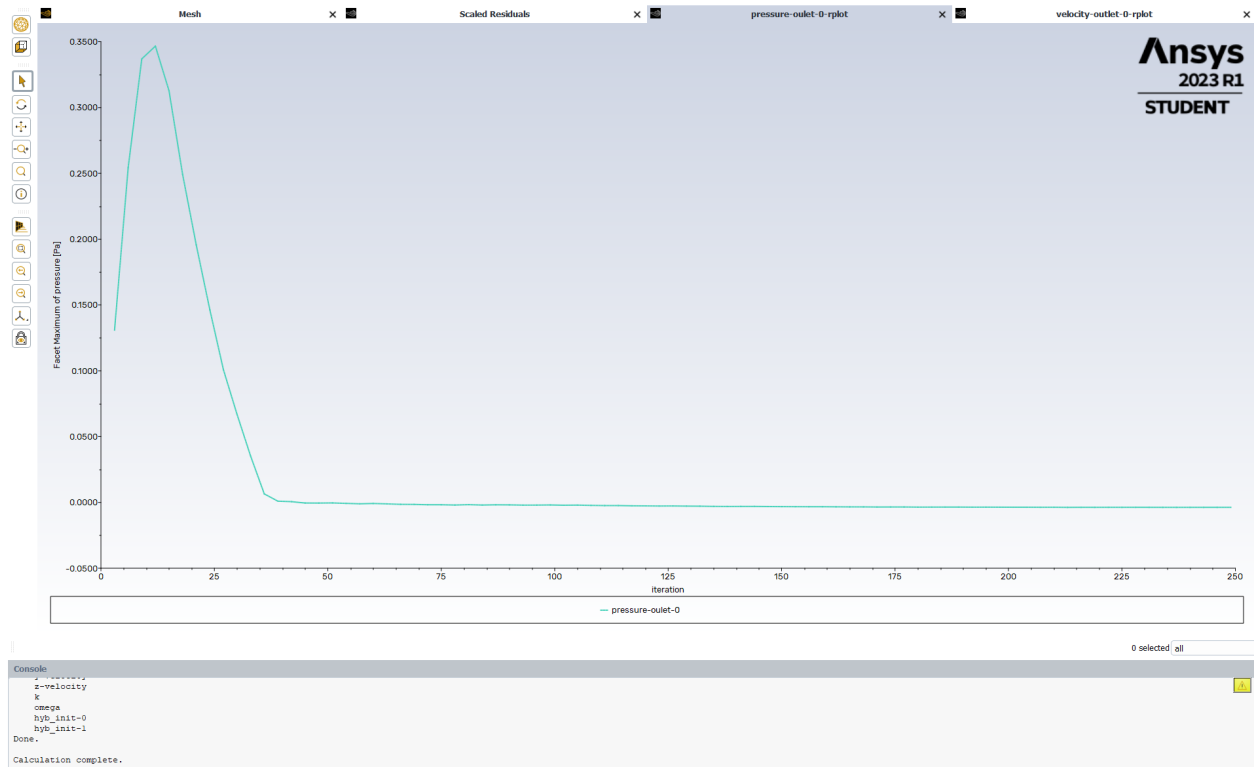
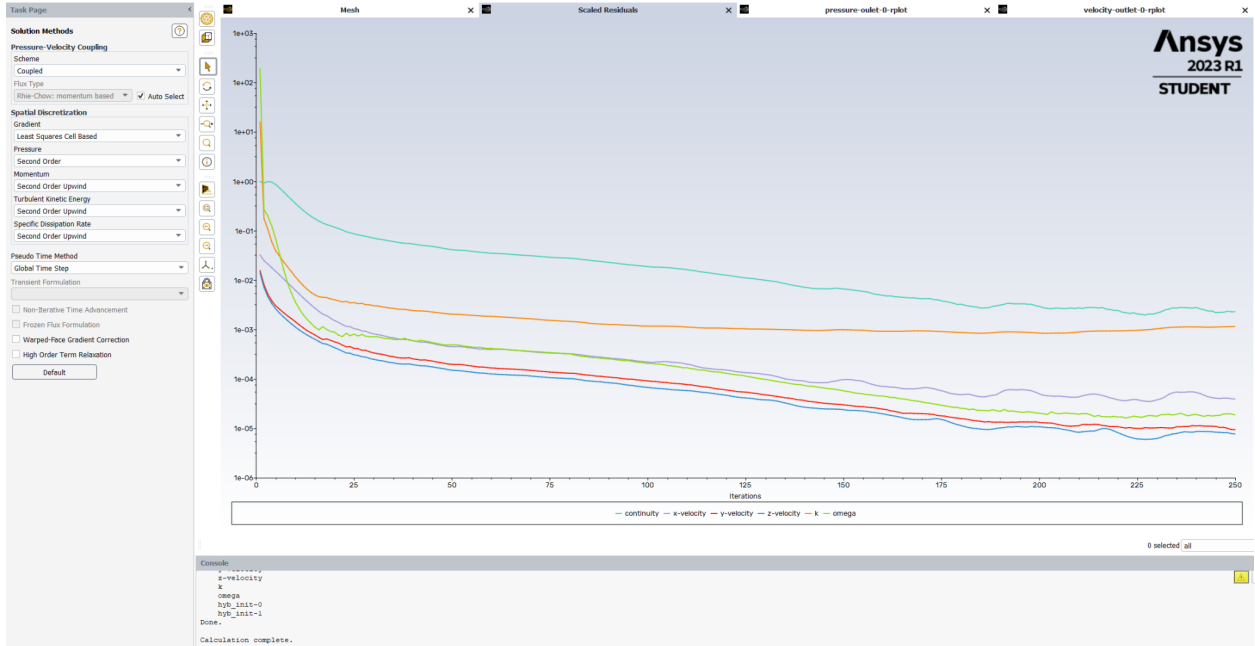
- 1 cfm => 0.000472 m³/s => (Q = Av => v = Q/A)
 - Area: 4903.491 mm² => 0.004903 m²

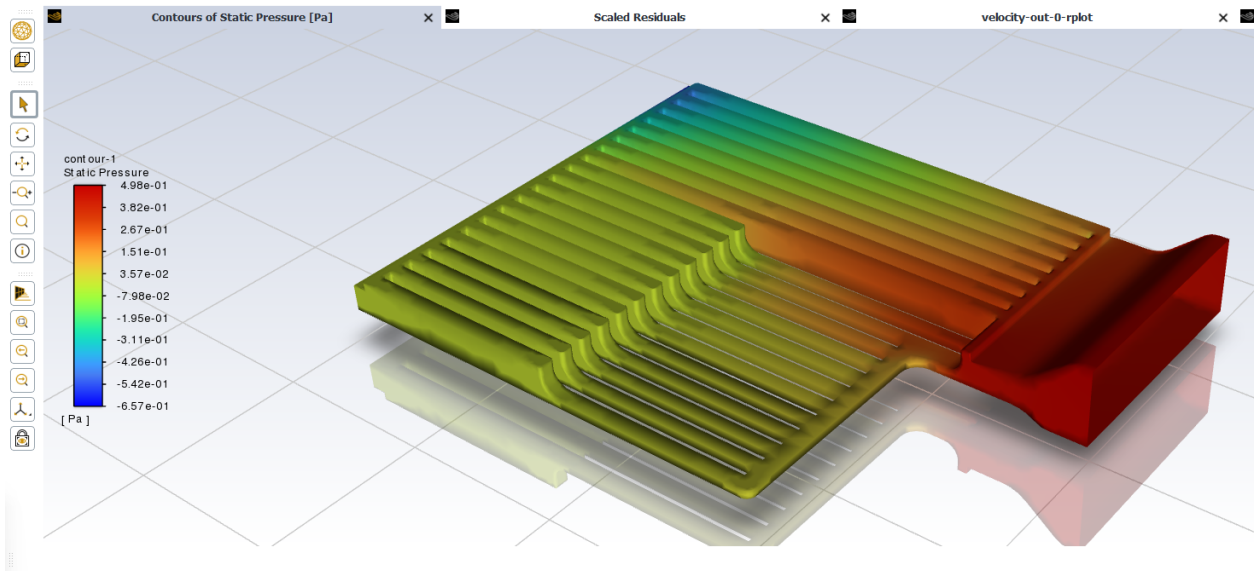
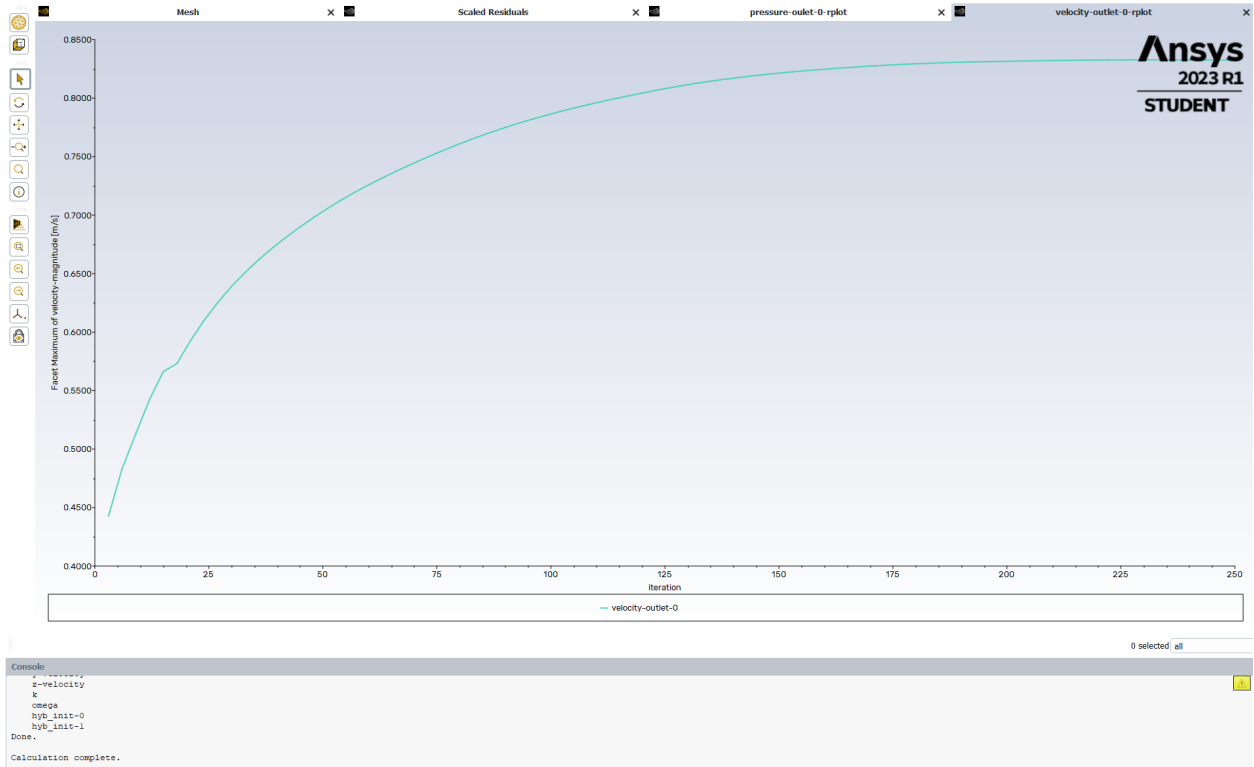
- Inlet Velocity Magnitude $v = 0.09627$ m/s
- Magnitude, Normal to Boundary
- Turbulence Specification Method: Intensity and Hydraulic Diameter
 - Turbulent Intensity: 5%
 - Hydraulic Diameter: $D_h = 4A_c/P_w$
 - $A_c = 0.004903 \text{ m}^2$
 - $P_w = 0.3252 \text{ m}$
 - $D_h = 0.0603 \text{ m}$
- Outflow
 - Flow Rate Weighting: 1
- Solution Methods

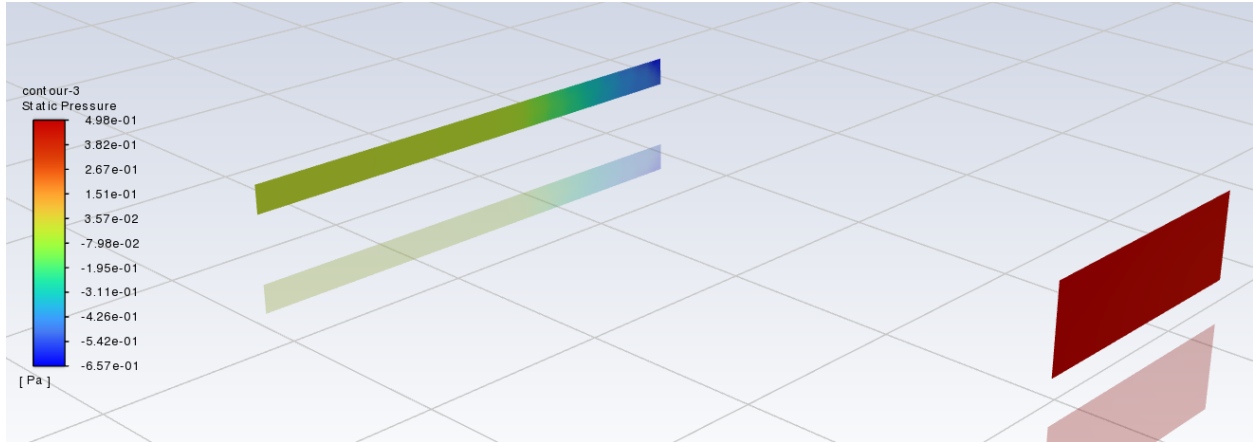


-
- Solution
 - 300 iterations

ME102B Group 5: Brad Ling, Shane Lee, David Kurniawan, Isak Knox, David Kurniawan







- Debugging
 - Reversed Flow
 - Reversed flow can occur when pressure gradients due to geometry mean that the flow wants to re-enter the domain at the location where an outlet/outflow has been specified
 - In the absence of flow separation on outflow boundary walls, reverse flow normally occurs only on a fraction of a pressure outlet boundary determined by the fact that for the neighboring cells near the outflow boundary exchanging momentum, the velocity correction obtained from the interior pressure field and the prescribed outflow pressure is sufficiently negative to cause reverse flow.
 - This means even the dynamic pressure available in these interior cells is not sufficient to allow flow out of the domain.
 - If it is known that this is not in agreement with observed flow one can overcome this only by reducing outlet gauge pressure and not by extending the outflow boundary.
 - If separation has occurred on outflow boundary walls then extension of the computational domain is warranted.
 - It is then logical that in any case the total pressure needs to be corrected for

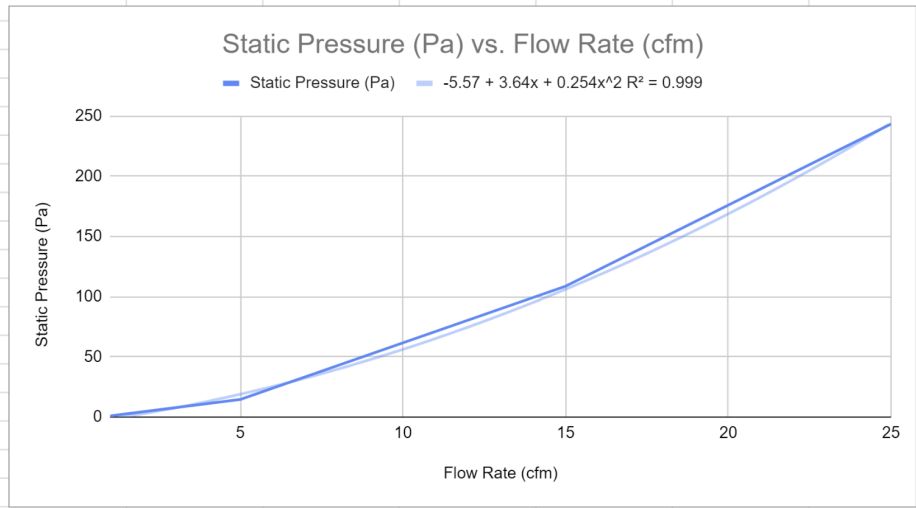
the artificial or numerical head added by the reverse flow

- First we need to understand that even in the simplest pipe flow total pressure as per Bernoulli equation will not remain constant along the pipe since there will be viscous losses in any real flow.
- If you want to get the correct total pressure corresponding to the portion of the flow exiting the domain, a work around is to obtain the averaged velocity components individually on the outflow plane and calculate the dynamic pressure and add this to the averaged static pressure.
- A little care is necessary here since if the outflow plane is normal to the x-axis, the average will have to be taken only for the positive part of the u-component and over the portion of the plane where it is positive.
- Some flow reversal can be tolerated, but will have an effect on mass-conservation and thus convergence
 - Solutions
 - Make mesh thin and long at the outlet to artificially “damp” the reverse flow
 - Move the outlet position further downstream
 - Make a better distribution of mesh sizes and elements leading up to the outlet
 - Grid size refinement
 - Decrease relaxation factor
 - Outlet Boundary Condition
 - Pressure Outlet vs Outflow
 - Boundary Condition Initialization
 - Initial Gauge Pressure
- System Impedance Curve
 - Obtain pressure drops at 5 flow rates => curve fitting/interpolation to obtain system impedance curve

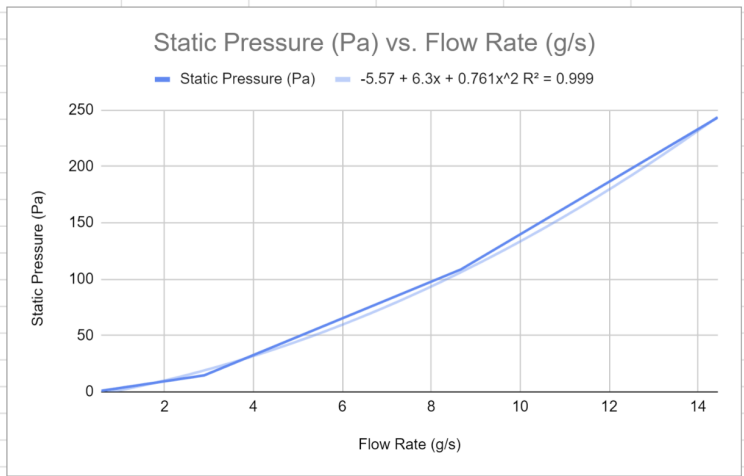
ME102B Group 5: Brad Ling, Shane Lee, David Kurniawan, Isak Knox, David Kurniawan

Ansys Fluent Vehicle Pad Heatsink System Impedance Curve

Flow Rate (cfm)	Static Pressure (Pa)
1	0.924
5	14.61
15	108.7
25	243.5



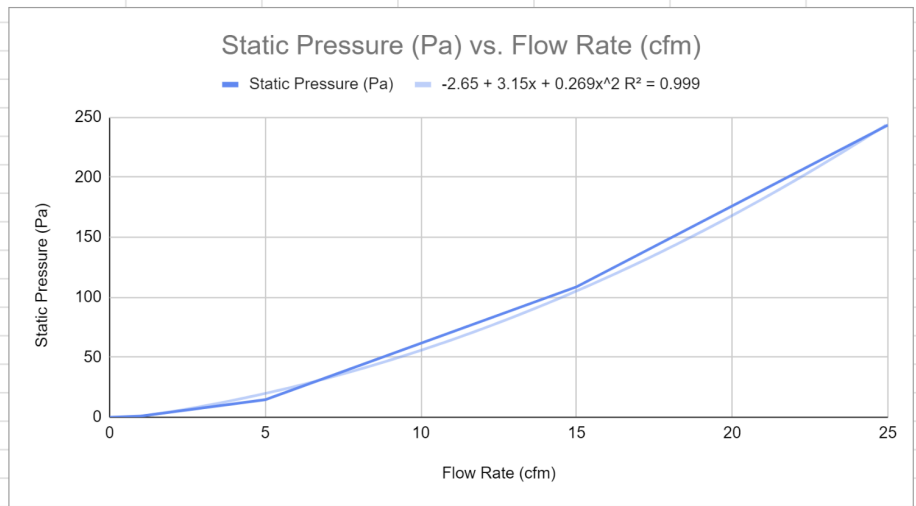
Air Density (kg/m ³)	Flow Rate (g/s)	Static Pressure (Pa)
1.225	0.5777916667	0.924
	2.888958333	14.61
ft ³ to m ³	8.666875	108.7
	14.44479167	243.5
min to s		
	0.01666666667	



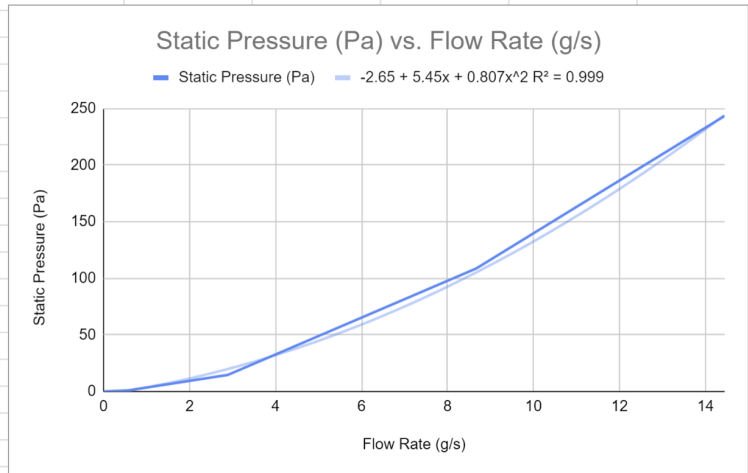
○ (0,0) Origin Added

Ansys Fluent Vehicle Pad Heatsink System Impedance Curve

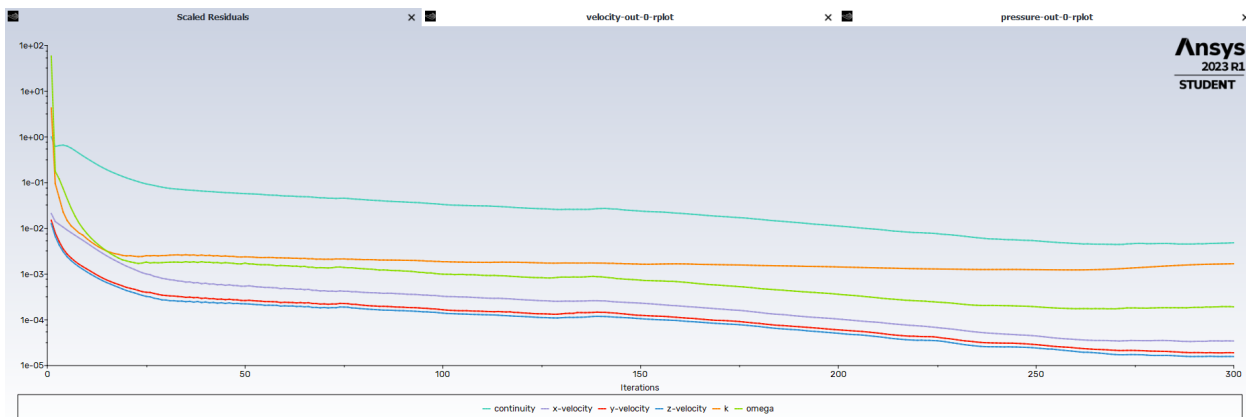
Flow Rate (cfm)	Static Pressure (Pa)
0	0
1	0.924
5	14.61
15	108.7
25	243.5



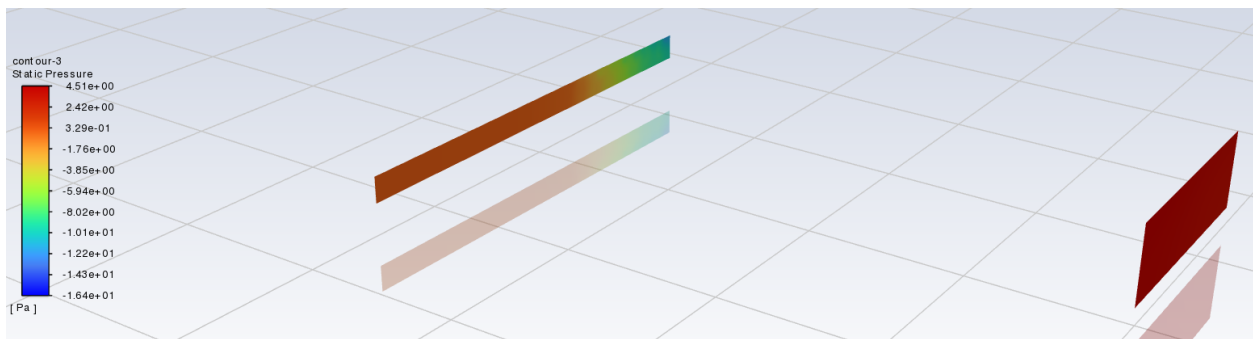
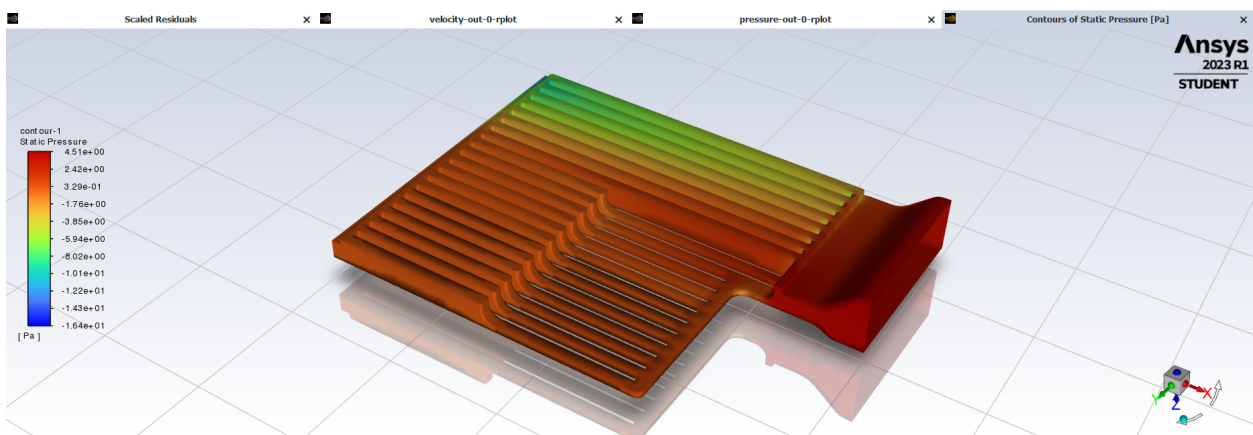
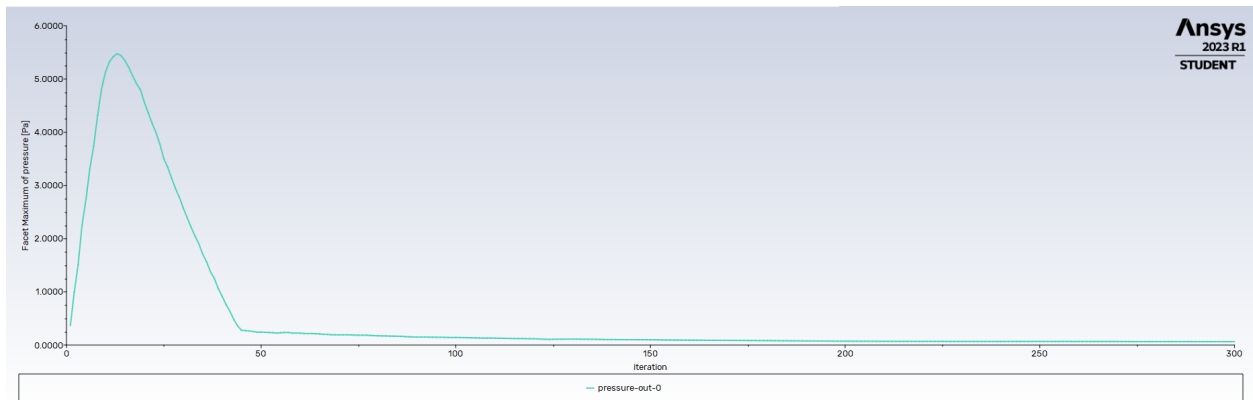
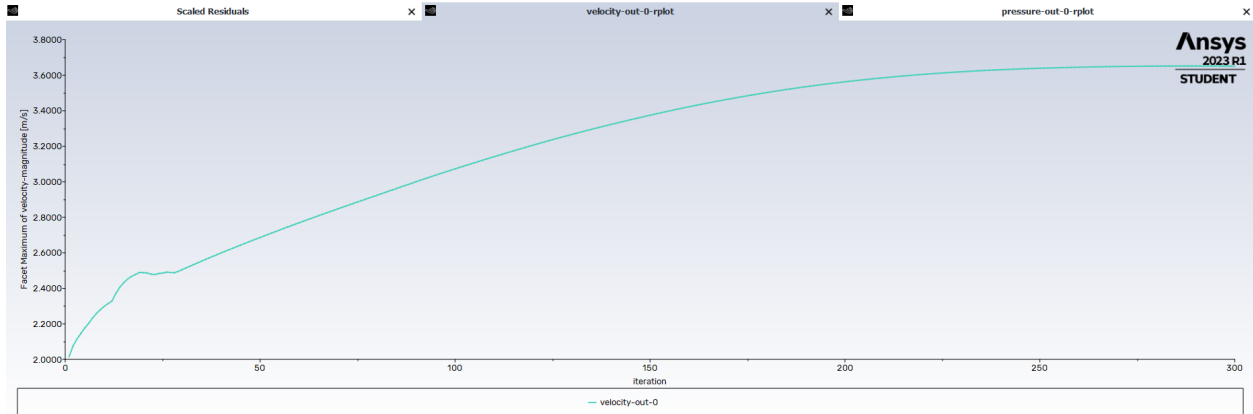
Air Density (kg/m ³)	Flow Rate (g/s)	Static Pressure (Pa)
1.225	0	0
	0.5777916667	0.924
ft ³ to m ³	2.888958333	14.61
0.0283	8.666875	108.7
	14.44479167	243.5
min to s		
0.01666666667		



- System Impedance Curve Accuracy
 - Pressure drop seems to be very high for the vehicle pad heatsink
 - Look into adding slant/draft onto corner section of the heatsink where the PCBA resides to reduce loss coefficient
 - Increase heat sink fin pitch
 - Target Maximum pressure drop for 60 cfm
 - 300 Pa
- Selected flow rates (cfm)
 - 1 cfm
 - 0.000472 m³/s ($Q = Av \Rightarrow v = Q/A$)
 - Area: 4903.491 mm² \Rightarrow 0.004903 m²
 - Inlet Velocity Magnitude $v = 0.09627$ m/s
 - 5 cfm
 - 0.00236 m³/s ($Q = Av \Rightarrow v = Q/A$)
 - Area: 4903.491 mm² \Rightarrow 0.004903 m²
 - Inlet Velocity Magnitude $v = 0.4813$ m/s



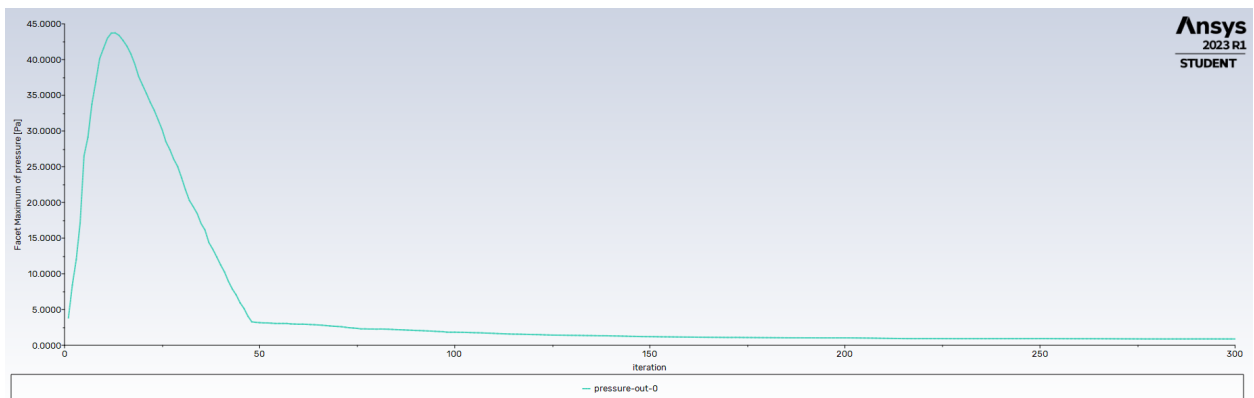
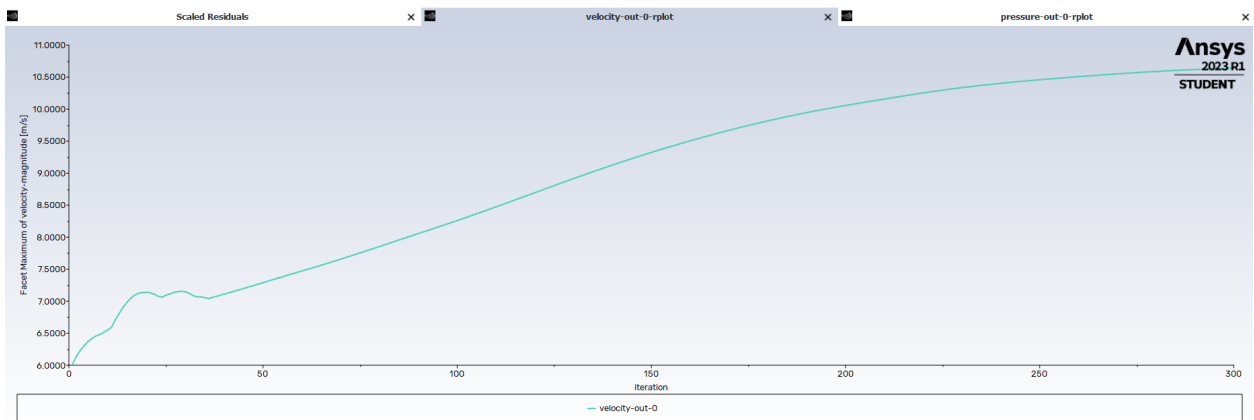
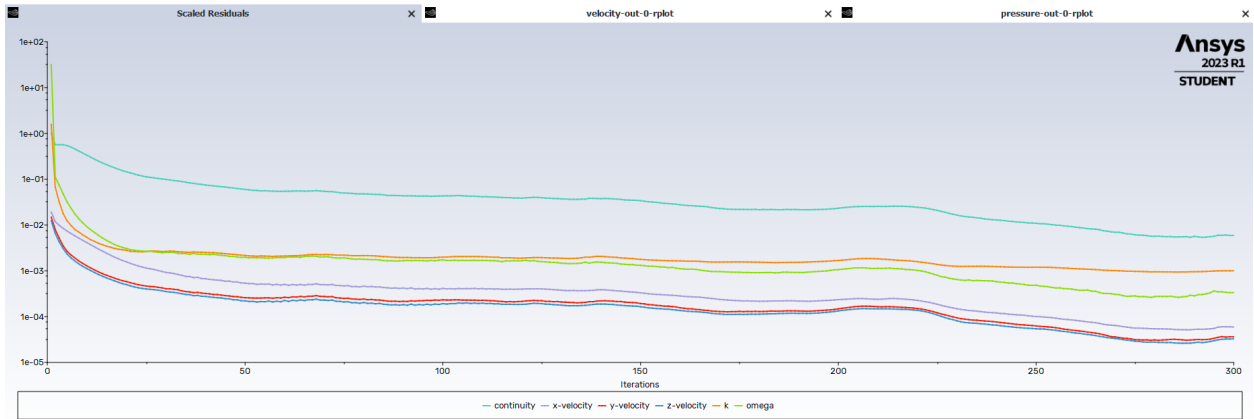
ME102B Group 5: Brad Ling, Shane Lee, David Kurniawan, Isak Knox, David Kurniawan

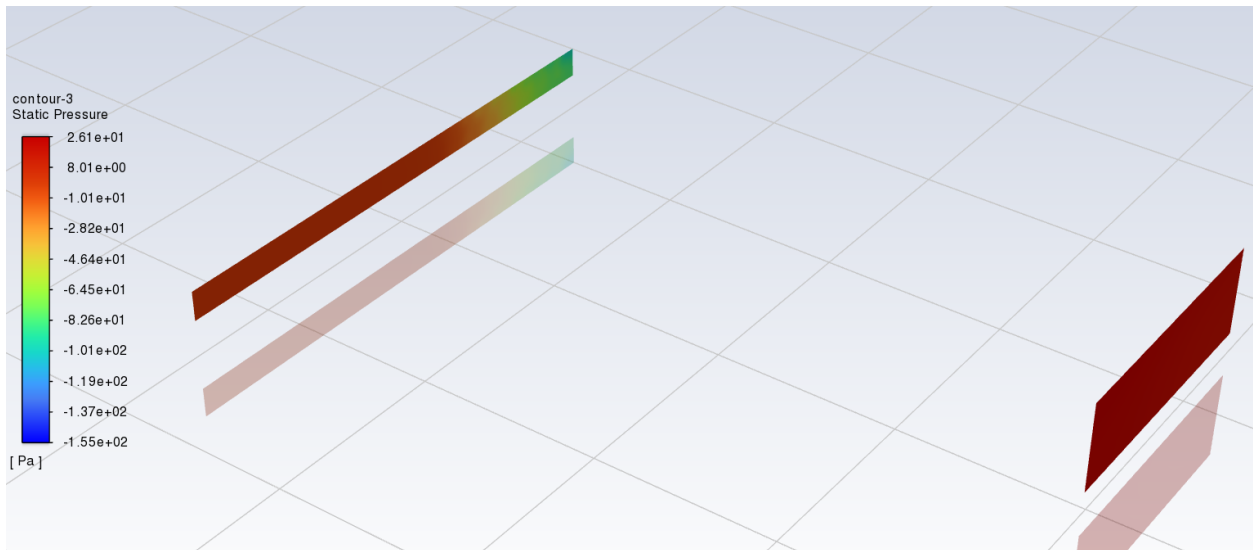
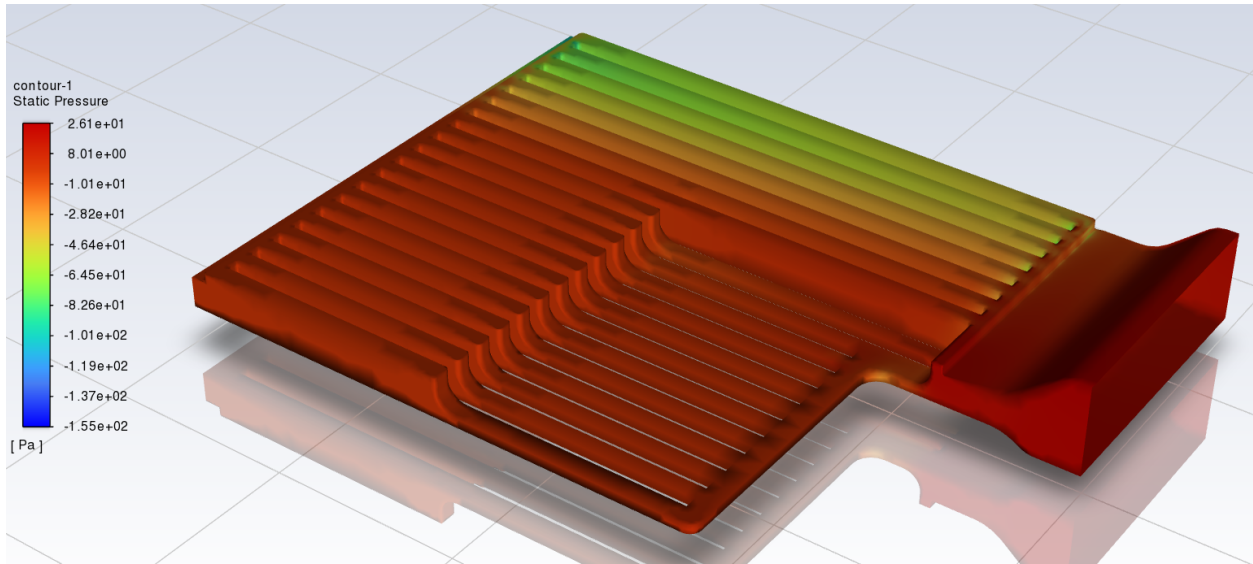


■ 10 cfm

ME102B Group 5: Brad Ling, Shane Lee, David Kurniawan, Isak Knox, David Kurniawan

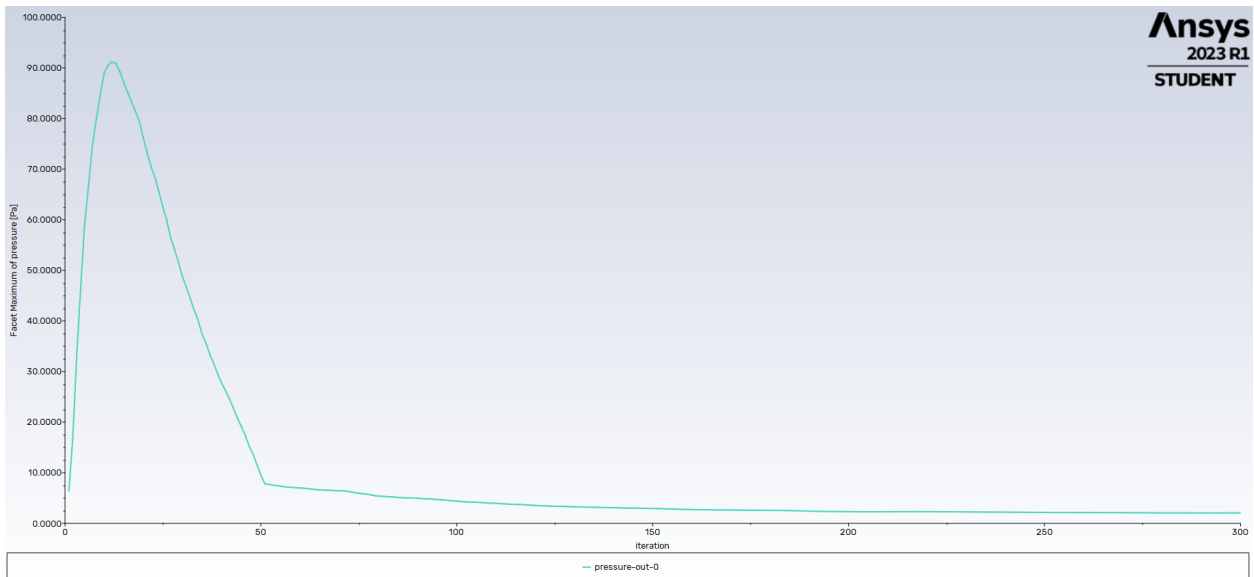
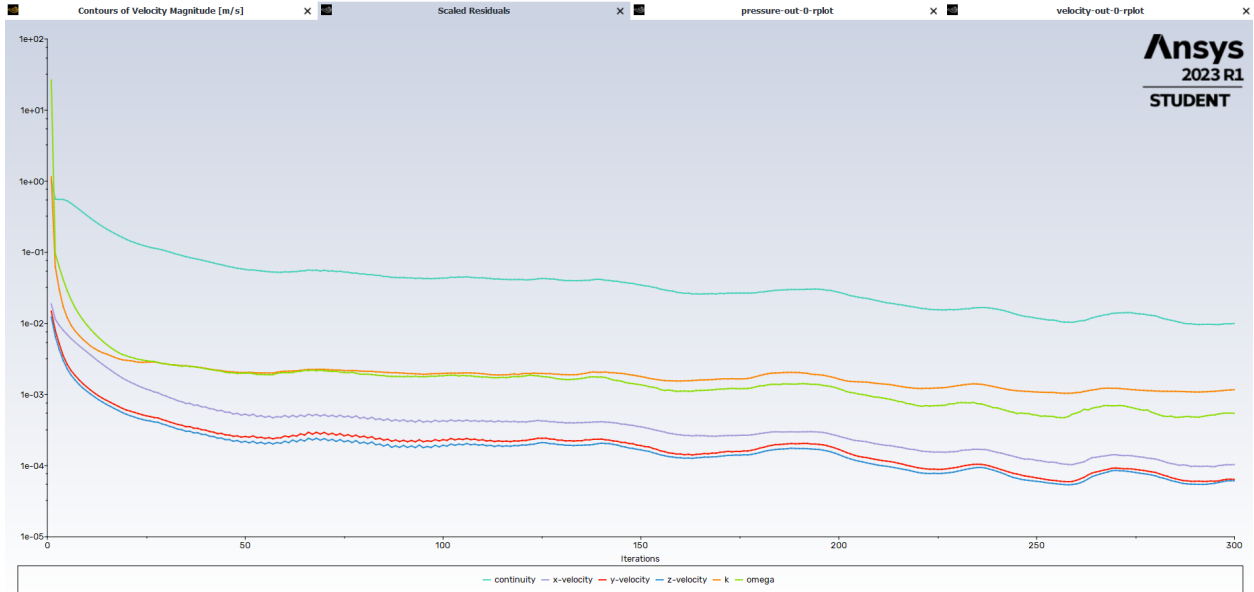
- 0.00472 m³/s
- 15 cfm
 - 0.00708 m³/s ($Q = Av \Rightarrow v = Q/A$)
 - Area: 4903.491 mm² \Rightarrow 0.004903 m²
 - Inlet Velocity Magnitude $v = 1.444$ m/s

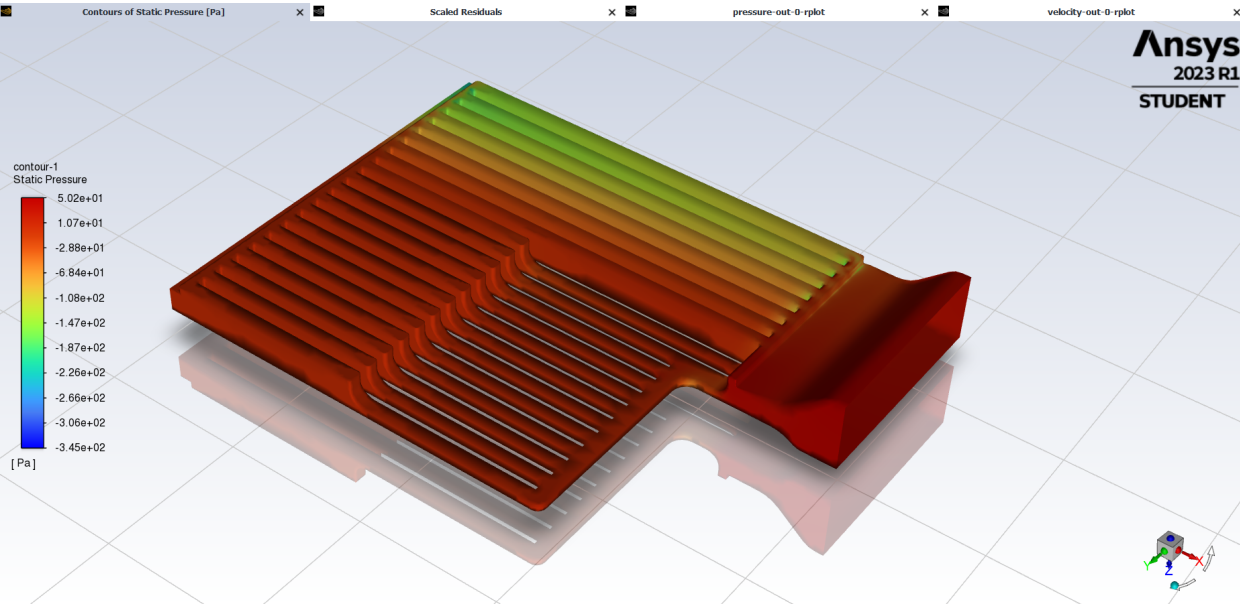
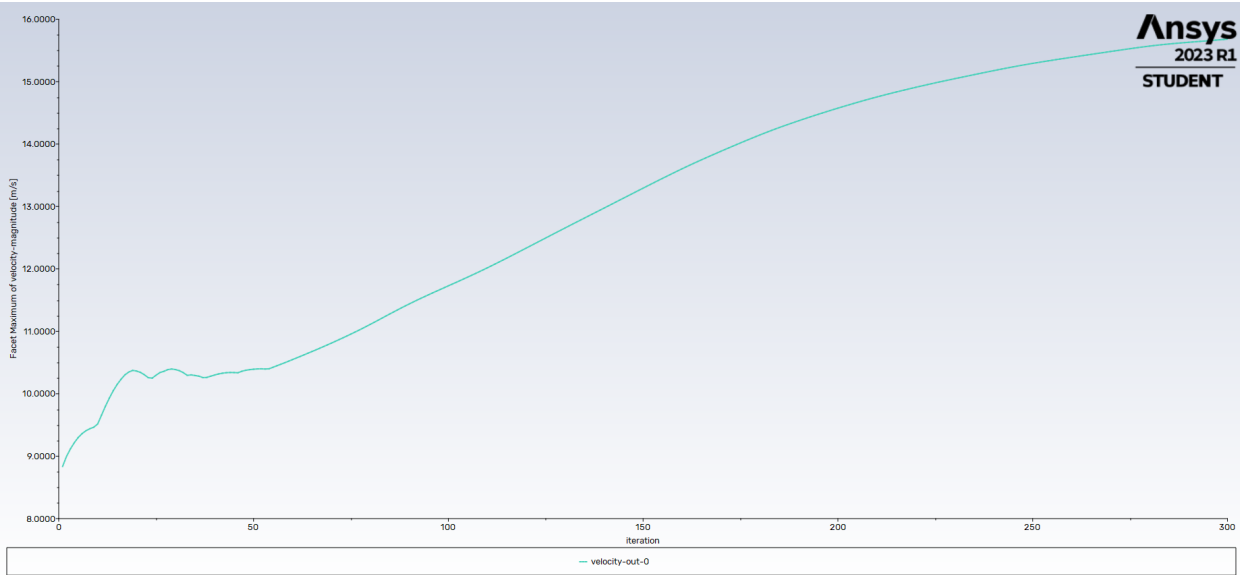


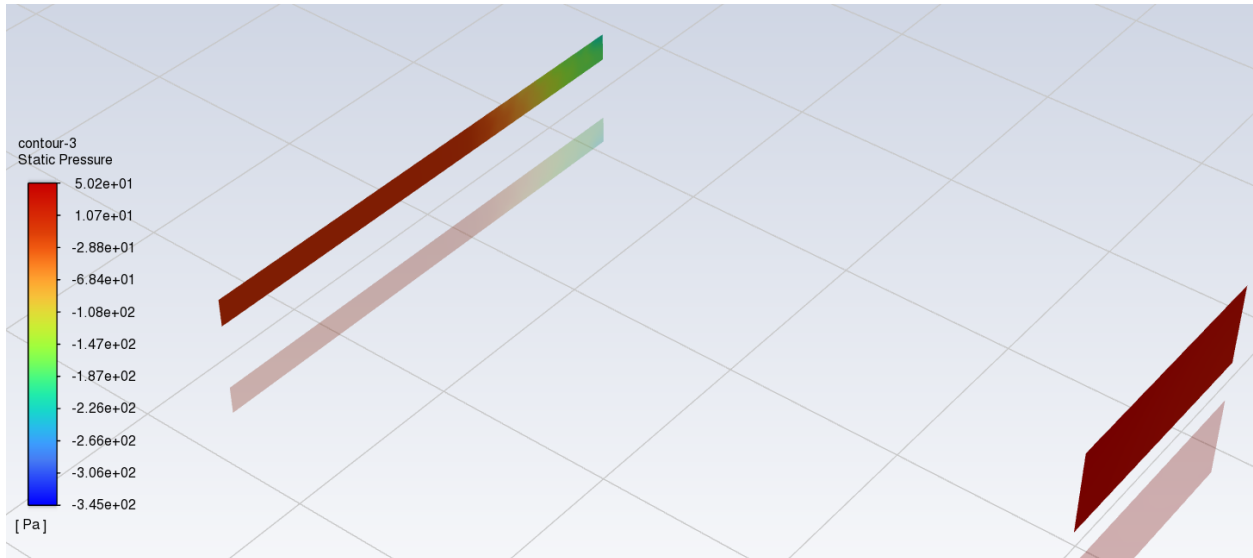


- 25 cfm
 - $0.0104 \text{ m}^3/\text{s}$ ($Q = Av \Rightarrow v = Q/A$)
 - Area: $4903.491 \text{ mm}^2 \Rightarrow 0.004903 \text{ m}^2$
 - Inlet Velocity Magnitude $v = 2.121 \text{ m/s}$

ME102B Group 5: Brad Ling, Shane Lee, David Kurniawan, Isak Knox, David Kurniawan







- 1 cfm
 - Flow Velocity Distribution
 - Pressure Drop Distribution
 - 0.924 Pa
- 5 cfm
 - Flow Velocity Distribution
 - Pressure Drop Distribution
 - 14.61 Pa
- 15 cfm
 - Flow Velocity Distribution
 - Pressure Drop Distribution
 - 108.7 Pa
- 25 cfm
 - Flow Velocity Distribution
 - Pressure Drop Distribution
 - 237.2 Pa
- 40 cfm
 - Flow Velocity Distribution
 - Pressure Drop Distribution
 - Pa
- 60 cfm
 - Flow Velocity Distribution
 - Pressure Drop Distribution
 - Pa
- Heat Transfer Coefficient, h Estimation
 - Methods
 - Apply losses => obtain a temperature distribution => use mean temperature relative to inlet temperature as

ΔT , use surface area from defeatured model => use q , A_s , and ΔT to get estimated h => compare to first principles conservative hand calc

- To get local h => get local Nu based on flow characteristics at certain regions (using Gnielinski => need Pr and Re which come from fluid properties and flow properties)

■ Ground Pad CFD Flow/Pressure Drop Analysis

- Normal Heatsink Model
- De-featured heatsink Model
- Fluid Volume Extract
- Mesh Workflow
 - Import defeatured CAD => surface mesh => generate fluid medium regions => volume mesh => solution mode
 - Note: Fluent Meshing vs Ansys Meshing
 - Cell types/ Methods:
 - Fluent Meshing's Mosaic-Enabled Parallel Poly-Hex Core Meshing combines high geometry fidelity, cell quality and fast solve time.
 - Ansys Meshing Sweep and Multi zone meshing enable users to create structured (primarily) hex meshes with intuitive control and flexibility.
 - Workflows
 - Fluent Meshing's task-based workflows are easy to use and tailored to the most common CFD applications.
 - Ansys Meshing provides a flexible environment allowing users to leverage smart physics-based global controls while also providing detailed local mesh control.
 - Usability Features
 - Fluent meshing offers the ability to create custom workflows that can include journal files, local sizing and automatic mesh improvement tasks.
 - Ansys meshing worksheets enable mesh operation recording and name selection definition based on size, location, or topology for mesh control
- Mesh Parameters & Setup
 - Local Sizing
 - Face Sizing

- 0.0003 m
 - Surface Mesh
 - Min Size
 - 0.0003 m
 - Max Size
 - 0.005 m
 - Growth Rate
 - 1.2
 - Size Functions
 - Curvature & Proximity
 - Curvature Normal Angle
 - 18
 - Mesh Quality
 - Skewness
- Ansys Meshing
 - Mesh Settings
 - Mesh Quality
 - 0.001 m Element Size
 - Note: Difficult to lower number of cells for Ansys mesh (Fluent mesh uses cells while Ansys uses elements/nodes => doubled mesh size and still didn't go below student license limit)
 - 0.008 Element Size
 - 0.008 element size was successful in reducing cell count under 512000 limit for student license
 - 414883 tetrahedral cells
 - Named Selections
 - Velocity Inlet
 - Pressure Outlet vs Outflow
 - Setting up Mesh Domain in Fluent (Mesh Check & Mesh Quality Evaluation)
 - Models
 - Material Properties
 - Boundary Conditions
 - Velocity Inlet
 - Cross-Sectional Area
 - Momentum Boundary Conditions
 - $1 \text{ cfm} \Rightarrow 0.000472 \text{ m}^3/\text{s} \Rightarrow (Q = Av \Rightarrow v = Q/A)$
 - Area: $4903.491 \text{ mm}^2 \Rightarrow 0.004903 \text{ m}^2$

- Inlet Velocity Magnitude $v = 0.09627$ m/s
- Magnitude, Normal to Boundary
- Turbulence Specification
Method: Intensity and Hydraulic Diameter
- Turbulent Intensity: 5%
- Hydraulic Diameter: $D_h = 4A_c/P_w$
- $A_c = 0.004903$ m²
- $P_w = 0.3252$ m
- $D_h = 0.0603$ m
- Outflow
 - Flow Rate Weighting: 1
- Solution Methods
 -
- Solution
 - 300 iterations
- Debugging
 - Reversed Flow
 - Reversed flow can occur when pressure gradients due to geometry mean that the flow wants to re-enter the domain at the location where an outlet/outflow has been specified
 - In the absence of flow separation on outflow boundary walls, reverse flow normally occurs only on a fraction of a pressure outlet boundary determined by the fact that for the neighboring cells near the outflow boundary exchanging momentum, the velocity correction obtained from the interior pressure field and the prescribed outflow pressure is sufficiently negative to cause reverse flow.
 - This means even the dynamic pressure available in these

interior cells is not sufficient to allow flow out of the domain.

- If it is known that this is not in agreement with observed flow one can overcome this only by reducing outlet gauge pressure and not by extending the outflow boundary.
- If separation has occurred on outflow boundary walls then extension of the computational domain is warranted.
- It is then logical that in any case the total pressure needs to be corrected for the artificial or numerical head added by the reverse flow
- First we need to understand that even in the simplest pipe flow total pressure as per Bernoulli equation will not remain constant along the pipe since there will be viscous losses in any real flow.
- If you want to get the correct total pressure corresponding to the portion of the flow exiting the domain, a work around is to obtain the averaged velocity components individually on the outflow plane and calculate the dynamic pressure and add this to the averaged static pressure.
- A little care is necessary here since if the outflow plane is normal to the x-axis, the average will have to be taken only for the positive part of the u-component and over the portion of the plane where it is positive.

- Some flow reversal can be tolerated, but will have an effect on mass-conservation and thus convergence
- Solutions
 - Make mesh thin and long at the outlet to artificially “damp” the reverse flow
 - Move the outlet position further downstream
 - Make a better distribution of mesh sizes and elements leading up to the outlet
 - Grid size refinement
 - Decrease relaxation factor
- Outlet Boundary Condition
 - Pressure Outlet vs Outflow
- Boundary Condition Initialization
 - Initial Gauge Pressure
- System Impedance Curve
 - Obtain pressure drops at 5 flow rates => curve fitting/interpolation to obtain system impedance curve
 - System Impedance Curve Accuracy
 - Pressure drop seems to be very high for the vehicle pad heatsink
 - Look into adding slant/draft onto corner section of the heatsink where the PCBA resides to reduce loss coefficient
 - Increase heat sink fin pitch
 - Target Maximum pressure drop for 60 cfm
 - 300 Pa
- Selected flow rates (cfm)
 - 1 cfm
 - $0.000472 \text{ m}^3/\text{s}$ ($Q = Av \Rightarrow v = Q/A$)
 - Area: $4903.491 \text{ mm}^2 \Rightarrow 0.004903 \text{ m}^2$

- Inlet Velocity Magnitude $v = 0.09627$ m/s
- 5 cfm
 - 0.00236 m³/s ($Q = Av \Rightarrow v = Q/A$)
 - Area: 4903.491 mm² $\Rightarrow 0.004903$ m²
 - Inlet Velocity Magnitude $v = 0.4813$ m/s
- 10 cfm
 - 0.00472 m³/s
- 15 cfm
 - 0.00708 m³/s ($Q = Av \Rightarrow v = Q/A$)
 - Area: 4903.491 mm² $\Rightarrow 0.004903$ m²
 - Inlet Velocity Magnitude $v = 1.444$ m/s
- 25 cfm
 - 0.0104 m³/s ($Q = Av \Rightarrow v = Q/A$)
 - Area: 4903.491 mm² $\Rightarrow 0.004903$ m²
 - Inlet Velocity Magnitude $v = 2.121$ m/s
- 1 cfm
 - Flow Velocity Distribution
 - Pressure Drop Distribution
 - 0.924 Pa
- 5 cfm
 - Flow Velocity Distribution
 - Pressure Drop Distribution
 - 14.61 Pa
- 15 cfm
 - Flow Velocity Distribution
 - Pressure Drop Distribution
 - 108.7 Pa
- 25 cfm
 - Flow Velocity Distribution
 - Pressure Drop Distribution
 - 237.2 Pa
- 40 cfm

- Flow Velocity Distribution
- Pressure Drop Distribution
- Pa
- 60 cfm
 - Flow Velocity Distribution
 - Pressure Drop Distribution
 - Pa
- Heat Transfer Coefficient, h Estimation
 - Methods
 - Apply losses => obtain a temperature distribution => use mean temperature relative to inlet temperature as ΔT , use surface area from defeatured model => use q , A_s , and ΔT to get estimated h => compare to first principles conservative hand calc
 - To get local h => get local Nu based on flow characteristics at certain regions (using Gnielinski => need Pr and Re which come from fluid properties and flow properties)

- **Heatsink Design**

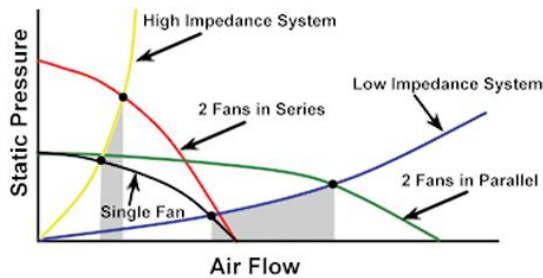
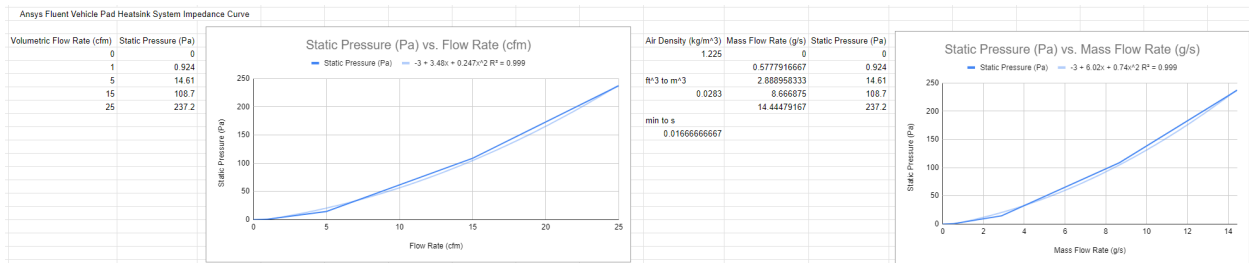
- **+** Wireless Charger | Heatsink Design Analysis
- **Heatsink Material**
 - Considerations
 - Thermal
 - Specific heat capacity
 - Important to note that we do not want high specific heat capacity as this will make the air flowing through the plate fins accept less heat due to the temperature delta between the convective surface area and the fluid medium being lower
 - Thermal conductivity
 - As high as possible, we want there to be a low thermal resistance path from magnetics or devices to the fluid medium
 - EMI/EMC
 - Magnetic permeability

- Don't want to divert flux density away from ferrite magnetic core which can weaken field strength at regions where we need it to augment inductive power transfer (reduced mutual inductance)
- Non-magnetically permeable material will help shield EMI from sensitive circuits
- Both copper and aluminum have a relative permeability of ~ 1 (ferrous materials can go up to the several hundreds)
- Manufacturing
 - Machinability
- Cost
 - Keep heatsink cost below \$700 piece price
 - Makes aluminum heatsink more preferred than copper (copper MSRP is at least double that of aluminum)
- Mechanical/Structural
 - Density
 - Material should have high specific strength (strength/density) such as Al 7075 or Al 6061
 - Copper is denser than aluminum on average ($\sim 2.7 \text{ g/cm}^3$ to 8.8 g/cm^3)
 - Young's Modulus
 - Yield Strength
 - UTS
 - 10^7 Endurance/Fatigue Strength
- Corrosion Resistance
 - Copper generally corrodes much faster than aluminum and will require additional plating for corrosion resistance
- **Fin Geometry**
 - Fin Width
 - Fin Pitch & Number Combinations (max width boundary condition)
 - Combination 1
 - Pitch: 12 mm
 - Width: 5 mm
 - Number: 19
 - Combination 2
 - Pitch: 15 mm
 - Width 5 mm
 - Number: 15
 - Combination 3
 - Width 4 mm
 - Combination 4

- Width 3 mm
- Combination 5
- Fin Profile
 - Limit to constant area and rectangular to simplify manufacturing considerations and cost
- Heatsink Fin Geometry Candidate Number 1
 - Current
- Heatsink Fin Geometry Candidate Number 2
 - Add in the draft/slant to PCBA corner
- Heatsink Fin Geometry Candidate Number 3
 - Add in the draft/slant to PCBA corner
 - Increase fin pitch for the heatsink + decrease fin count

● **Fan Selection Study**

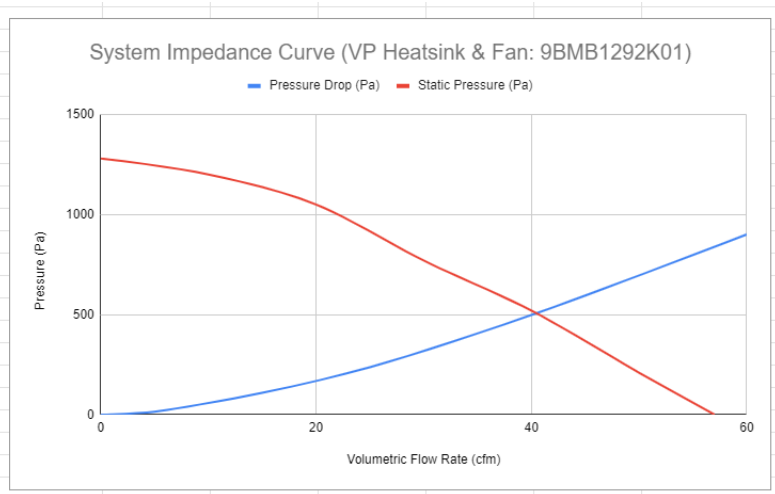
- 🇸🇬 Wireless Charger | Heatsink Design Analysis
- Obtain system impedance curve for the heatsink (from CFD) => need to select a fan with enough head/static pressure to provide the flow rate required at the system operating point (essentially, the system operating point needs to be to the right of the needed flow rate for the heatsink)
 - How to obtain system impedance curve
 - Get pressure drops for various flow rates => fit curve
 - Compare system impedance curve for both analytical calculation using darcy-weisbach equation as well as CFD results
 - System Impedance Curve of VP Heatsink from CFD:



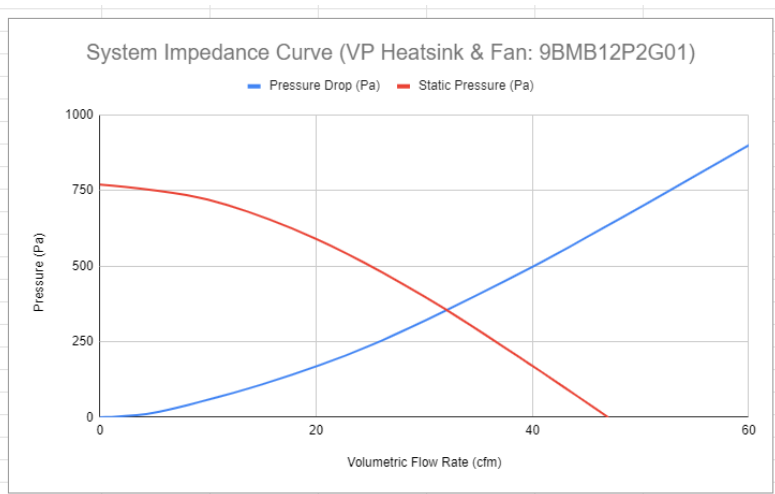
- - What is our system operating point?
 - What flow rate is required to achieve necessary heat transfer

ME102B Group 5: Brad Ling, Shane Lee, David Kurniawan, Isak Knox, David Kurniawan

System Operating Point		
Fan Model	9BMB12P2K01	
Volumetric Flow Rate (cfm)	Pressure Drop (Pa)	Static Pressure (Pa)
0	0	
1	0.924	
5	14.61	
15	108.7	
25	237.2	
40	497.6	
60	900	
0		1280
10		1200
20		1050
30		770
40		520
50		210
57		0



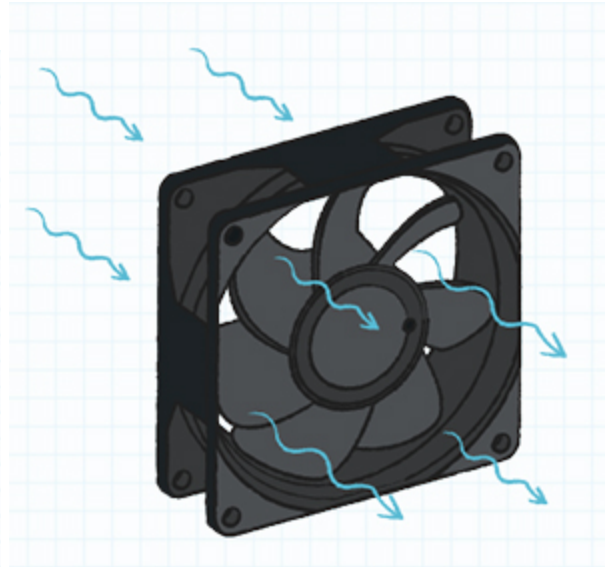
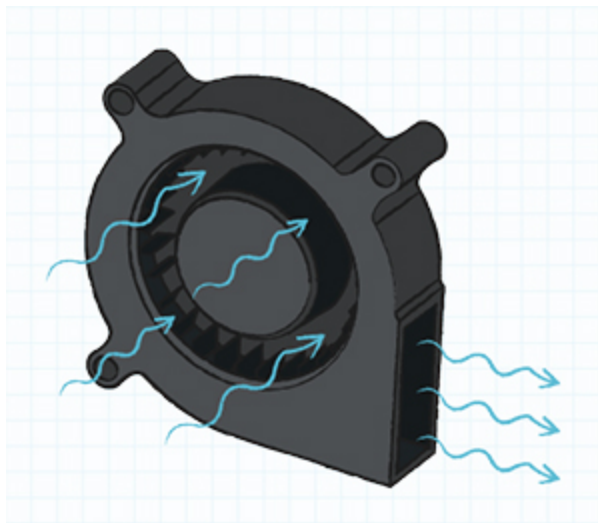
System Operating Point		
Fan Model	9BMB12P2G01	
Volumetric Flow Rate (cfm)	Pressure Drop (Pa)	Static Pressure (Pa)
0	0	
1	0.924	
5	14.61	
15	108.7	
25	237.2	
40	497.6	
60	900	
0		770
10		720
20		590
30		400
40		170
47		0



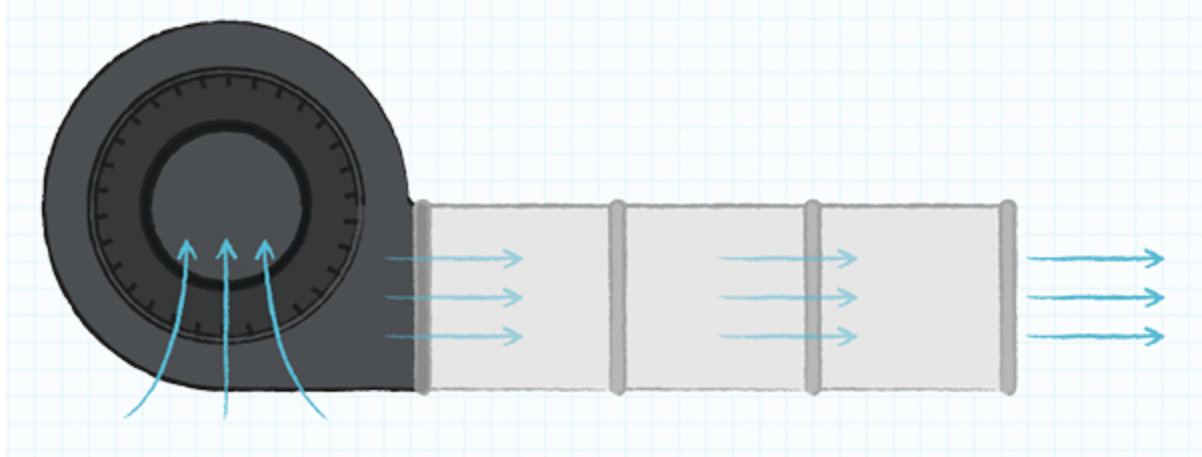
- Number of Fans
 - Configuration => Parallel
 - Number of fans in parallel
 - Fans in parallel lead to increased flow rate with no change in maximum static pressure/head, and progressively increased head/static pressure up to the maximum flow rate of a single fan
 - What flow rate (CFM)?
 - Flow velocity needed for the thermal management system
 - Total channel air flow area (Wetted area) => volumetric flow rate
 - Conservation of mass (mass continuity) => use density of air to get mass flow rate from volumetric flow rate
 - Assuming constant fluid density throughout the flow channel => both the mass flow rate and volumetric flow rate should remain the same => have the volumetric flow rate at the fan inlet and thus the needed total output flow rate => determine if 1 fan is sufficient or if 2+ fans are needed (objective function should be

to minimize the fan volume and fan power draw while providing minor margin on needed flow rate per fan)

- Fan Electrical Parameters
 - Nominal Operating Voltage
 - 5V or 12V => 12V (reduced losses for same power draw + higher velocities as higher voltages produce higher motor speeds - ignoring no-load and needed torque for system inertia, etc.)
 - Potentially look into 24V fans (higher speeds achievable with lower current draw for same power draw => better efficiency)
 - Control Scheme
 - PWM Duty Cycle
 - 100% Duty Cycle Power Draw
 - Speed Sensor
 - In-built tachometer preferred
- Fan Size Constraints
 - Vehicle Pad
 - Lower profile than the vehicle pad thickness
 - Ground Pad
 - Clearance from heatsink fins to the base plate of the ground pad: 30 mm
 - Tentative Maximum thickness: 20 mm
- Fan Formfactor
 - Axial vs Radial Fans
 - Radial fans would allow us to eliminate some of the steep pressure drops we would see from the shroud based on the relative size mismatch between fan and the heatsink inlet section of the duct
 - Much lower profile for the ground pad enclosure => less impact from the angle of the enclosure side walls for the FOD radar FOV
 - The airflow that axial fans produce is high volume, but low pressure, which makes them well-suited for cooling equipment and spaces both small and large due to airflow being evenly distributed in a defined area
 - As high-pressure, low-volume output devices, centrifugal fans essentially pressurize air within the fan housing, which works to produce a steady, high-pressure stream of air, but at more limited volumes compared to axial versions



Axial Fans	Radial Fans
<ul style="list-style-type: none"> ● High volume / low pressure ● Airflow parallel to axis ● Higher operating speed than centrifugal ● Compact designs ● Lower power usage than centrifugal ● Less audible noise than centrifugal ● Typically less expensive than centrifugal 	<ul style="list-style-type: none"> ● High pressure / low volume ● Airflow perpendicular to axis ● Lower operating speed than axial ● Better for specific directed cooling ● Typically uses more power than axial ● More audible noise than axial ● Durable and resistant to harsh environments



- Vehicle Pad Fan Selection
 - Centrifugal/Radial Fan
 - Axial fans have too much height => centrifugal/radial fans have a more low-profile formfactor
 - Fan Options

- - Ground Pad Fan Selection

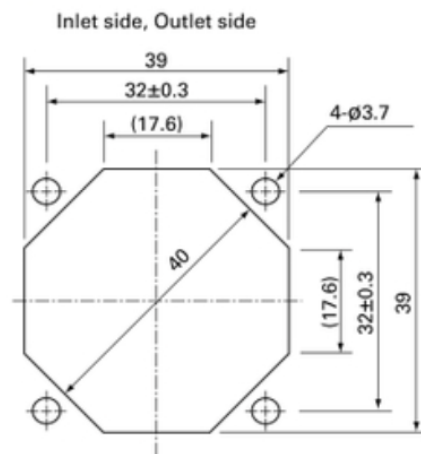
- - Ground Pad Fan Selection
 - Axial Fan

- - Ground Pad Fan Selection
 - Axial Fan
 - Either a single axial fan or an array of axial fans depending on required PQ flow characteristics

- - Ground Pad Fan Selection
 - Fan Position

- - Ground Pad Fan Selection
 - Fan Position
 - In order to accommodate the constraints around the air gap actuation system, the decision was made to place the fans on the underside of the fins rather than having them be placed to the side of the heatsink

- - Ground Pad Fan Selection
 - Potential Fan (60 x 25)



- - Ground Pad Fan Selection
 - Fan Size Constraints

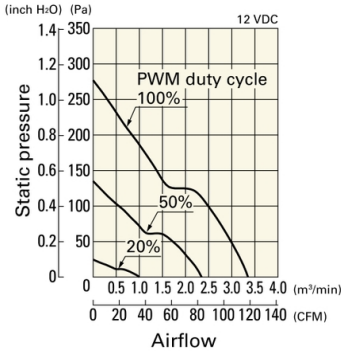
- - Ground Pad Fan Selection
 - Fan Size Constraints
 - 80 square to 100 square (mm)
 - Want to maximize coverage over all the fins => likely a 92 x 92 mm fan
 - Number of fans: 3
 - What is the new static pressure requirement for the fans?
 - Static pressure becomes the likely bottleneck
 - Our static pressure needed should be lower as well as there is less pressure drop from flow inlets to exhausts, albeit a greater loss factor from the axial fan pushing/intaking air at 90 degrees to the heatsink fin channels
 - Why is this a concern?
 - We want to see if we can go down to 20 mm wide fans to double the thickness available for a shroud to direct air flow to minimize recirculation?
 - How bad is recirculation for thermals?
 - Depends on the delta T of the air between inlet and exhaust

- What is the new flow rate requirement for the fans? (3 in parallel should lead to lower flow rate required per fan)
- Potential Fan:
 - PN: 9HV0912P4G0011
 - PQ Curve:

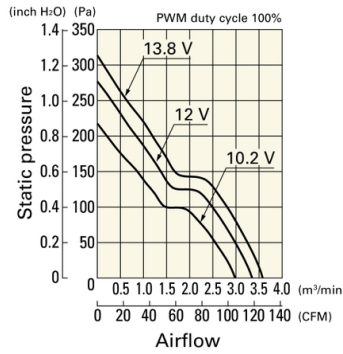
Airflow - Static Pressure Characteristics / PWM Duty - Speed Characteristics Example

9HV0912P4G001 With pulse sensor with PWM control

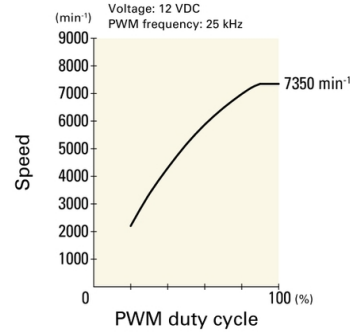
PWM duty cycle



Operating voltage range

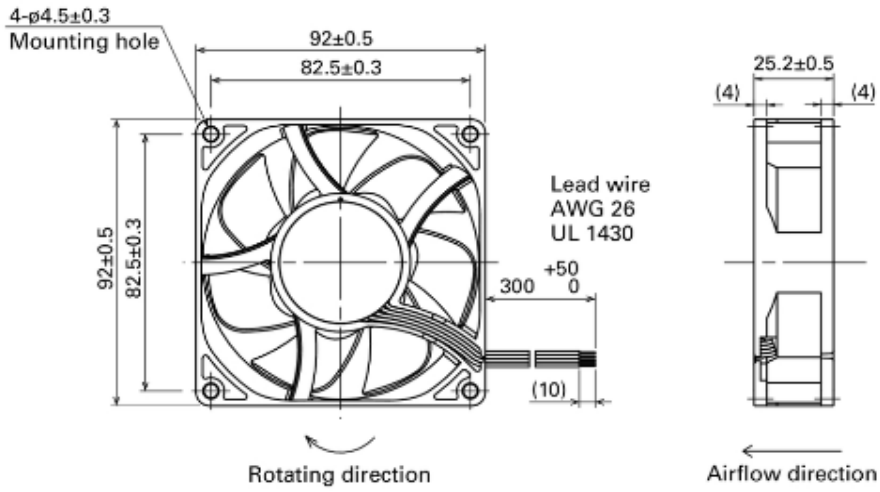


PWM duty - Speed characteristics example

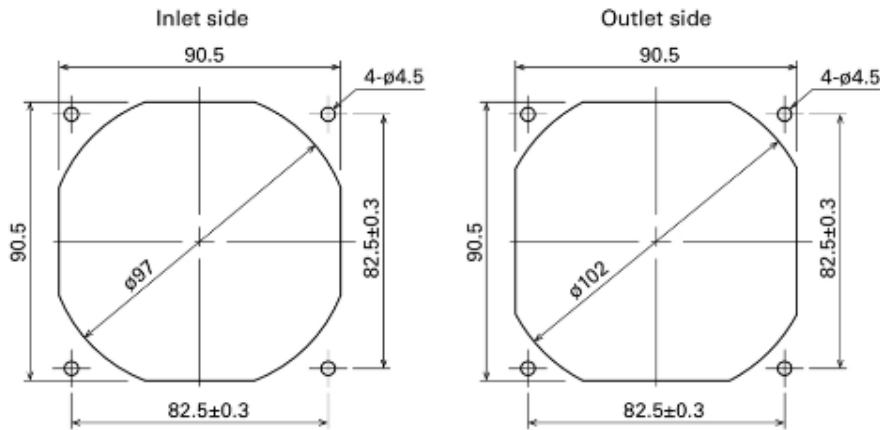


- Dimensions:

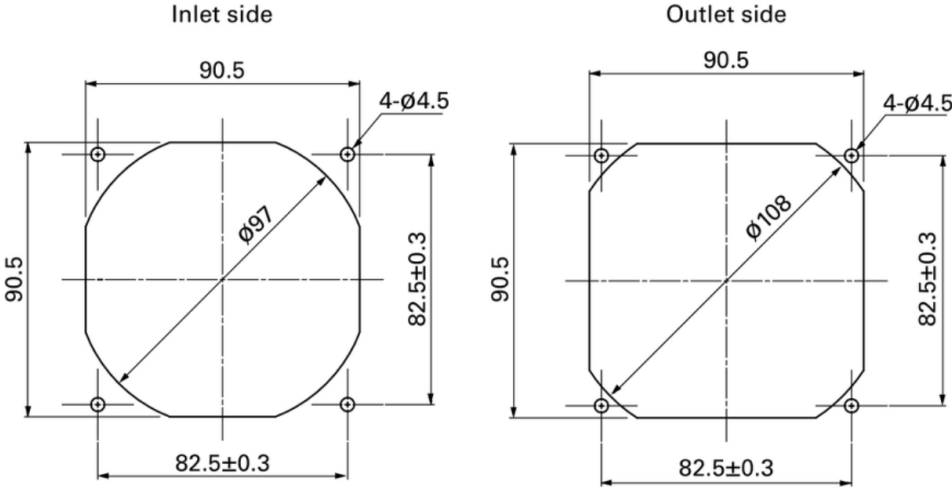
Dimensions (unit: mm) (With ribs)



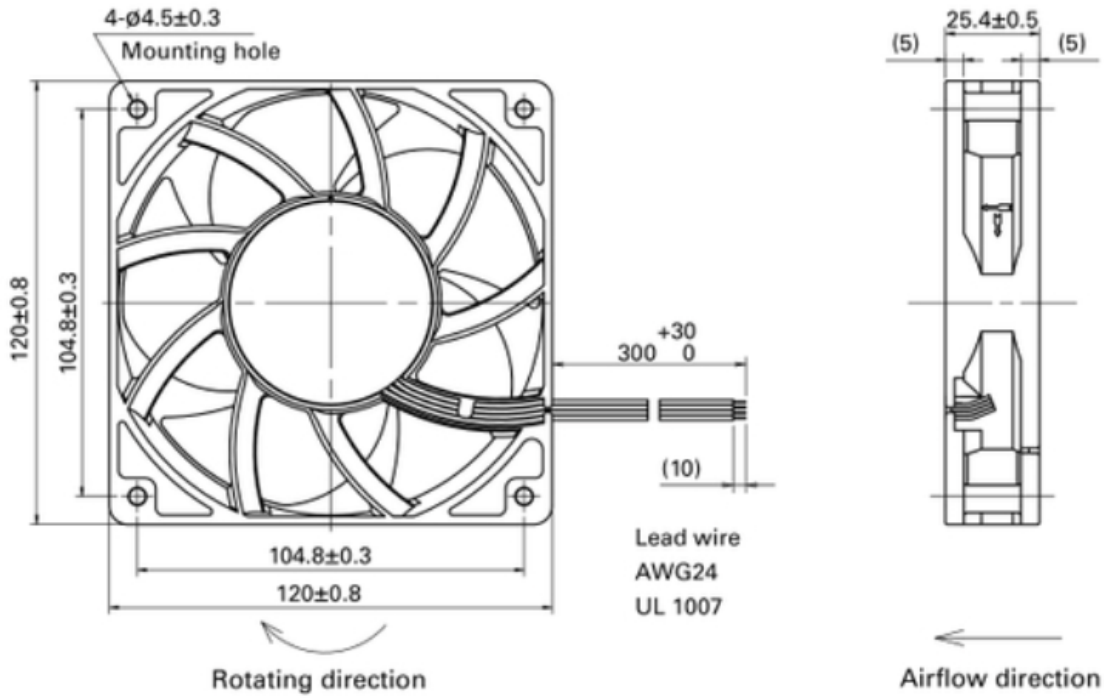
Reference Dimensions of Mounting Holes and Vent Opening (unit: mm)



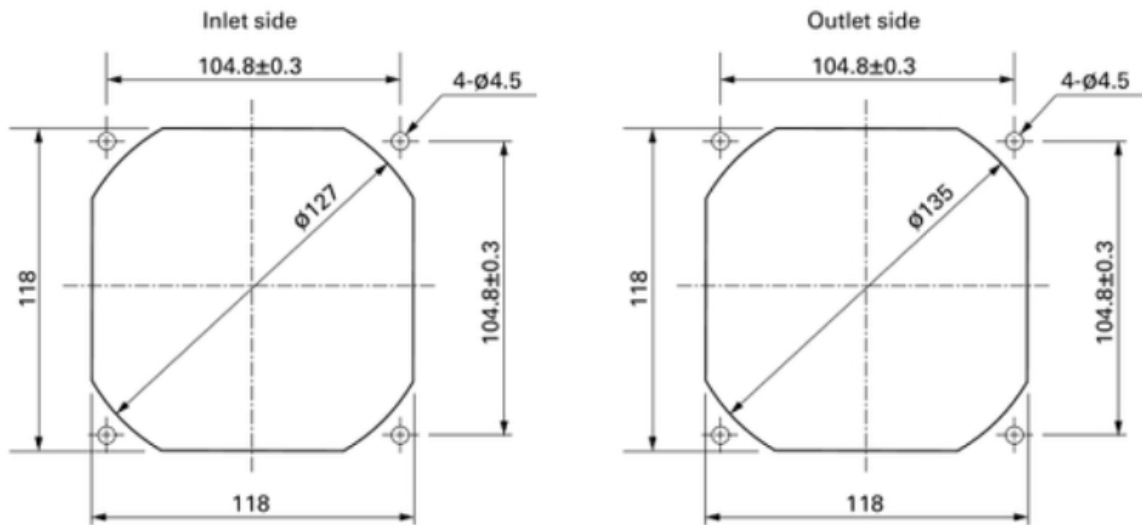
■ Reference Dimensions of Mounting Holes and Vent Opening (unit: mm)



Dimensions (unit: mm) (Ribbed frame with pulse sensor with PWM control)



Reference Dimensions of Mounting Holes and Vent Opening (unit: mm)



- **Magnetic Coupler Thermal Management**
 - Magnetic Core Thermal Interface Stack (Rth Ferrite → Heatsink)
 - [+ Wireless Charger | Heatsink Design Analysis](#)

- **+** Wireless Charger | Vehicle Pad | Component Thermal Limits & Losses
- Ferrite
 - Anisotropic Thermal Conductivity
 - Specific Heat Capacity
 - Thickness
 - Area
- Thermal Interface Material
 - Thermal Conductivity
 - Specific Heat Capacity
 - Thickness
 - Area
- Aluminum Heatsink
 - Thermal Conductivity
 - Specific Heat Capacity
 - Thickness
 - Area
- Heatsink Fin Channel Internal Ambient Air
 - Temperature
 - Surface Area
 - Convection Coefficient
- Thermal Resistances
 - $R_{th_TIM_Ferrite}$ (Contact)
 - R_{th_TIM} (Conduction)
 - $R_{th_TIM_Heatsink}$ (Contact)
 - $R_{th_Heatsink}$ (Conduction)
 - $R_{th_Heatsink_Air}$ (Convection)
- **Litz Wire Induction Coil Thermal Interface Stack (R_{th} Winding → Heatsink)**
 - **+** Wireless Charger | Heatsink Design Analysis
 - **+** Wireless Charger | Vehicle Pad | Component Thermal Limits & Losses
 - Copper Litz Wire Winding
 - Thermal Interface Material
 - Ferrite Core
 - Thermal Interface Material
 - Aluminum Heatsink
 - Heatsink Fin Channel Internal Ambient Air
 - Thermal Resistances
 - $R_{th_Winding}$ (Conduction)
 - $R_{th_Winding_TIM}$ (Contact)
 - R_{th_TIM} (Conduction)
 - $R_{th_TIM_Ferrite}$ (Contact)
 - $R_{th_Ferrite}$ (Conduction)

- Rth_TIM_Ferrite (Contact)
- Rth_TIM (Conduction)
- Rth_TIM_Heatsink (Contact)
- Rth_Heatsink (Conduction)
- Rth_Heatsink_Air (Convection)
- **Magnetics Thermal Limits**
 - Manganese Zinc Ferrite
 - Curie Point
 - Litz Wire Winding
 - Copper
 - Enamel Insulation (Polyimide)
- **Magnetics Losses**
 - Core Losses
 - Hysteresis Losses
 - Eddy Current Losses
 - Winding Losses
 - Resistive Losses (AC Current Carrying Conductor)
 - Skin Effect
 - Proximity Effect
- **Magnetics Thermal Modeling Techniques**
 - Challenges
 - Methods/Techniques
 - Thermal modeling of magnetic components is generally not standardized in the same manner that semiconductor packages and PCBs are which can be attributed to the following factors:
 - Complex, heterogeneous construction of the magnetic components and variability in construction of magnetic designs (windings in particular); a magnetics components comprises several bodies made of different materials with different material properties with some of them being active with regard to being loss generating sources directly involved in power conversion processes such as the magnetic core and the winding (different winding types such as wire wound, litz wire bundles, foil, planar, bar, etc.). Other components are passive such as the coil bobbin or insulating trays, the casing, etc. Each of these components behaves differently from an electromagnetic and thermal perspective which only increases complexity
 - Effective thermal conductivities for the winding construction are not trivial when considering the winding body consists of litz wire insulated in a polyimide enamel. Additionally, number of conductors or turns can add additional complexity as the winding can be made from just a few turns with a few parallel

conductors, to hundreds of turns with many parallel conductors which increases model granularity needed for sufficient accuracy

- Disparity of size and aspect ratios between the core and winding which forces a very demanding mesh when simulating magnetic components via FEA simulation
- 3D temperature distributions are generally the reality as opposed to simple 1D or even 2D heat fluxes seen in semiconductor packages. This is generally due to the complex non-uniform geometries of magnetic components and their arrangement over a PCB layout with different thermal interfaces and conductive/convective/radiative dissipation paths. As a result, the resolution of the heat equation for 3D in heterogeneous magnetics components is too complex to be directly formulated analytically, hence the need to use numerical solvers like FEM in order to increase accuracy and ease of modeling the interaction between each region or body of the component. This requires a good understanding and model of the loss densities to ensure the distribution is accurate based on various effects including high frequency operation and thermal-mechanical stresses.
- Generally, the more accurate the model, the easier it is to understand where margin can be gained to optimize the design and improve power density.
- The objective of this effort is to develop improved FEA-based thermal models with the following objectives and contributions
 - Simplified 3D FEA thermal models that ensure convergence with the end goal of relatively accurate temperature prediction with much faster simulations, regardless of geometric complexity. A potential solution that will be investigated is generic thermal homogenization for any type of winding construction.
 - Generating analytic thermal models from numerical FEA simulations in order to avoid the loss of accuracy from mathematical simplifications. The difficulty in this approach comes from FEM models providing temperature estimations for each element in the mesh which means the resultant matrix of resulting temperatures can be on the order of millions of elements which is not feasible for any analytical and mathematical calculations. As such, an objective will be to obtain a simplified matrix model from FEA output results in order to combine the accuracy and versatility of FEA tools with the simplicity of a linear thermal impedance state space matrix.

- Stretch objective of integrating previously mentioned models within an optimization model by taking advantage of fast and simplified 3D FEA combined with generated analytic thermal models to get optimized designs for magnetic components that ensure safe thermal operation below established limits
-


- ***Semiconductor Device Thermal Management***

- **+** Wireless Charger | Vehicle Pad | Component Thermal Limits & Losses
 - **Semiconductor Losses**
 - Switching Losses
 - Conduction Losses
 - Power Diodes
 - **Semiconductor Device Thermal Modeling**
 - Due to complex internal constructions of semiconductor devices, MOSFETs and diodes are generally modeled using simple, compact thermal resistance models described in their datasheets for various stack ups along the geometry (i.e. $R_{\text{junction-to-case}}$, $R_{\text{junction-to-ambient}}$, etc.) or using built-in package geometries in the modeling software libraries
 - These simplifications are made to reduce computational power needed for system-level thermal simulation
-

- ***Electronics Device/Component Thermal Management***

- **+** Wireless Charger | Vehicle Pad | Component Thermal Limits & Losses
 - Compensation Network Capacitor
 - Relay
 - Current Sense
 - Voltage Sense
 - Over-Voltage Protection
 - Filter Circuits
 - PCB
 - Metal Fraction percentage with regards to layer trace volume and thus loss quantity
 - Generally imported as an ODB++ file and evaluating the above-mentioned average metal fractions in different layers to understand effective thermal conductivity of the PCB to conserve compute from the cost of meshing PCB traces and vias.
-


- **Component Thermal Limits**

-  Wireless Charger | Vehicle Pad | Component Thermal Limits & Losses
 - Winding Bobbin Tray (Nylon PA12 Glass Bead Filler - MJF)
 - 175 C
 - PCB (FR4)
 - 130 C
 - Top Cover (Nylon PA12 Glass Bead Filler - MJF)
 - 175 C
 - Magnetic Core (MnZn Ferrite)
 - 265 C (Curie Point)
 - Thermal Runaway is induced at much lower temperatures (130-140C)
 - Litz Wire Winding (Copper)
 - 200 C
 - Litz Wire Enamel Insulation (Kapton/Polyimide)
 - 315 C
 - Thermal Interface Material - TIM (Silicone)
 - 160C+
 - Heatsink (Aluminum)
 - 170 C
 - PCB Components
 - MOSFETs
 - Capacitors
 - Resistors
 - IC's
-

- **Lumped Parameter RC Thermal Network Model Development**


- What is a LPTN?
 - Lumped Parameter Thermal Network
 - Circuit analogs for thermal management to provide a simple system-level analysis and temperature prediction framework
 - Why?
 - Relatively robust and simple way to model and capture thermal performance of a system => make predictions with relatively low computing cost and high accuracy once estimated parameters have been fit to real data
-

- **Thermal Sensor Suite Selection Study & Position**

-  Wireless Charger | Thermal Sensor Selection
- Thermal Sensor Options

- Thermistors
 - PCB Negative Temperature Coefficient (NTC) Resistor
 - Negative correlation between resistance and temperature
- Resistance Temperature Detectors (RTDs)
 - Positive correlation between resistance and temperature
- Thermocouple
- Considerations
 - Sensor accuracy
 - Sensor sensitivity
 - Environment
 - Noise
 - Sensor temperature sensing range
 - Sensor operating temperature
 - Sensor output type
 - Analog
 - Digital
- Sensor Attachment Methods
 - Thermally conductive adhesive
 - Soldered onto PCB
- Thermal Sensor Map
 - How do we determine this?
 - Obtain temperature distribution of critical and highest loss components from simulation => where are all the hot spots/regions with smallest thermal margin to thermal limits
 - Place a sensor in each of these locations (1 per component) => total sensor count
 - Mandatory
 - 1+ on the core
 - 1+ on the coil
 - 1 near the FETs for the inverter stage
 - 1 near the gate drivers
 - # for other electronics (Filter caps, resonant tank caps, over-voltage protection, relays, etc.)
 - 1 for magnetic coupler ambient air temperature
 - 1 for heatsink ambient air temperature
 - Or place 1 sensor for an overall region and extrapolate temperatures using thermal network
 - Much simpler, especially if the hot spots are overlapping => 1D approximations for the RC thermal network stack become much simpler and applicable

- **Thermal Interface Material Properties & Selection**

-  Wireless Charger | TIM Material Development
- Thermal conductivity
 - $> 3 \text{ W/m-K}$ (target: 4 W/m-K)
- Open time
 - At least 20 minutes to be able to ensure proper assembly of the vertical stack
- Cure method
 - Either room temperature cure or heat/temp cure below 150C
- Pre-cure viscosity
 - Potting encapsulant (SC 324, SC 320) vs gap filler (SC 1600)
- Compound type
 - Silicone encapsulant preferred over epoxy formulations as epoxy is more brittle and has lower operating temperature range
- Considerations
 - Thermal conductivity
 - Gap fill
 - Dispense process
 - Cure method and time
 - Specific heat capacity
 - Viscosity
 - Adhesive strength
 - Shear strength
 - Elastic modulus
 - Dielectric strength
- TIM Formfactors
 - Gap Filler
 - Generally thixotropic/shear-thinning
 - Potting Encapsulant
 - Gap Pad
 - Grease
 - Adhesives
- Material Types
 - Silicone
 - More viscous than epoxies
 - Have higher operating temperatures
 - Epoxy
 - Lower viscosity
 - More brittle, especially at higher temperatures
 - Acrylic
 - Urethane
- Total TIM Volume Estimation

- Determine volume of TIM to purchase

- ***Fluids Reference Properties:***

Table 1. Properties of water vs. temperature, with pressure constant at 101.3 kPa (absolute)

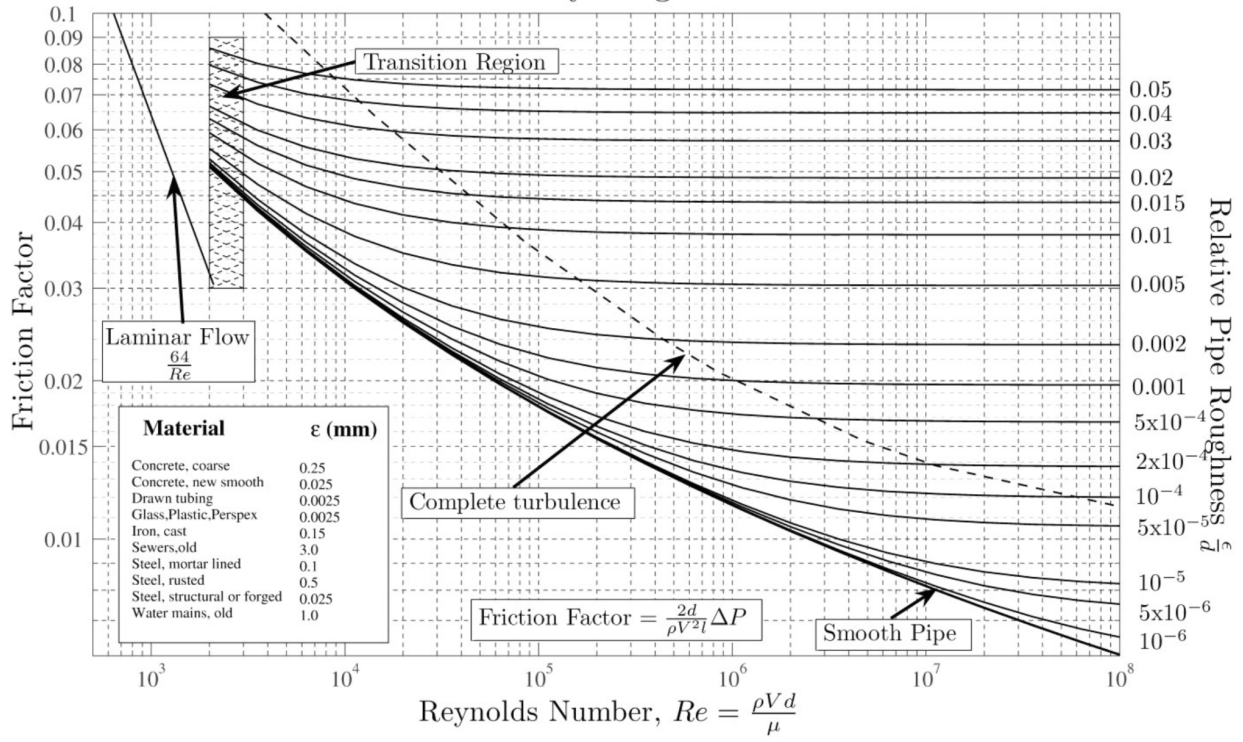
Temperature, T (°C)	Density, ρ (kg/m ³)	Dynamic Viscosity, μ (s·Pa = N·s/m ² = kg/m·s)	Kinematic Viscosity, ν (m ² /s)
0	999.9	1.79×10^{-3}	1.79×10^{-6}
5	1000	1.52×10^{-3}	1.52×10^{-6}
10	999.7	1.31×10^{-3}	1.31×10^{-6}
15	999.1	1.14×10^{-3}	1.14×10^{-6}
20	998.2	1.00×10^{-3}	1.00×10^{-6}
40	992.2	0.65×10^{-3}	0.655×10^{-6}
80	971.8	0.35×10^{-3}	0.360×10^{-6}
100	958.4	0.28×10^{-3}	0.292×10^{-6}

Note: by definition $\mu \equiv \rho\nu$

Table 2. Properties of dry air vs. temperature, with pressure constant at 101.3 kPa (absolute)

Temperature, T (°C)	Density, ρ (kg/m ³)	Dynamic Viscosity, μ (s·Pa = kg/m·s)	Kinematic Viscosity, ν (m ² /s)
0	1.29	1.71×10^{-5}	1.32×10^{-5}
5	1.27	1.73×10^{-5}	1.36×10^{-5}
10	1.25	1.76×10^{-5}	1.41×10^{-5}
15	1.23	1.80×10^{-5}	1.47×10^{-5}
20	1.20	1.82×10^{-5}	1.51×10^{-5}
40	1.13	1.87×10^{-5}	1.66×10^{-5}
80	1.00	2.07×10^{-5}	2.07×10^{-5}
100	0.95	2.17×10^{-5}	2.29×10^{-5}

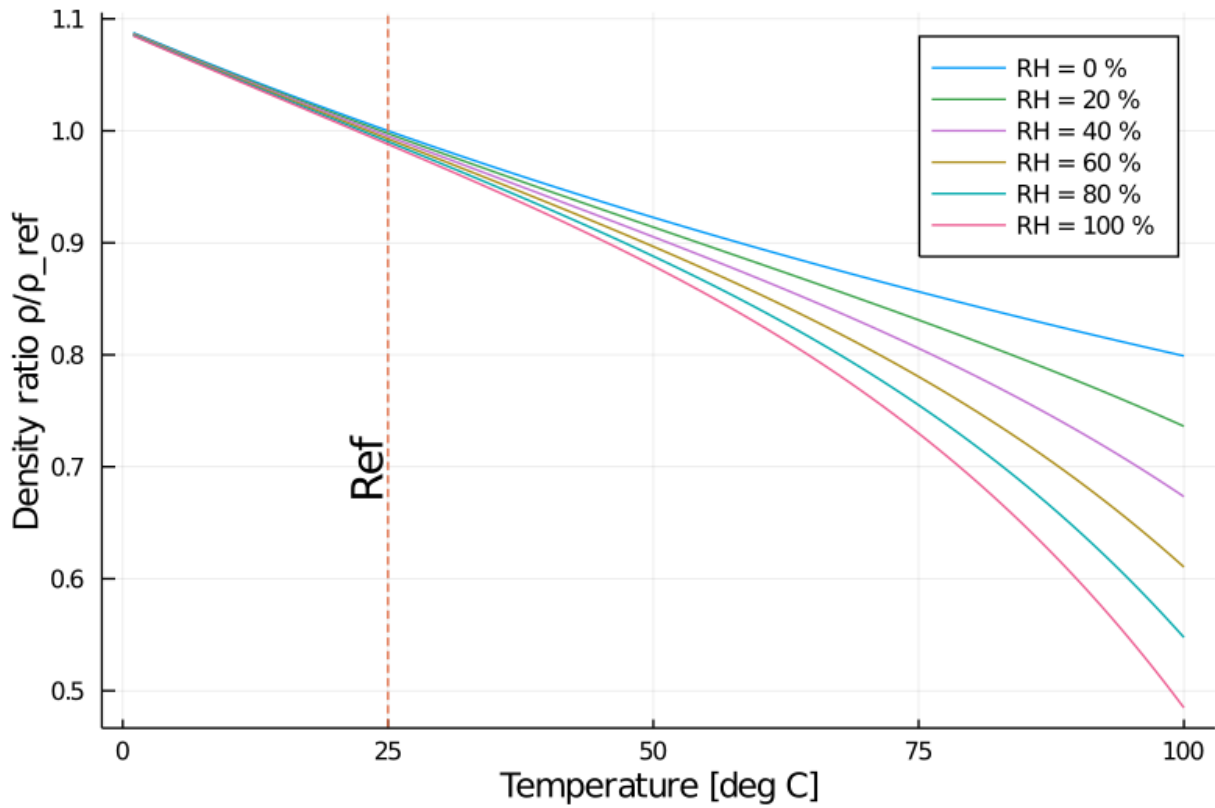
Moody Diagram



ME102B Group 5: Brad Ling, Shane Lee, David Kurniawan, Isak Knox, David Kurniawan

Resistance Coefficients $K = h_m/[V^2/(2g)]$ for Open Valves, Elbows and Tees

Nominal diameter, mm									
	Screwed				Flanged				
	12.7	25.4	50.8	101.6	25.4	50.8	101.6	203.2	508
Valves (fully open)									
Globe	14	8.2	6.9	5.7	13	8.5	6	5.8	5.5
Gate	0.3	0.24	0.16	0.11	0.8	0.35	0.16	0.07	0.03
Swing check	5.1	2.9	2.1	2.0	2.0	2.0	2.0	2.0	2.0
Angle	9.0	4.7	2.0	1.0	4.5	2.4	2.0	2.0	2.0
Elbows:									
45° regular	0.39	0.32	0.3	0.29					
45° long radius					0.21	0.20	0.19	0.16	0.14
90° regular	2.0	1.5	0.95	0.64	0.50	0.39	0.30	0.26	0.21
90° long radius	1.0	0.72	0.41	0.23	0.40	0.30	0.19	0.15	0.10
180° regular	2.0	1.5	0.95	0.64	0.41	0.35	0.30	0.25	0.20
180° long radius					0.40	0.30	0.21	0.15	0.10
Tees:									
Line flow	0.90	0.90	0.90	0.90	0.24	0.19	0.14	0.10	0.07
Branch flow	2.4	1.8	1.4	1.1	1.0	0.80	0.64	0.58	0.41



Dry Air Density in relation to temperature and relative humidity

Appendix E: Air Gap Actuation with ~17kg

- Video Link GDrive ([link](#))

Appendix F: Entrepreneurship Award

